

AD-A013 194

THE PIEN WAVEMAKING RESISTANCE COMPUTATION PROGRAM -PART
I. THEORETICAL BASIS AND PROGRAMMING TECHNIQUE

Ruey Chen

Naval Ship Research and Development Center
Bethesda, Maryland

April 1975

DISTRIBUTED BY:

NTIS

National Technical Information Service
U. S. DEPARTMENT OF COMMERCE

ADA013194

225133

NAVAL SHIP RESEARCH AND DEVELOPMENT CENTER

Bethesda, Md. 20084



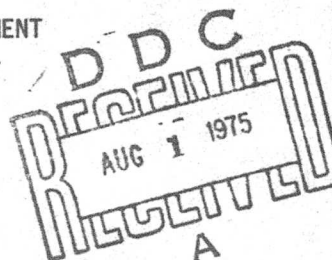
THE PIEN WAVEMAKING RESISTANCE COMPUTATION PROGRAM - PART 1: THEORETICAL BASIS AND PROGRAMMING TECHNIQUE

by
Ruey Chen

APPROVED FOR PUBLIC RELEASE: DISTRIBUTION UNLIMITED

COMPUTATION AND MATHEMATICS DEPARTMENT
RESEARCH AND DEVELOPMENT REPORT

Reproduced by
**NATIONAL TECHNICAL
INFORMATION SERVICE**
U S Department of Commerce
Springfield VA 22151



April 1975

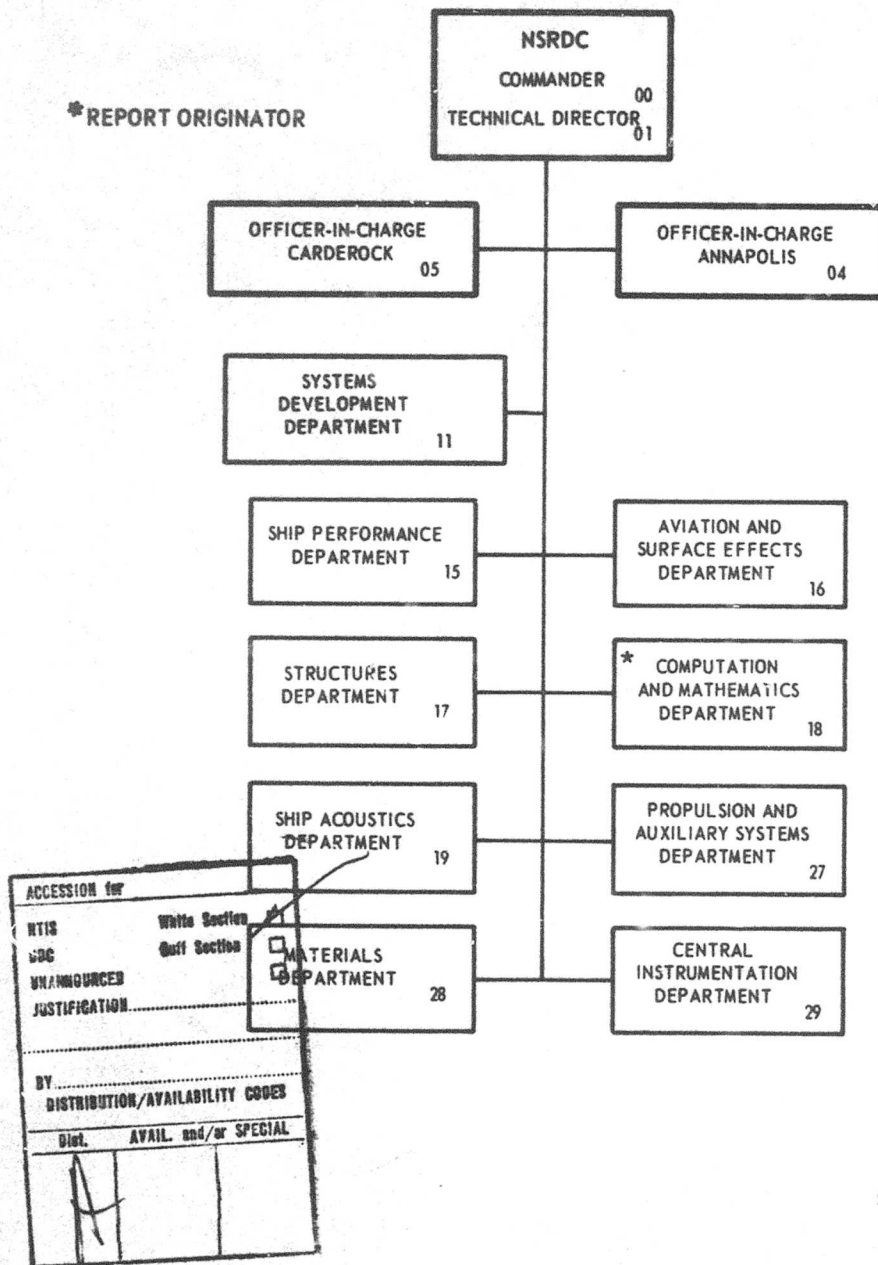
Report 4370

The Naval Ship Research and Development Center is a U. S. Navy center for laboratory effort directed at achieving improved sea and air vehicles. It was formed in March 1967 by merging the David Taylor Model Basin at Carderock, Maryland with the Marine Engineering Laboratory at Annapolis, Maryland.

Naval Ship Research and Development Center
Bethesda, Md. 20034

MAJOR NSRDC ORGANIZATIONAL COMPONENTS

*REPORT ORIGINATOR



UNCLASSIFIED

SECURITY CLASSIFICATION OF THIS PAGE (When Data Entered)

REPORT DOCUMENTATION PAGE		READ INSTRUCTIONS BEFORE COMPLETING FORM
1. REPORT NUMBER 4370	2. GOVT ACCESSION NO.	3. RECIPIENT'S CATALOG NUMBER
4. TITLE (and Subtitle) THE PIEN WAVEMAKING RESISTANCE COMPUTATION PROGRAM - PART 1: THEORETICAL BASIS AND PROGRAMMING TECHNIQUE		5. TYPE OF REPORT & PERIOD COVERED
7. AUTHOR(s) Ruey Chen		6. PERFORMING ORG. REPORT NUMBER
9. PERFORMING ORGANIZATION NAME AND ADDRESS Naval Ship Research and Development Center Bethesda, Maryland 20084		8. CONTRACT OR GRANT NUMBER(s)
11. CONTROLLING OFFICE NAME AND ADDRESS		10. PROGRAM ELEMENT, PROJECT, TASK AREA & WORK UNIT NUMBERS Task SF35421007 Work Unit 1-1521-018
13. MONITORING AGENCY NAME & ADDRESS (if different from Controlling Office)		12. REPORT DATE April 1975
		13. NUMBER OF PAGES 148 149
		14. SECURITY CLASS. (of this report) UNCLASSIFIED
		15a. DECLASSIFICATION/DOWNGRADING SCHEDULE
16. DISTRIBUTION STATEMENT (of this Report) APPROVED FOR PUBLIC RELEASE; DISTRIBUTION UNLIMITED		
17. DISTRIBUTION STATEMENT (of the abstract entered in Block 20, if different from Report)		
18. SUPPLEMENTARY NOTES		
19. KEY WORDS (Continue on reverse side if necessary and identify by block number) Wavemaking Resistance, Ship Hull Form Design, Singularity Distribution, Source-Sink, Doublet, Stream-Line Tracing		
20. ABSTRACT (Continue on reverse side if necessary and identify by block number) The waves produced at the rear of a ship as it travels at the water's surface are directly related to a component of the ship resistance known as wavemaking resistance. Pien's Wavemaking Resistance Computation Program adapts Havelock's mathematical representation of this phenomenon to provide the ship designer with a relatively quick and inexpensive way of determining the wavemaking resistance of his proposed design. This computer program can also be used in determining the optimum hull form which has the least theoretical wavemaking resistance. Applied initially for the development of small		

DD FORM 1 JAN 73 1473

EDITION OF 1 NOV 65 IS OBSOLETE
S/N 0102-014-6601

UNCLASSIFIED

SECURITY CLASSIFICATION OF THIS PAGE (When Data Entered)

UNCLASSIFIED

SECURITY CLASSIFICATION OF THIS PAGE(When Data Entered)

20. (Continued)

waterplane area twin hull and single hull ships, the Pien program produced predicted wavemaking resistances which compared favorably with those measured from actual experimental model tests. Use of the Pien program in the design of other type ships appears promising. The Pien Wavemaking Resistance Program, written in FORTRAN and developed for use with the CDC 6000 series computers, has been documented in two volumes--Part 1, the theory underlying the logic of the program, and Part 2, the Users Manual, Naval Ship Research and Development Center Report 4371, which explains the preparation of input and the use of the program.

ia

UNCLASSIFIED

SECURITY CLASSIFICATION OF THIS PAGE(When Data Entered)

FOREWORD

This work was performed as part of the Hull Form Design Procedure Documentation project being conducted by the Ship Performance Department. It was carried out within the Graphics Systems Development Group of the Computer Sciences Division. The Pien program is documented in two parts: Part 1, Theoretical Basis and Programming Technique, Naval Ship Research and Development Report 4370; Part 2, the Users Manual, Naval Ship Research and Development Report 4371.

TABLE OF CONTENTS

	Page
I. INTRODUCTION.....	7
II. THEORETICAL BASIS.....	9
WAVE AMPLITUDE FUNCTIONS OF A POINT SOURCE.....	9
VELOCITY COMPONENTS OF A POINT SOURCE.....	12
III. APPLICATION OF THE THEORY.....	14
η -SURFACE AND COORDINATE SYSTEMS.....	15
SINGULARITY DISTRIBUTIONS.....	17
PARAMETRIC REPRESENTATION OF SINGULARITY DISTRIBUTIONS.....	18
WAVE AMPLITUDE FUNCTIONS.....	22
COEFFICIENT OF WAVEMAKING RESISTANCE.....	30
OPTIMIZATION OF WAVEMAKING RESISTANCE.....	30
STREAMLINE FUNCTIONS AND VELOCITY COMPONENTS.....	38
STREAMLINE TRACING.....	42
IV. DESCRIPTION OF THE COMPUTER PROGRAM.....	43
PROGRAM STRUCTURE.....	43
SUBROUTINE DESCRIPTIONS.....	49
ACKNOWLEDGMENT.....	103
APPENDIX A - VARIABLES IN COMMON.....	105
APPENDIX B - COMPARISONS OF COEFFICIENTS OF THEORETICAL WAVEMAKING RESISTANCE AND RESIDUAL RESISTANCE OF SWATH'S III, IV, V, AND RC-2.....	119
REFERENCES.....	149

Preceding page blank

LIST OF FIGURES

	Page
Figure 1 - Coordinate Systems and n -Surface for Location of Singularity Distributions.....	15
Figure 2 - Approximation of n -Surface for a Forebody by Three Straight-Line Segments.....	16
Figure 3 - Singularity Distribution on Forebody and Aftbody....	19
Figure 4 - Flow Chart of the Optimization Process.....	36
Figure 5 - Program Overlay Structure.....	43
Figure 6 - Block Diagram for (1,0) Overlay - Input Data Processing.....	44
Figure 7 - Block Diagram for (2,0) Overlay - Wavemaking Resistance Computation.....	45
Figure 8 - Block Diagram for (2,0) Overlay - Wavemaking Resistance Optimization.....	46
Figure 9 - Block Diagram for (3,0) Overlay - Streamline Tracing.....	47
Figure 10 - Abbreviated Lines and Profile for SWATH III Represented by Models 5276 and 5276E.....	121
Figure 11 - Ship and Experimental Model Test Data for SWATH III (Model 5276).....	122
Figure 12 - Residual and Wavemaking Resistance Coefficients versus Speed-Length Ratio for SWATH III (Model 5276) at a 32-Foot Draft.....	123
Figure 13 - Residual and Wavemaking Resistance Coefficients versus Speed-Length Ratio for SWATH III (Model 5276) at a 28-Foot Draft.....	124
Figure 14 - Residual and Wavemaking Resistance Coefficients versus Speed-Length Ratio for SWATH III (Model 5276) at a 25-Foot Draft.....	125
Figure 15 - Ship and Experimental Model Test Data for SWATH III (Model 5276E).....	126
Figure 16 - Residual and Wavemaking Resistance Coefficients versus Speed-Length Ratio for SWATH III (Model 5276E) at a 32-Foot Draft.....	127
Figure 17 - Residual and Wavemaking Resistance Coefficients versus Speed-Length Ratio for SWATH III (Model 5276E) at a 28-Foot Draft.....	128

	Page
Figure 18 - Residual and Wavemaking Resistance Coefficients versus Speed-Length Ratio for SWATH III (Model 5276E) at a 25-Foot Draft.....	129
Figure 19 - Abbreviated Lines and Profile for SWATH IV Represented by Model 5287.....	130
Figure 20 - Abbreviated Body Plan for SWATH IV (Model 5287)...	131
Figure 21 - Ship and Experimental Model Test Data for SWATH IV (Model 5287).....	132
Figure 22 - Residual and Wavemaking Resistance Coefficients versus Speed-Length Ratio for SWATH IV (Model 5287) at a 32-Foot Draft.....	133
Figure 23 - Residual and Wavemaking Resistance Coefficients versus Speed-Length Ratio for SWATH IV (Model 5287) at a 28-Foot Draft.....	134
Figure 24 - Residual and Wavemaking Resistance Coefficients versus Speed-Length Ratio for SWATH IV (Model 5287) at a 25-Foot Draft.....	135
Figure 25 - Abbreviated Lines and Profile for SWATH V Represented by Model 5301.....	136
Figure 26 - Ship and Experimental Model Test Data for SWATH V (Model 5301).....	137
Figure 27 - Residual and Wavemaking Resistance Coefficients versus Speed-Length Ratio for SWATH V (Model 5301) at a 36.27-Foot Draft.....	138
Figure 28 - Residual and Wavemaking Resistance Coefficients versus Speed-Length Ratio for SWATH V (Model 5301) at a 32-Foot Draft.....	139
Figure 29 - Residual and Wavemaking Resistance Coefficients versus Speed-Length Ratio for SWATH V (Model 5301) at a 26.27-Foot Draft.....	140
Figure 30 - Abbreviated Lines and Profile for SWATH V Represented by Model 5301-1.....	141
Figure 31 - Ship and Experimental Model Test Data for SWATH V (Model 5301-1).....	142
Figure 32 - Residual and Wavemaking Resistance Coefficients versus Speed-Length Ratio for SWATH V (Model 5301-1) at a 38-Foot Draft.....	143
Figure 33 - Residual and Wavemaking Resistance Coefficients versus Speed-Length Ratio for SWATH V (Model 5301-1) at a 32-Foot Draft.....	144

	Page
Figure 34 - Abbreviated Lines and Profile for SWATH RC-2.....	145
Figure 35 - Ship and Experimental Model Test Data for SWATH RC-2.....	146
Figure 36 - Residual and Wavemaking Resistance Coefficients versus Speed-Length Ratio for SWATH RC-2 at a 28-Foot Draft.....	147
Figure 37 - Residual and Wavemaking Resistance Coefficients versus Speed-Length Ratio for SWATH RC-2 at a 21-Foot Draft.....	148

I. INTRODUCTION

During the period 1963-1966, Dr. P. C. Pien of the Naval Ship Research and Development Center conducted an investigation into the application of existing wavemaking resistance theory^{1 2 3} to the design of practical ship hull forms. During the three years of the study, Dr. Pien developed several computer programs which were later used in designing the hulls of various ship models. The procedures developed and the resistances obtained were documented by Pien.^{4 5 6} Although the models built from these designs had low resistances, the agreement between the values of the experimental and theoretical resistances was unsatisfactory.

With the recent surge of interest in unconventional hull forms, such as catamarans, small waterplane area twin-hull (SWATH) ships and small waterplane area single-hull (SWASH) ships for which little or no experimental information is available, the theoretical approach to ship design has assumed a new importance. Accordingly, the programs developed earlier by Dr. Pien have been redesigned into a new program called "The Pien Wave-making Resistance Computation Program." This program computes and prints out the wavemaking resistance coefficients (C_W) for various ship speeds. It can also compute the frictional resistance coefficients (C_f) and therefore the effective horsepower (EHP) for various ship speeds. Using this program, the designer is able to predict the resistance of a SWATH or SWASH ship of a particular design without undergoing the expense of building and testing a scale model.

The Pien program has been used successfully in the past few years for the design of several SWATH ships, models of which have actually been built. Experimental results have shown close agreement with the resistances predicted by the Pien program.⁸ (See also Appendix B.)

The Pien program consists of about 60 individual subroutines assembled into three main overlays which are available either on disk or on magnetic tape. These routines are coded in CDC Fortran Extended for use on the CDC 6000-series computers. The program requires a minimum of 35K octal core

¹A complete list of references is given on page 149.

for execution. An interactive graphics capability operable on the CDC 6000/1700/274 computer configuration is being developed as a separate program.

Documentation of the Pien program has been prepared in two parts. The first describes the theoretical basis and programming technique, and is intended primarily for those who wish to review the theoretical equations or understand the coding of the program. The second, the User's Manual,⁹ is intended for those who are responsible for designing a ship hull with low wavemaking resistance or for computing the wavemaking resistance of a ship hull for which the singularity distribution is known. Programming knowledge is not essential to understand the Users Manual.

II. THEORETICAL BASIS

Normal pressures vary along the length of a deeply submerged body traveling horizontally at a steady speed. If the fluid surrounding the body is nonviscous, the net force of these various pressures is zero. However, when a body travels on or near the surface, the variations in pressure along the length of the body cause waves to form which themselves affect the distribution of the pressures along the hull so that a net fore-and-aft force, called wavemaking resistance, is created. A great deal of research has been devoted to the development of theoretical methods for calculating wavemaking resistance and to their experimental verification. One such method involves determining the flow around the hull, and hence the normal pressure distribution, and then integrating the fore-and-aft components of these pressures over the hull surface. This method was developed in 1898 by Michell for a thin ship moving over the surface of a nonviscous fluid.¹ Another method is that used by the Pien program which adapts Havelock's mathematical representation of the wave system generated by the ship at a great distance astern^{2 3} to compute the wavemaking resistance as determined by the flow of energy necessary to maintain the wave system.

A ship hull moving through water can be hydrodynamically represented by singularity distributions. The basic element of a singularity distribution is a simple point source. From it, a point doublet can be derived. Since a line source and doublet and a surface source and doublet can all be expressed in terms of a point source, only those equations of amplitude function and induced velocity components of a point source are given.

WAVE AMPLITUDE FUNCTIONS OF A POINT SOURCE

The gravity waves created by a point source with a steady motion under a free surface have two parts:

$$\zeta(x,y) = \zeta_w(x,y) + \zeta_l(x,y)^* \quad (1)$$

*The coordinate systems are assumed to move with the ship, with the z-axis vertically upward, $z = 0$ on still-water surface, and the x-axis opposite to the ship's course.

where $\zeta_w(x,y)$ is the free-wave pattern
 $\zeta_l(x,y)$ is the local disturbance

The free-wave pattern is the cause of wave resistance; the local disturbance has nothing to do with the transfer of the wave energy.

Sir Thomas H. Havelock's papers treated a free-wave pattern as a resultant of the "elementary waves," and obtained the following extremely simple and elegant relationship between the elementary waves and the wave-making resistance. For a moving point source located at a point (ξ, η, ζ) , the free surface wave elevation can be expressed in the x-y-z coordinate system as

$$\zeta_w(x,y) = \frac{M \cdot K_0}{\pi \cdot U} \int_{-\frac{\pi}{2}}^{\alpha} \sec^3 \theta \cdot e^{-k_0 \cdot \zeta} \cdot \sec^2 \theta \cdot \cos R \cdot d\theta \quad (2)$$

where $R = k_0 \sec^2 \theta \cdot [(x - \xi) \cdot \cos \theta + (y - \eta) \cdot \sin \theta]$
 $K_0 = g/V^2$
 $M =$ Source strength
 $U =$ Speed of advance
 $\theta =$ Angle between wave direction and x-axis
 $\alpha = \tan^{-1} (-x/y)$

Introducing

$$R_0 = X \cdot \cos \theta + y \cdot \sin \theta \quad (3)$$

$$S = \xi \cdot \cos \theta + \eta \cdot \sin \theta \quad (4)$$

we can write

$$R = k_0 \cdot \sec^2 \theta \cdot (R_0 - S) \quad (5)$$

and

$$\begin{aligned} \cos R = & \cos (k_0 \cdot \sec^2 \theta \cdot S) \cdot \cos (k_0 \cdot \sec^2 \theta \cdot R_0) \\ & + \sin (k_0 \cdot \sec^2 \theta \cdot S) \cdot \sin (k_0 \cdot \sec^2 \theta \cdot R_0) \end{aligned} \quad (6)$$

From equations (2) and (6) we have

$$\begin{aligned} \zeta_w(x,y) = & \int_{-\pi/2}^{\alpha} A_c(\theta, \xi, \zeta) \cdot \cos (K_0 \cdot \sec^2 \theta \cdot R_0) \cdot d\theta \\ & + \int_{-\pi/2}^{\alpha} A_s(\theta, \xi, \zeta) \cdot \sin (K_0 \cdot \sec^2 \theta \cdot R_0) \cdot d\theta \end{aligned} \quad (7)$$

$$\text{where } A_c(\theta, \xi, \zeta) = \frac{M \cdot K_0}{\pi \cdot U} \cdot \sec^3 \theta \cdot e^{k_0 \cdot \zeta \cdot \sec^2 \theta} \cdot \cos(k_0 \cdot \sec^2 \theta \cdot S)$$

$$A_s(\theta, \xi, \zeta) = \frac{M \cdot k_0}{\pi \cdot U} \cdot \sec^3 \theta \cdot e^{k_0 \cdot \zeta \cdot \sec^2 \theta} \cdot \sin(k_0 \cdot \sec^2 \theta \cdot S)$$

Since R_0 is the distance between the point (x,y) and the origin, the free-wave system $\zeta_w(x,y)$ as shown by Equation (7) consists of two components: namely, a cosine-wave system with an amplitude function $A_c(\theta, \xi, \zeta)$, and a sine-wave system with an amplitude function $A_s(\theta, \xi, \zeta)$.

The computation of the wavemaking resistance for a surface or a line singularity distribution is based on the results of a point singularity moving underneath a free surface. For a moving point source located at a point (ξ, η, ζ) , a three-dimensional surface-wave system is created.

Havelock obtained the following general expression for wavemaking resistance in regard to a point source:

$$R_w = \pi \cdot \rho \cdot U^2 \cdot \int_0^{\pi/2} [A_c(\theta, \xi, \zeta)]^2 + [A_s(\theta, \xi, \zeta)]^2 \cdot \cos^3 \theta \cdot d\theta \quad (8)$$

where ρ is the water density.

VELOCITY COMPONENTS OF A POINT SOURCE

When the singularity distribution representing a hull form is known, the hull geometry can be obtained by tracing a number of streamlines. These streamlines define a closed stream surface to approximate the hull geometry. Each streamline is determined from a set of first-order differential equations

$$\frac{dy}{dx} = \frac{v}{U + u}$$

$$\frac{dz}{dx} = \frac{w}{U + u}$$

where U is the uniform stream velocity, and u , v , and w are the induced velocity components resulting from a given singularity distribution. Since the induced velocity components of a given singularity distribution can be derived from point sources alone, only the expressions needed for computing the induced velocity components for a point source will be given here. Theoretically, the induced velocity components of a point source should take into consideration the free surface effects. However, at the present time it is only practical to trace streamlines under the assumption that the free surface is a rigid wall. This is equivalent to assuming a double model in an infinite fluid without a free surface. Under the rigid wall condition, another point source is introduced as the mirror image for each point source under a free surface. Thus, the velocity potential of a point source under a free surface can be derived as follows:

$$\phi = \frac{M}{4\pi \cdot r}$$

where M = point source strength

$$r = \sqrt{(x - \xi)^2 + (y - \eta)^2 + (z - \zeta)^2}$$

The induced velocity components are as follows

$$u = -\frac{M \cdot (x - \xi)}{4\pi \cdot r^3} \quad (9)$$

$$v = -\frac{M \cdot (y - \eta)}{4\pi \cdot r^3}$$

$$w = -\frac{M \cdot (z - \zeta)}{4\pi \cdot r^3}$$

III. APPLICATION OF THE THEORY

Michell's thin-ship wavemaking resistance theory rests on two basic assumptions that limit its usefulness for the design of practical hull forms: The first is that the ship is thin and the free-surface wave slope is small; the second is that no viscosity effects exist. Although no satisfactory method for dealing with viscosity effects has yet been devised, ways have been found for dealing with the thin-ship assumption.

For a thin ship, the flow over the ship's surface is essentially two-dimensional, so that the hull form may be represented by a source distribution on a central plane and the density of the source distribution may be assumed to be proportional to the waterline slope at various depths. In reality, however, a practical hull form must have a beam-draft ratio greater than 2, and the flow around it will be highly three-dimensional.

Inui¹⁰ used an inverse method in which known singularity distributions were used as the starting point and the corresponding hull form geometry was obtained by tracing streamlines of the singularity distributions. These same singularity distributions were also used to compute the wavemaking resistance. He obtained close agreement between experimental results and theoretical predictions by building his experimental model to conform with the steam surface. The Pien program uses Inui's inverse method technique.

However, Inui's approach, too, has shortcomings: The hull form is nearly as impractical as Michell's—due to the small beam draft—and the streamline tracing must be performed under zero Froude number conditions. Although the Pien program must also operate under the zero Froude number conditions, since tracing streamlines at nonzero Froude number conditions is extremely difficult, the problem of the small beam-draft ratio has been solved. The Pien program uses a subsurface (η -surface) rather than a central plane as the location of the singularity distribution. This technique is explained in the following sections.

η -SURFACE AND COORDINATE SYSTEMS

In the past, the singularity distribution has customarily been located on the centerline plane of a ship, a fact which has resulted in the beam-draft ratio, B/T , always being less than 2.0. To obtain more practical B/T values—values greater than 2.0—the Pien program defines the singularity distribution on an η -surface as follows:

$$\eta = \pm f(\xi, \zeta) \quad (11)$$

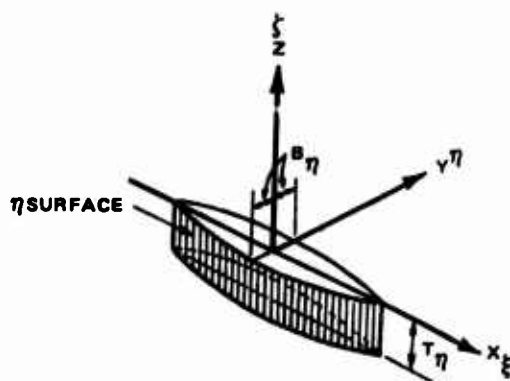


Figure 1 - Coordinate Systems and η -Surface for Location of Singularity Distributions

where ξ , η , and ζ are the coordinates of a rectangular coordinate system with the origin at the midship on the undisturbed free surface.

Let's define

$$\eta = B_{\eta} \cdot (1 - \xi^n) \quad (12)$$

where n is an even integer number and Equation (12) represents a vertical strut-like surface, its beam controlled by B_{η} and its waterline controlled by n .

To facilitate numerical integration, a waterline of an η -surface is further simplified by being represented as a number of first-degree

polynomials or straight-line segments. Figure 2 shows the forebody of the η -surface as approximated by three straight-line segments:

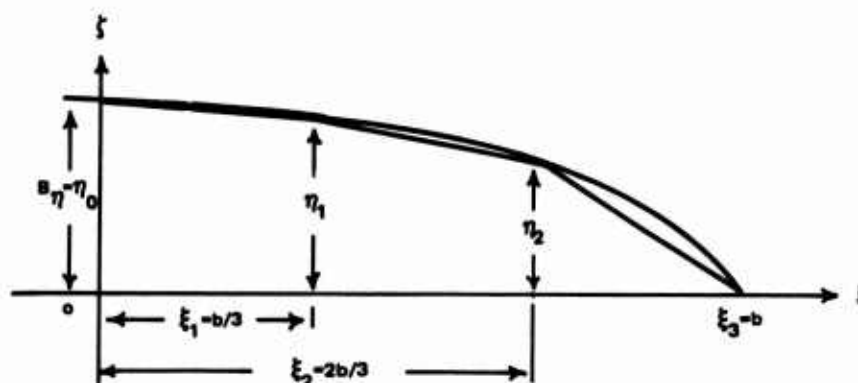


Figure 2 - Approximation of η -Surface for a Forebody by Three Straight-Line Segments

Each of the straight-line segments can be expressed by the following equation

$$\eta = B_{\eta} \cdot (A_1 \cdot \xi + A_2) \quad (13)$$

where $A_1 = \frac{\eta_k - \eta_{k+1}}{B_{\eta} \cdot (\xi_k - \xi_{k+1})}$

$$A_2 = \frac{\xi_k \cdot \eta_{k+1} - \xi_{k+1} \cdot \eta_k}{B_{\eta} \cdot (\xi_k - \xi_{k+1})}$$

The η -surface is then represented by K piecewise straight-line segments as

$$\eta = \frac{\eta_k - \eta_{k+1}}{\xi_k - \xi_{k+1}} \cdot \xi + \frac{\xi_k \cdot \eta_{k+1} - \xi_{k+1} \cdot \eta_k}{\xi_k - \xi_{k+1}} \quad (14)$$

where $k = 0, 1, 2 \dots K$

In the computer program, K is arbitrarily set less than 5, i.e., $1 \leq k \leq 4$.

By varying the parameters of the η -surface and the singularity distribution, a large family of different hull forms can be generated. By choosing the appropriate beam B_{η} and depth T_{η} of the η -surface, the required B/T value of a set of ship hull forms can be obtained.

SINGULARITY DISTRIBUTIONS

The singularity density distribution, defined as the singularity strength per unit area per unit velocity of a moving ship, $\frac{M}{U}$, can be expressed in the following way:

$$m(\xi, \zeta) = \sum_{i=0}^I \sum_{j=0}^J C_{ij} \cdot \xi^i \cdot \zeta^j \quad (15)$$

Equation (15) can then be expressed in any one of the following forms:

- As a Surface Source-Sink and Doublet

After arbitrarily choosing $I = 5$ and $J = 3$, the strength of a singularity distribution of surface source-sink or doublet can be expressed as

$$m_s(\xi, \zeta) = \sum_{i=0}^5 \sum_{j=0}^3 C_{ij} \cdot \xi^i \cdot \zeta^j \quad (16)$$

For the purpose of controlling the hull geometry, it is convenient to rewrite Equation (16) as follows:

$$\begin{aligned} m_s(\xi, \zeta) &= \sum_{j=0}^3 \left(\sum_{i=0}^5 C_{ij} \cdot \xi^i \right) \cdot \zeta^j \\ &= \sum_{j=0}^3 e_j \cdot \zeta^j \end{aligned} \quad (17)$$

$$\text{with } e_j = \sum_{i=0}^5 C_{ij} \cdot \xi^i \quad (18)$$

where $j = 0, 1, 2$ or 3

The singularity with e_0 of Equation (18) is independent of the depth. It contributes the most to ship displacement. The singularities with e_1 through e_3 are more influential on the lower waterlines and thus primarily affect the shape of the sections.

- As a Vertical Line Source-Sink and Doublet

The strength of a vertical line source-sink or doublet can be expressed as

$$m_v(\zeta) = \sum_{j=0}^3 C_j \cdot \zeta^j \quad (19)$$

- As a Horizontal Line Source-Sink and Doublet

The strength of a horizontal line source-sink or doublet can be expressed as

$$m_h(\xi) = \sum_{i=0}^5 C_i \cdot \xi^i \quad (20)$$

Both vertical and horizontal line source-sinks and doublets can be placed at any location along the ship length and depth that is desirable.

- As a Bottom Source-Sink and Doublet

(Not yet coded into the computer program)

To obtain a flat bottom, a bottom singularity distribution is introduced on a horizontal plane, η_b , slightly above the required flat-bottom location. The density distribution is determined so that the downward induced velocity on the flat bottom is zero. The strength of a bottom singularity distribution may be expressed in the following way:

$$m(\xi, \eta) = \sum_{i=0}^5 \sum_{j=0}^3 C_{ij} \cdot \xi^i \cdot \eta^j \quad (21)$$

To summarize, not only the point source-sink and doublet distributions but also the surface and line source-sink and doublet distributions are available for use in any combination with the particular η -surface chosen. Thus, a large family of practical hull forms can be represented.

PARAMETRIC REPRESENTATION OF SINGULARITY DISTRIBUTIONS

To improve control over the hull geometry, six parameters—E, B, V, Y, TE, and TM—are chosen for each half body (Figure 3).

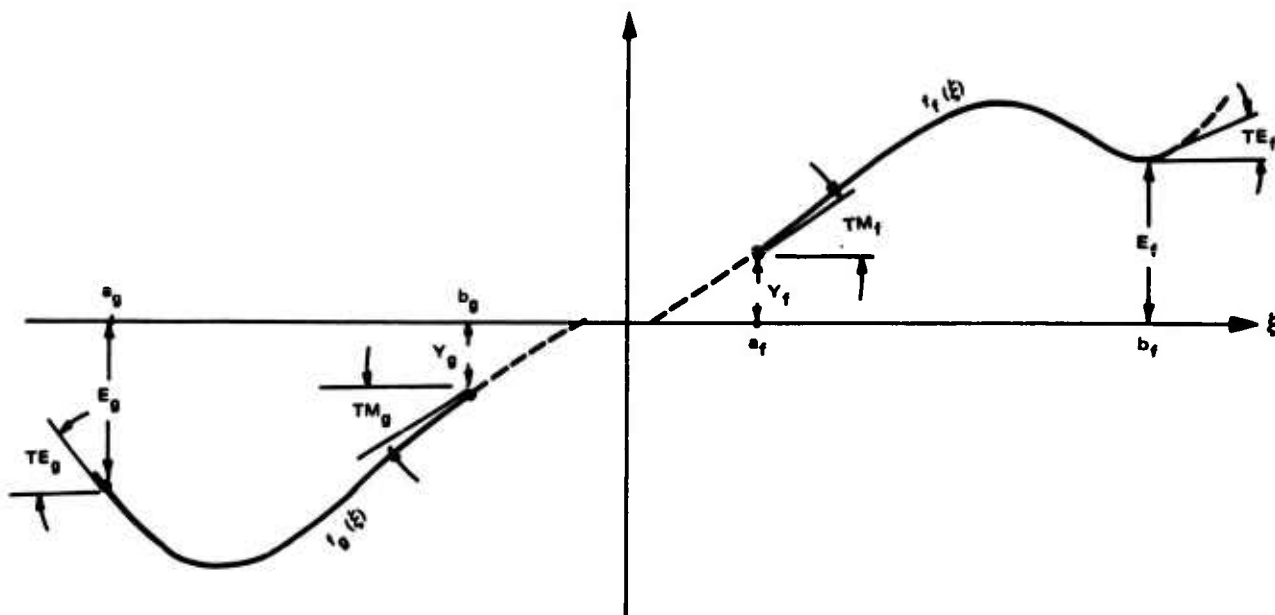


Figure 3 - Singularity Distribution on Forebody and Aftbody

In Figure 3, B_f is defined as the area under the curve $f_f(\xi)$ between the abscissas a_f and b_f , (and, similarly, B_g for the curve $f_g(\xi)$). V_f and V_g are the moments of the areas B_f and B_g , respectively, about the $\xi = 0$ axis. E_f and Y_f are function values of $f_f(\xi)$ at $\xi = b_f$, and $\xi = a_f$, respectively. TE_f and TM_f are the slopes at points b_f and a_f .

For surface source-sink and horizontal-line source-sink, E and TE are grossly related to the entrance angle of the waterline; B to the midship section area; V to the displacement volume; and Y and TM to the parallel middle body. For the surface doublet and horizontal-line doublet, V is related to the center of buoyancy, and B to the displacement volume.

These six parameters are related to the coefficients of the forebody (Equation (15)) in the following way:

$$\begin{aligned}
 e_j(b_f) &= \sum_{i=0}^5 C_{ij} \cdot b_f^i &= (E_f)_j \\
 \int_{a_f}^{b_f} e_j(\xi) \cdot d\xi &= \sum_{i=0}^5 \frac{1}{i+1} C_{ij} \cdot (b_f^{i+1} - a_f^{i+1}) &= (B_f)_j \\
 \int_{a_f}^{b_f} \xi \cdot e_j(\xi) \cdot d\xi &= \sum_{i=0}^5 \frac{1}{i+2} C_{ij} \cdot (b_f^{i+2} - a_f^{i+2}) &= (V_f)_j \\
 e_j(a_f) &= \sum_{i=0}^5 C_{ij} \cdot a_f^i &= (Y_f)_j \\
 \left. \frac{\partial e_j(\xi)}{\partial \xi} \right|_{\xi=b_f} &= \sum_{i=0}^5 i \cdot C_{ij} \cdot b_f^{i-1} &= (TE_f)_j \\
 \left. \frac{\partial e_j(\xi)}{\partial \xi} \right|_{\xi=a_f} &= \sum_{i=0}^5 i \cdot C_{ij} \cdot a_f^{i-1} &= (TM_f)_j
 \end{aligned} \tag{22}$$

where $j = 0, 1, 2, \text{ or } 3$

Equation (22) can then be written in a matrix form as shown in Equation (23). For ease of referencing, the left-hand portion of the matrix representation is noted as Matrix (23a); the middle portion as Matrix (23b); and the right-hand portion as Matrix (23c).

(23a) (23b) (23c)

$$[P]_j = [Q] \cdot [C]_j \tag{23}$$

where $j = 0, 1, 2, \text{ or } 3,$

$$\text{and } [P]_j = \begin{bmatrix} E_f \\ B_f \\ V_f \\ Y_f \\ TE_f \\ TM_f \end{bmatrix}_j \quad \text{and } [C]_j = \begin{bmatrix} C_0 \\ C_1 \\ C_2 \\ C_3 \\ C_4 \\ C_5 \end{bmatrix}_j$$

The elements q_{ki} of $[Q]$ are:

$$\begin{aligned} q_{0i} &= b_f^i \\ q_{1i} &= \frac{1}{i+1} (b_f^{i+1} - a_f^{i+1}) \\ q_{2i} &= \frac{1}{i+2} (b_f^{i+2} - a_f^{i+2}) \\ q_{3i} &= a_f^i \\ q_{4i} &= i \cdot b_f^{i-1} \\ q_{5i} &= i \cdot a_f^{i-1} \end{aligned}$$

with $i = 0, 1, 2, 3, 4$, and 5

Since the determinant of $[Q]$ will not be zero, $[Q]$ can be inverted to $[Q]^{-1}$. For later referencing, $[Q]^{-1}$ will be referred to as Matrix [24].

We can write

$$[C]_j = [Q]^{-1} \cdot [P]_j \quad (25)$$

The expressions of Equations (22) through (25) apply to the forebody. The aftbody can be expressed in a similar manner.

WAVE AMPLITUDE FUNCTIONS

With density distributions known and the η -surface given, the wave amplitude functions $A_c(\theta, \xi, \zeta)$ and $A_s(\theta, \xi, \zeta)$ can be obtained by a surface integration over the singularity distribution area. The η -surface is symmetrical with respect to $\eta = 0$. One half of the distribution is on the positive side of the η -surface and the other half is on the negative side. For the positive side, using Equation (7), we have

$$\begin{aligned} A_c(\theta, \xi, \zeta) &= \frac{1}{2} \cdot \frac{M \cdot K_0}{U \cdot \pi} \cdot \sec^3 \theta \cdot e^{-k_0 \cdot \zeta \cdot \sec^2 \theta} \cdot \cos(K_0 \cdot \xi \cdot \sec \theta \\ &\quad + K_0 \cdot \eta \cdot \tan \theta \cdot \sec \theta) \\ &= \frac{1}{2} \cdot m \cdot \frac{K_0}{\pi} \cdot \sec^3 \theta \cdot e^{-k_0 \cdot \zeta \cdot \sec^2 \theta} \cdot \cos(F_1 \cdot \xi + F_2 \cdot \eta) \end{aligned} \quad (26)$$

$$\text{where } F_1 = K_0 \cdot \sec \theta$$

$$F_2 = K_0 \cdot \sec \theta \cdot \tan \theta$$

For the negative side, using Equation (7), we have

$$A_s(\theta, \xi, \zeta) = \frac{1}{2} \cdot m \cdot \frac{K_0}{\pi} \cdot \sec^3 \theta \cdot e^{-k_0 \cdot \zeta \cdot \sec^2 \theta} \cdot \cos(F_1 \cdot \xi - F_2 \cdot \eta) \quad (27)$$

Combining the equations of (26) and (27), we get the amplitude function of a cosine elementary wave system ranging from $-\pi/2$ to $\pi/2$.

$$\begin{aligned} A_c(\theta, \xi, \zeta) &= \frac{1}{2} \cdot m \cdot \frac{K_0}{\pi} \cdot \sec^3 \theta \cdot e^{-k_0 \cdot \zeta \cdot \sec^2 \theta} \cdot \cos(F_1 \cdot \xi + F_2 \cdot \eta) \\ &\quad + \frac{1}{2} \cdot m \cdot \frac{K_0}{\pi} \cdot \sec^3 \theta \cdot e^{-k_0 \cdot \zeta \cdot \sec^2 \theta} \cdot \cos(F_1 \cdot \xi - F_2 \cdot \eta) \\ &= \frac{1}{2} \cdot m \cdot \frac{K_0}{\pi} \cdot \sec^3 \theta \cdot e^{-k_0 \cdot \zeta \cdot \sec^2 \theta} [\cos(F_1 \cdot \xi + F_2 \cdot \eta) \\ &\quad + \cos(F_1 \cdot \xi - F_2 \cdot \eta)] \\ &= m \cdot \frac{K_0}{\pi} \cdot \sec^3 \theta \cdot e^{-k_0 \cdot \zeta \cdot \sec^2 \theta} \cdot \cos(F_1 \cdot \xi) \cdot \cos(F_2 \cdot \eta) \end{aligned} \quad (28)$$

After integration over the distribution surface, we have

$$\begin{aligned}
 A_c(\theta) &= \sum_{i=0}^I \sum_{j=0}^J C_{ij} \cdot \frac{k_0}{\pi} \cdot \sec^3 \theta \int_{-T_n}^0 \zeta^j \cdot e^{-k_0 \cdot \zeta \cdot \sec^2 \theta} d\zeta \\
 &\quad \cdot \int_a^b \xi^i \cdot \cos(F_1 \cdot \xi) \cdot \cos(F_2 \cdot \eta) \cdot d\xi \\
 &= \frac{k_0}{\pi} \cdot \sec^3 \theta \cdot \sum_{i=0}^I \sum_{j=0}^J C_{ij} \cdot Z^j \cdot \chi_c^i
 \end{aligned} \tag{29}$$

where

$$Z^j = \int_{-T_n}^0 \zeta^j \cdot e^{-k_0 \cdot \zeta \cdot \sec^2 \theta} \cdot d\zeta \tag{30}$$

$$\chi_c^i = \int_a^b \xi^i \cdot \cos(F_1 \cdot \xi) \cdot \cos(F_2 \cdot \eta) \cdot d\xi \tag{31}$$

Likewise, for the sine amplitude functions over the range of $-\pi/2$ to $\pi/2$, we have

$$\begin{aligned}
 A_s(\theta) &= m \cdot \frac{k}{\pi} \cdot \sec^3 \theta \cdot e^{-k_0 \cdot \zeta \cdot \sec^2 \theta} \cdot \sin(F_1 \cdot \xi) \cdot \cos(F_2 \cdot \eta) \\
 &= \frac{k_0}{\pi} \cdot \sec^3 \theta \cdot \sum_{i=0}^I \sum_{j=0}^J C_{ij} \cdot Z^j \cdot \chi_s^i
 \end{aligned} \tag{32}$$

$$\text{where } \chi_s^i = \int_a^b \xi^i \cdot \sin(F_1 \cdot \xi) \cdot \cos(F_2 \cdot \eta) \cdot d\xi \tag{33}$$

The representations of the wave amplitudes for the various singularity distributions are derived in the following ways:

● Surface Source-Sink

By substituting Equation (13) into Equation (31), we have for the k th line segment (see Figure 2)

$$\begin{aligned} (X_c^i)_{ss} &= \int_{\xi_k}^{\xi_{k+1}} \xi^i \cdot \cos(F_1 \cdot \xi) \cdot \cos\{F_2 \cdot [B_n \cdot (A_1 \cdot \xi + A_2) + d]\} d\xi \\ &= \int_{\xi_k}^{\xi_{k+1}} \xi^i \cdot \cos(F_1 \cdot \xi) \cdot \cos(H \cdot \xi + G) \cdot d\xi \end{aligned} \quad (34)$$

where $H = F_2 \cdot B_n \cdot A_1$

$G = F_2 \cdot (B_n \cdot A_2 + d)$

$d = \text{distance from centerplane to } \zeta - \xi \text{ plane}$

$$\begin{aligned} (X_c^i)_{ss} &= \frac{1}{2} \int_{\xi_k}^{\xi_{k+1}} \xi^i \cdot \left\{ \cos[(H + F_1) \cdot \xi + G] + \cos[(H - F_1) \cdot \xi + G] \right\} d\xi \\ &= \frac{1}{2} \left\{ \cos G \cdot \int_{\xi_k}^{\xi_{k+1}} \xi^i \cdot \cos[(H + F_1) \cdot \xi] \cdot d\xi \right. \\ &\quad - \sin G \cdot \int_{\xi_k}^{\xi_{k+1}} \xi^i \cdot \sin[(H + F_1) \cdot \xi] \cdot d\xi \\ &\quad + \cos G \cdot \int_{\xi_k}^{\xi_{k+1}} \xi^i \cdot \cos[(H - F_1) \cdot \xi] \cdot d\xi \\ &\quad \left. - \sin G \cdot \int_{\xi_k}^{\xi_{k+1}} \xi^i \cdot \sin[(H - F_1) \cdot \xi] \cdot d\xi \right\} \end{aligned} \quad (35)$$

where $i = 0, 1, 2, 3, 4, \text{ or } 5$

Likewise, Equation (33) can be expanded into

$$\begin{aligned}
 (X_s^i)_{ss} = & \frac{1}{2} \left\{ \cos G \cdot \int_{\xi_k}^{\xi_{k+1}} \xi^i \cdot \sin [(H + F_1) \cdot \xi] \cdot d\xi \right. \\
 & + \sin G \cdot \int_{\xi_k}^{\xi_{k+1}} \xi^i \cdot \cos [(H + F_1) \cdot \xi] \cdot d\xi \\
 & - \cos G \cdot \int_{\xi_k}^{\xi_{k+1}} \xi^i \cdot \sin [(H - F_1) \cdot \xi] \cdot d\xi \\
 & \left. - \sin G \cdot \int_{\xi_k}^{\xi_{k+1}} \xi^i \cdot \cos [(H - F_1) \cdot \xi] \cdot d\xi \right\} \quad (36)
 \end{aligned}$$

where $i = 0, 1, 2, 3, 4, \text{ or } 5$

Solutions of Equations (35) and (36) can be obtained functionally. By summing the individual contributions of each line segment, the total value is obtained.

The amplitude functions of the cosine wave and sine wave follow:

$$(A_c(\theta))_{ss} = \frac{K_0}{\pi} \cdot \sec^3 \theta \cdot \sum_{i=0}^5 \sum_{j=0}^3 C_{ij} \cdot Z^j \cdot (X_c^i)_{ss} \quad (37)$$

$$(A_s(\theta))_{ss} = \frac{K_0}{\pi} \cdot \sec^3 \theta \cdot \sum_{i=0}^5 \sum_{j=0}^3 C_{ij} \cdot Z^j \cdot (X_s^i)_{ss} \quad (38)$$

● Surface Doublet

By partially differentiating Equation (29) with respect to ξ and η , the amplitude function of a cosine wave can be obtained.

$$(A_c(\theta))_{sd} = \frac{\partial(A_c(\theta))}{\partial \xi} \cdot XD + \frac{\partial(A_c(\theta))}{\partial \eta} \cdot YD$$

$$\begin{aligned}
&= \frac{k_0}{\pi} \cdot \sec^3 \theta \cdot \sum_{i=0}^I \sum_{j=0}^J C_{ij} \cdot Z^j \cdot \left(\frac{\partial \chi_c^i}{\partial \xi} \cdot XD + \frac{\partial \chi_c^i}{\partial \eta} \cdot YD \right) \\
&= \frac{k_0}{\pi} \cdot \sec^3 \theta \cdot \sum_{i=0}^I \sum_{j=0}^J C_{ij} \cdot Z^j \cdot (\chi_c^i)_{sd} \quad (39)
\end{aligned}$$

where $(\chi_c^i)_{sd} = \frac{\partial \chi_c^i}{\partial \xi} \cdot XD + \frac{\partial \chi_c^i}{\partial \eta} \cdot YD$

$$\begin{aligned}
&= XD \int_a^b [-F_1 \cdot \xi^i \cdot \sin(F_1 \cdot \xi) + i \cdot \xi^{i-1} \cdot \cos(F_1 \cdot \xi)] \\
&\quad \cdot \cos(F_2 \cdot \eta) \cdot d\xi \\
&\quad - YD \int_a^b F_2 \cdot \xi^i \cdot \cos(F_1 \cdot \xi) \cdot \sin(F_2 \cdot \eta) \cdot d\xi \quad (40)
\end{aligned}$$

where $i = 0, 1, 2, 3, 4, \text{ or } 5$.

XD and YD are the doublet components in the ξ - and η -directions, respectively, and ξ^i and ξ^{i-1} are the doublet strengths. When the direction of the doublet is pointing to the ξ -direction, we have

$$XD = 1.0$$

$$YD = 0.0$$

Likewise, the amplitude function of the sine wave is

$$\begin{aligned}
(A_s(\theta))_{sd} &= \frac{\partial(A_s(\theta))}{\partial \xi} \cdot XD + \frac{\partial(A_s(\theta))}{\partial \eta} \cdot YD \\
&= \frac{k_0}{\pi} \cdot \sec^3 \theta \cdot \sum_{i=0}^I \sum_{j=0}^J C_{ij} \cdot Z^j \cdot (\chi_s^i)_{sd} \quad (41)
\end{aligned}$$

$$\begin{aligned}
\text{where } (X_s^i)_{sd} = & XD \int_a^b [F_1 \cdot \xi^i \cdot \cos (F_1 \cdot \xi) + i \cdot \xi^{i-1} \cdot \sin (F_1 \cdot \xi)] \\
& \cdot \cos (F_2 \cdot \eta) \cdot d\xi \\
& - YD \int_a^b F_2 \cdot \xi^i \cdot \sin (F_1 \cdot \xi) \cdot \sin (F_2 \cdot \eta) \cdot d\xi \quad (42)
\end{aligned}$$

● Point Source-Sink

The wave amplitude functions of cosine and sine waves created by a traveling point source-sink can be deduced from Equations (28) and (32), respectively.

$$(A_c(\theta))_{ps} = \frac{k_0}{\pi} \cdot \sec^3 \theta \cdot m \cdot e^{-k_0 \cdot z \cdot \sec^2 \theta} \cdot \cos (F_1 \cdot \xi) \cdot \cos (F_2 \cdot \eta) \quad (43)$$

$$(A_s(\theta))_{ps} = \frac{k_0}{\pi} \cdot \sec^3 \theta \cdot m \cdot e^{-k_0 \cdot z \cdot \sec^2 \theta} \cdot \sin (F_1 \cdot \xi) \cdot \cos (F_2 \cdot \eta) \quad (44)$$

● Point Doublet

By partially differentiating Equations (43) and (44) with respect to ξ , the wave amplitude function will be given as

$$\begin{aligned}
(A_c(\theta))_{pd} = & \frac{k_0}{\pi} \cdot \sec^3 \theta \cdot m \cdot e^{-k_0 \cdot z \cdot \sec^2 \theta} [-F_1 \cdot \sin (F_1 \cdot \xi) \\
& \cdot \cos (F_2 \cdot \eta)] \quad (45)
\end{aligned}$$

$$\begin{aligned}
(A_s(\theta))_{pd} = & \frac{k_0}{\pi} \cdot \sec^3 \theta \cdot m \cdot e^{-k_0 \cdot z \cdot \sec^2 \theta} [F_1 \cdot \cos (F_1 \cdot \xi) \\
& \cdot \cos (F_2 \cdot \eta)] \quad (46)
\end{aligned}$$

• Vertical Line Source-Sink

From Equations (29) and (32), the amplitude functions of cosine and sine waves created by a vertical line source-sink may be written

$$(A_c(\theta))_{vs} = \frac{k_0}{\pi} \cdot \sec^3 \theta \cdot \sum_{j=0}^3 C_j \cdot \int_a^b \zeta^j \cdot e^{-k_0 \cdot \zeta \cdot \sec^2 \theta} \cdot d\zeta \cdot \cos(F_1 \cdot \xi) \cdot \cos(F_2 \cdot \eta) \quad (47)$$

$$(A_s(\theta))_{vs} = \frac{k_0}{\pi} \cdot \sec^3 \theta \cdot \sum_{j=0}^3 C_j \cdot \int_a^b \zeta^j \cdot e^{-k_0 \cdot \zeta \cdot \sec^2 \theta} \cdot d\zeta \cdot \sin(F_1 \cdot \xi) \cdot \cos(F_2 \cdot \eta) \quad (48)$$

• Vertical Line Doublet

By partially differentiating Equations (47) and (48) with respect to ξ , the amplitude functions of cosine and sine wave created by a vertical line doublet can be expressed

$$(A_c(\theta))_{vd} = \frac{k_0}{\pi} \cdot \sec^3 \theta \cdot \sum_{j=0}^3 C_j \cdot \int_a^b \zeta^j \cdot e^{-k_0 \cdot \zeta \cdot \sec^2 \theta} \cdot d\zeta \cdot [-F_1 \cdot \sin(F_1 \cdot \xi) \cdot \cos(F_2 \cdot \eta)] \quad (49)$$

$$(A_s(\theta))_{vd} = \frac{k_0}{\pi} \cdot \sec^3 \theta \cdot \sum_{j=0}^3 C_j \cdot \int_a^b \zeta^j \cdot e^{-k_0 \cdot \zeta \cdot \sec^2 \theta} \cdot d\zeta \cdot [F_2 \cdot \cos(F_1 \cdot \xi) \cdot \cos(F_2 \cdot \eta)] \quad (50)$$

• Horizontal Line Source-Sink

From Equations (29) and (32), the amplitude functions of cosine and sine waves created by a horizontal line source-sink may be written

$$(A_c(\theta))_{hs} = \frac{k_0}{\pi} \cdot \sec^3 \theta \cdot \sum_{i=0}^5 C_i \cdot e^{-k_0 \cdot z \cdot \sec^2 \theta} \cdot \int_a^b \xi^i \cdot \cos(F_1 \cdot \xi) \cdot \cos(F_2 \cdot \eta) \cdot d\xi \quad (51)$$

$$(A_s(\theta))_{hs} = \frac{k_0}{\pi} \cdot \sec^3 \theta \cdot \sum_{i=0}^5 C_i \cdot e^{-k_0 \cdot z \cdot \sec^2 \theta} \cdot \int_a^b \xi^i \cdot \sin(F_1 \cdot \xi) \cdot \cos(F_2 \cdot \eta) \cdot d\xi \quad (52)$$

• Horizontal Line Doublet

By partially differentiating Equations (51) and (52) with respect to ξ , the amplitude functions of cosine and sine wave created by a horizontal line doublet can be written

$$(A_c(\theta))_{hd} = \frac{k_0}{\pi} \cdot \sec^3 \theta \cdot \sum_{i=0}^5 C_i \cdot e^{-k_0 \cdot z \cdot \sec^2 \theta} \cdot [-F_1 \int_a^b \xi^i \cdot \sin(F_1 \cdot \xi) \cdot \cos(F_2 \cdot \eta) \cdot d\xi] \quad (53)$$

$$(A_s(\theta))_{hd} = \frac{k_0}{\pi} \cdot \sec^3 \theta \cdot \sum_{i=0}^5 C_i \cdot e^{-k_0 \cdot z \cdot \sec^2 \theta} \cdot [F_1 \int_a^b \xi^i \cdot \cos(F_1 \cdot \xi) \cdot \cos(F_2 \cdot \eta) \cdot d\xi] \quad (54)$$

COEFFICIENT OF WAVEMAKING RESISTANCE

Equation (8) indicates the wavemaking resistance of a ship. A non-dimensional coefficient, C_w , of wavemaking resistance is defined as

$$C_w = \frac{R_w}{1/2 \cdot \rho \cdot U^2 \cdot L^2} = \frac{k_0^2}{2\pi} \int_0^{\pi/2} (A_c(\theta)^2 + A_s(\theta)^2) \cdot \sec^3 \theta \cdot d\theta \quad (55)$$

where L is a suitably chosen length.

Since the free-surface disturbance is assumed to be small where the boundary condition is linearized in the theory, the total wave amplitudes $A_c(\theta)$ and $A_s(\theta)$ are the sums of those various singularity elements

$$\begin{aligned} A_c(\theta) = & (A_c(\theta))_{ss} + (A_c(\theta))_{sd} + (A_c(\theta))_{ps} + (A_c(\theta))_{pd} + (A_c(\theta))_{vs} \\ & + (A_c(\theta))_{vd} + (A_c(\theta))_{hs} + (A_c(\theta))_{hd} \end{aligned} \quad (56)$$

$$\begin{aligned} A_s(\theta) = & (A_s(\theta))_{ss} + (A_s(\theta))_{sd} + (A_s(\theta))_{ps} + (A_s(\theta))_{pd} + (A_s(\theta))_{vs} \\ & + (A_s(\theta))_{vd} + (A_s(\theta))_{hs} + (A_s(\theta))_{hd} \end{aligned} \quad (57)$$

OPTIMIZATION OF WAVEMAKING RESISTANCE

Calculating wavemaking resistance from a set of given singularity distributions has already been discussed in great detail. The Pien program's main objective is to obtain a set of singularity distributions that will generate a hull geometry which satisfies the design conditions and at the same time has good resistance performance.

Two approaches to optimization are possible. In one of these, a hull form is already known, and the singularity distribution representing the hull form can be modified. In this case, the objective is to improve the resistance performance in the following way, with or without specifying changes in the hull beam and displacement. The modifying singularity distribution (Equation (15)) is introduced, using only one value of j at a

time. The coefficient in the chosen modifying singularity distribution is determined by optimizing the wavemaking resistance of all of the singularity distributions within the constraints imposed on the modifying singularity distribution. When this has been done, the hull geometry is computed to determine whether or not it is practical. If it is, another modifying singularity distribution with a different j value is chosen and the optimization computation repeated. If it is not, a different set of constraints, or even a different modifying singularity distribution, is tried. If neither of these techniques provides a more satisfactory result, the result obtained before the current optimization attempt should be used.

The procedure just described derives a new design by improving an existing design through optimization. This method works well when the parent form to be used has a known singularity distribution. The new design is achieved by imposing appropriate constraints on the modifying singularity distributions of the parent form. When there is no appropriate parent form available, the entire singularity distribution for the new design has to be obtained from the optimization process. It is advisable to start the first step of the optimization procedure with a smaller displacement and beam than would likely be suitable. The modifying singularity distribution chosen for subsequent steps of the optimization and the constraints specified will then be guided by the result of the previous step. The optimization process used is as follows:

For a value of j corresponding to each term of Equation (15), there is a wave amplitude function $d_{ij} \cdot Z^j \cdot X^i$. By applying Equations (30) and (31) an arbitrary wave amplitude function defined as

$$\sum_{i=0}^5 d_{ij} \cdot Z^j \cdot X^i \quad (58)$$

is introduced. This wave system is designed to partially eliminate the wave system generated by the existing wave amplitudes of the original singularity distributions (Equations (56) and (57)).

The six coefficients of Equation (58)

$$d_{ij} \quad i = 0, 1, 2, 3, 4, 5 \quad (59)$$

where $j = 0, 1, 2$, or 3 , are to be selected under a set of design constraints and by an optimization procedure.

Assume from Equations (55) and (58)

$$\begin{aligned} C_w &= \frac{k_0^2}{2\pi} \int_0^{\frac{\pi}{2}} \left[\left(\sum_{i=0}^5 d_{ij} \cdot z^j \cdot \chi_c^i + A_c(\theta) \right)^2 + \left(\sum_{i=0}^5 d_{ij} \cdot z^i \cdot \chi_s^j + A_s(\theta) \right)^2 \right] \\ &\quad \cdot \sec^3 \theta \cdot d\theta \\ &= \frac{k_0^2}{2} \int_0^{\frac{\pi}{2}} \left\{ \sum_{k=0}^5 \left[\sum_{i=0}^5 (d_{kj} \cdot d_{ij}) \cdot t_c^i \cdot t_c^k + 2 \cdot d_{kj} \cdot t_s^k \cdot A_s(\theta) \right] \right. \\ &\quad \left. + A_c(\theta) \right\} d\theta \\ &\quad + \frac{k_0^2}{2\pi} \int_0^{\frac{\pi}{2}} \left\{ \sum_{k=0}^5 \left[\sum_{i=0}^5 (d_{kj} \cdot d_{ij}) \cdot t_s^i \cdot t_s^k + 2 \cdot d_{kj} \cdot t_s^k \cdot A_s(\theta) \right] \right. \\ &\quad \left. + A_s(\theta) \right\} d\theta \quad (60) \end{aligned}$$

where A_s and A_c are free-wave amplitudes of the original singularity distribution and

$$\begin{aligned} t_c^i &= \int_0^{\frac{\pi}{2}} z^j \cdot \chi_c^i \cdot \sec^3 \theta \cdot d\theta \\ t_s^i &= \int_0^{\frac{\pi}{2}} z^j \cdot \chi_s^i \cdot \sec^3 \theta \cdot d\theta, \quad (61) \end{aligned}$$

where $j = 0, 1, 2$, or 3

The variables Z^j , x_c^i and x_s^i are defined in Equations (30), (31), and (33), respectively.

After the terms shown in the first integral of the expanded form of Equation (60) are expanded, they can be rearranged as a 7X7 matrix

$$[B]_j \quad (62)$$

where $j = 0, 1, 2$, or 3 and the elements b_{ki} of $[B]_j$ are

$$\begin{aligned} b_{0i} &= d_{0j} \cdot t_c^0 (d_{ij} \cdot t_c^i + A_c) \\ b_{1i} &= d_{1j} \cdot t_c^1 (d_{ij} \cdot t_c^i + A_c) \\ b_{2i} &= d_{2j} \cdot t_c^2 (d_{ij} \cdot t_c^i + A_c) \\ b_{3i} &= d_{3j} \cdot t_c^3 (d_{ij} \cdot t_c^i + A_c) \\ b_{4i} &= d_{4j} \cdot t_c^4 (d_{ij} \cdot t_c^i + A_c) \\ b_{5i} &= d_{5j} \cdot t_c^5 (d_{ij} \cdot t_c^i + A_c) \\ b_{6i} &= A_c (d_{ij} \cdot t_c^i + A_c) \end{aligned}$$

where $i = 0, 1, 2, 3, 4$, and 5 .

After separating the d_{ki} from each term, the remaining terms can be written as

$$\begin{bmatrix} t_c^0 (t_c^0 + A_c) & t_c^0 (t_c^1 + A_c) & . & . & . & . & t_c^0 (t_c^5 + A_c) \\ t_c^1 (t_c^0 + A_c) & t_c^1 (t_c^1 + A_c) & . & . & . & . & t_c^1 (t_c^5 + A_c) \\ . & . & . & . & . & . & . \\ . & . & . & . & . & . & . \\ . & . & . & . & . & . & . \\ A_c (t_c^0 + A_c) & A_c (t_c^1 + A_c) & . & . & . & . & A_c (t_c^5 + A_c) \end{bmatrix} \quad (63)$$

In a similar way, the terms of the second integral of Equation (60) are expanded and then rearranged as a 7X7 matrix form

$$[B]_j \quad (64)$$

The elements b_{ki} of $[B]_j$ are

$$\begin{aligned} b_{0i} &= d_{0j} \cdot t_s^0 (d_{ij} \cdot t_s^i + A_s) \\ b_{1i} &= d_{1j} \cdot t_s^1 (d_{ij} \cdot t_s^i + A_s) \\ b_{2i} &= d_{2j} \cdot t_s^2 (d_{ij} \cdot t_s^i + A_s) \\ b_{3i} &= d_{3j} \cdot t_s^3 (d_{ij} \cdot t_s^i + A_s) \\ b_{4i} &= d_{4j} \cdot t_s^4 (d_{ij} \cdot t_s^i + A_s) \\ b_{5i} &= d_{5j} \cdot t_s^5 (d_{ij} \cdot t_s^i + A_s) \\ b_{6i} &= A_s (d_{ij} \cdot t_s^i + A_s) \end{aligned}$$

where $i = 0, 1, 2, 3, 4, \text{ and } 5$.

After separating the d_{ki} from each term, the remaining terms can be written as

$$\begin{bmatrix} t_s^0 (t_s^0 + A_s) & t_s^0 (t_s^1 + A_s) & . & . & . & . & t_s^0 (t_s^5 + A_s) \\ t_s^1 (t_s^0 + A_s) & t_s^1 (t_s^1 + A_s) & . & . & . & . & t_s^1 (t_s^5 + A_s) \\ . & . & . & . & . & . & . \\ . & . & . & . & . & . & . \\ . & . & . & . & . & . & . \\ A_s (t_s^0 + A_s) & t_s (t_s^1 + A_s) & . & . & . & . & A_s (t_s^5 + A_s) \end{bmatrix} \quad (65)$$

The six coefficients defined in Equation (58) are the only unknowns of the Equation (60). These six numbers can be expressed parametrically as E, B, V, Y, TE, TM by Equation (22). An exponential random search method¹¹ was used to search for a minimum value of C_w by randomly varying the six parameters within the range of their search limits (or design constraints).

Equation (58), the added wave amplitude function, may be any one of the following singularity distributions in which j will have the value 0, 1, 2, or 3:

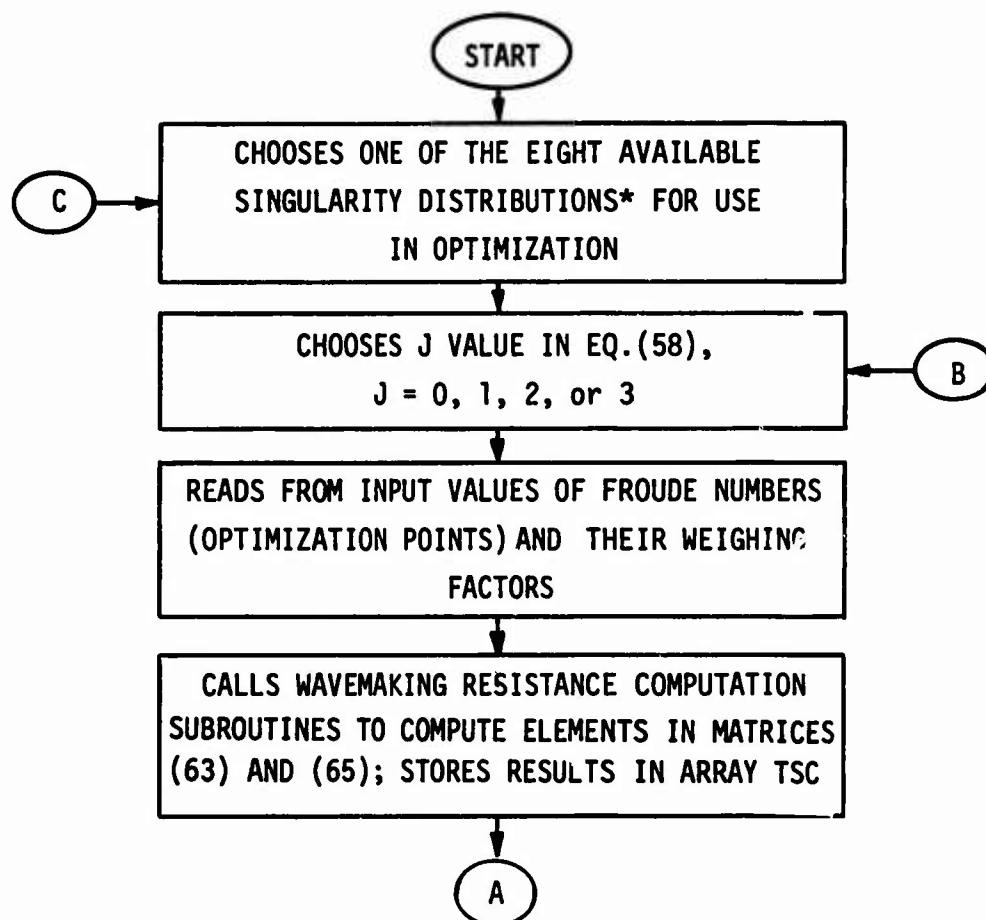
- surface source-sink
- surface doublet
- horizontal line source-sink
- horizontal line doublet

Singularity distribution of vertical line and bottom can easily be included in the optimization process at some future time.

After one optimization iteration, values of the six numbers (d_{ij})

just selected are lumped into $\sum_{i=0}^5 C_{ij}$ of A_C and A_S of Equation (60) to

form the new singularity distribution. The second optimization iteration is then begun, with $j = 0, 1, 2$, or 3 , to find another set of d_{ij} . This process will be repeated over and over until the value of C_W can no longer be reduced. Figure 4 shows the flow diagram of this optimization process.



* Singularity distributions available:

- Surface source-sink, forebody
- Surface Source-sink, aftbody
- Surface doublet, forebody
- Surface doublet, aftbody
- Horizontal line source-sink, forebody
- Horizontal line source-sink, aftbody
- Horizontal line doublet, forebody
- Horizontal line doublet, aftbody

Figure 4 - Flow Chart of the Optimization Process

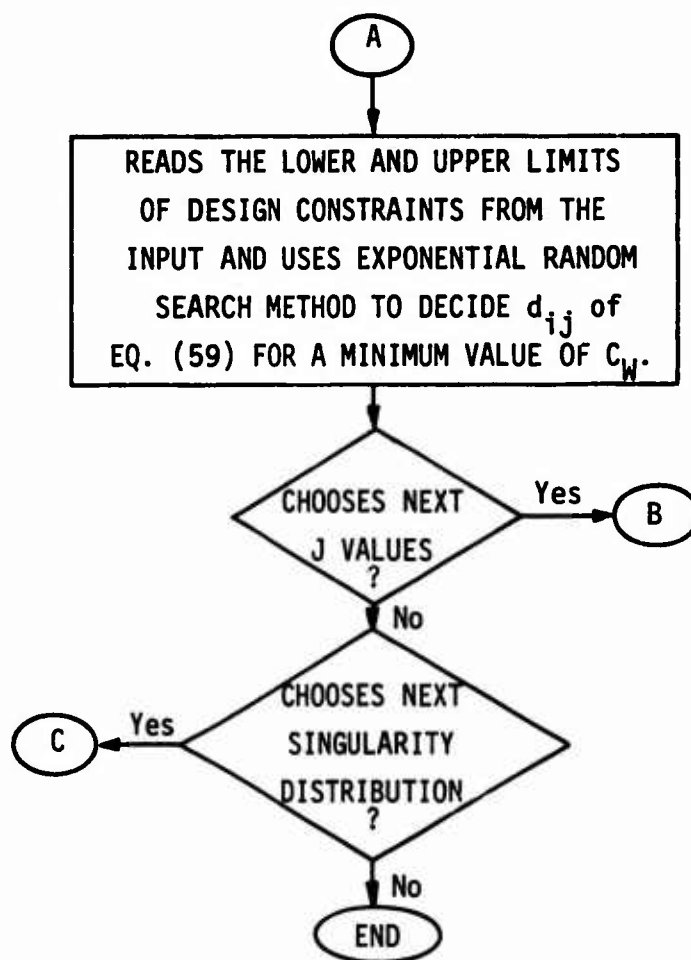


Figure 4 - Flow Chart of the Optimization Process - Continued

From the foregoing discussion, it is clear that a great deal of human judgment must be used in an optimization procedure. This judgment can be exercised most effectively in conjunction with interactive graphics. A graphics capability is being developed as a separate program.

STREAMLINE FUNCTIONS AND VELOCITY COMPONENTS

The velocity potential ϕ is given by the three dimensional singularity distribution regarding the distribution as symmetrical to the free surface. The velocity components u , v , and w are induced by the singularity distributions at any field point (x, y, z) .

• Surface Source Sink

$$\phi_{ss} = - \sum_{i=0}^5 \sum_{j=0}^3 C_{ij} \cdot \frac{U}{4\pi} \int_a^b \int_{-T_\eta}^{T_\eta} \frac{\xi^i \cdot \zeta^j \cdot d\xi \cdot d\zeta}{r} \quad (66)$$

$$u_{ss} = - \frac{\partial \phi_{ss}}{\partial x} = \sum_{i=0}^5 \sum_{j=0}^3 C_{ij} \cdot \frac{U}{4\pi} \int_a^b \int_{-T_\eta}^{T_\eta} \frac{(\xi-x) \cdot \xi^i \cdot \zeta^j \cdot d\xi \cdot d\zeta}{r^3} \quad (67)$$

$$v_{ss} = - \frac{\partial \phi_{ss}}{\partial y} = \sum_{i=0}^5 \sum_{j=0}^3 C_{ij} \cdot \frac{U}{4\pi} \int_a^b \int_{-T_\eta}^{T_\eta} \frac{(n-y) \cdot \xi^i \cdot \zeta^j \cdot d\xi \cdot d\zeta}{r^3} \quad (68)$$

$$w_{ss} = - \frac{\partial \phi_{ss}}{\partial z} = \sum_{i=0}^5 \sum_{j=0}^3 C_{ij} \cdot \frac{U}{4\pi} \int_a^b \int_{-T_\eta}^{T_\eta} \frac{(\zeta-z) \cdot \xi^i \cdot \zeta^j \cdot d\xi \cdot d\zeta}{r^3} \quad (69)$$

$$\text{where } r = \sqrt{(x-\xi)^2 + (y-n)^2 + (z-\zeta)^2}$$

• Surface Doublet

$$\phi_{sd} = - \sum_{i=0}^5 \sum_{j=0}^3 C_{ij} \cdot \frac{U}{4\pi} \int_a^b \int_{-T_\eta}^{T_\eta} \frac{R \cdot \xi^i \cdot \zeta^j \cdot d\xi \cdot d\zeta}{r^3} \quad (70)$$

$$u_{sd} = - \frac{\partial \phi_{sd}}{\partial x} = \sum_{i=0}^5 \sum_{j=0}^3 C_{ij} \cdot \frac{U}{4\pi} \int_a^b \int_{-T_\eta}^{T_\eta} \left[\frac{\xi}{r^3} - \frac{3(x-\xi) \cdot R}{r^5} \right] \cdot \xi^i \cdot \zeta^j \cdot d\xi \cdot d\zeta \quad (71)$$

$$v_{sd} = - \frac{\partial \phi_{sd}}{\partial y} = \sum_{i=0}^5 \sum_{j=0}^3 C_{ij} \cdot \frac{U}{4\pi} \int_a^b \int_{-T_n}^{T_n} \left[\frac{m}{r^3} - \frac{3(y-\eta) \cdot R}{r^5} \right] \cdot \xi^i \cdot \zeta^j \cdot d\xi \cdot d\zeta \quad (72)$$

$$w_{sd} = - \frac{\partial \phi_{sd}}{\partial z} = \sum_{i=0}^5 \sum_{j=0}^3 C_{ij} \cdot \frac{U}{4\pi} \int_a^b \int_{-T_n}^{T_n} \left[\frac{n}{r^3} - \frac{3(Z-\zeta) \cdot R}{r^5} \right] \cdot \xi^i \cdot \zeta^j \cdot d\xi \cdot d\zeta \quad (73)$$

where $R = (x-\xi) \cdot l + (y-\eta) \cdot m + (z-\zeta) \cdot n$

l, m and n are directional cosines

● Point Source-Sink

$$\phi_{ps} = - \frac{U}{4\pi} \cdot \frac{m}{r} \quad (74)$$

$$u_{ps} = - \frac{\partial \phi_{ps}}{\partial x} = \frac{U}{4\pi} \cdot \frac{m \cdot (x-\xi)}{r^3} \quad (75)$$

$$v_{ps} = - \frac{\partial \phi_{ps}}{\partial y} = \frac{U}{4\pi} \cdot \frac{m \cdot (y-\eta)}{r^3} \quad (76)$$

$$w_{ps} = - \frac{\partial \phi_{ps}}{\partial z} = \frac{U}{4\pi} \cdot \frac{m \cdot (z-\zeta)}{r^3} \quad (77)$$

where m is the strength of the source-sink divided by ship speed.

● Point Doublet

$$\phi_{pd} = - \frac{U}{4\pi} \cdot \frac{m \cdot (x-\xi)}{r^3} \quad (78)$$

$$u_{pd} = - \frac{\partial \phi_{pd}}{\partial x} = \frac{U}{4\pi} \cdot \left[\frac{m}{r^3} - \frac{3m \cdot (x-\xi)^2}{r^5} \right] \quad (79)$$

$$v_{pd} = - \frac{\partial \phi_{pd}}{\partial y} = \frac{U}{4\pi} \cdot \left[\frac{-3m \cdot (x-\xi) \cdot (y-\eta)}{r^5} \right] \quad (80)$$

$$w_{pd} = - \frac{\partial \phi_{pd}}{\partial z} = \frac{U}{4\pi} \cdot \left[\frac{-3m \cdot (x-\xi) \cdot (z-\zeta)}{r^5} \right] \quad (81)$$

where m is the strength of the doublet divided by ship speed.

● Vertical Line Source Sink

$$\phi_{vs} = - \sum_{j=0}^3 C_j \cdot \frac{U}{4\pi} \int_a^b \frac{\zeta^j \cdot d\zeta}{r} \quad (82)$$

$$u_{vs} = - \frac{\partial \phi_{vs}}{\partial x} = \sum_{j=0}^3 C_j \cdot \frac{U}{4\pi} \int_a^b \frac{(\xi-x) \cdot \zeta^j \cdot d\zeta}{r^3} \quad (83)$$

$$v_{vs} = - \frac{\partial \phi_{vs}}{\partial y} = \sum_{j=0}^3 C_j \cdot \frac{U}{4\pi} \int_a^b \frac{(\eta-y) \cdot \zeta^j \cdot d\zeta}{r^3} \quad (84)$$

$$w_{vs} = - \frac{\partial \phi_{vs}}{\partial z} = \sum_{j=0}^3 C_j \cdot \frac{U}{4\pi} \int_a^b \frac{(\zeta-z) \cdot \zeta^j \cdot d\zeta}{r^3} \quad (85)$$

where the line source-sink extends in depth from a to b and is located perpendicular to the $\xi-\eta$ plane.

● Vertical Line Doublet

$$\phi_{vd} = - \sum_{j=0}^3 C_j \cdot \frac{U}{4\pi} \int_a^b \frac{(x-\xi) \cdot \zeta^j \cdot d\zeta}{r^3} \quad (86)$$

$$u_{vd} = \frac{\partial \phi_{vd}}{\partial x} = \sum_{j=0}^3 C_j \cdot \frac{U}{4\pi} \int_a^b \left[\frac{1}{r^3} - \frac{3(x-\xi)^2}{r^5} \right] \cdot \zeta^j \cdot d\zeta \quad (87)$$

$$v_{vd} = - \frac{\partial \phi_{vd}}{\partial y} = \sum_{j=0}^3 C_j \cdot \frac{U}{4\pi} \int_a^b \frac{-3 (x-\xi) \cdot (y-\eta) \cdot \zeta^j \cdot d\zeta}{r^5} \quad (88)$$

$$w_{vd} = - \frac{\partial \phi_{vd}}{\partial z} = \sum_{j=0}^3 C_j \cdot \frac{U}{4\pi} \int_a^b \frac{-3 (x-\xi) \cdot (z-\zeta) \cdot \zeta^j \cdot d\zeta}{r^5} \quad (89)$$

where the line doublet extends in depth from a to b and is located perpendicular to the ξ - η plane.

● Horizontal Line Source-Sink

$$\phi_{hs} = - \sum_{i=0}^5 C_i \cdot \frac{U}{4\pi} \int_a^b \frac{\xi^i \cdot d\xi \cdot d\zeta}{r} \quad (90)$$

$$u_{hs} = - \frac{\partial \phi_{hs}}{\partial x} = \sum_{i=0}^5 C_i \cdot \frac{U}{4\pi} \cdot \int_a^b \frac{(\xi-x) \cdot \xi^i \cdot d\xi}{r^3} \quad (91)$$

$$v_{hs} = - \frac{\partial \phi_{hs}}{\partial y} = \sum_{i=0}^5 C_i \cdot \frac{U}{4\pi} \cdot \int_a^b \frac{(\eta-y) \cdot \xi^i \cdot d\xi}{r^3} \quad (92)$$

$$w_{hs} = - \frac{\partial \phi_{hs}}{\partial z} = \sum_{i=0}^5 C_i \cdot \frac{U}{4\pi} \cdot \int_a^b \frac{(\zeta-z) \cdot \xi^i \cdot d\xi}{r^3} \quad (93)$$

where the horizontal line source-sink extends in the x-direction from a to b and is located perpendicular to the η - ξ plane.

● Horizontal Line Doublet

$$\phi_{hd} = - \sum_{i=0}^5 C_i \cdot \frac{U}{4\pi} \int_a^b \frac{(x-\xi) \cdot \xi^i \cdot d\xi}{r^3} \quad (94)$$

$$u_{hd} = - \frac{\partial \phi_{hd}}{\partial x} = \sum_{i=0}^5 C_i \cdot \frac{U}{4\pi} \int_a^b \left[\frac{1}{r^3} - \frac{3 (x-\xi)^2}{r^5} \right] \cdot \xi^i \cdot d\xi \quad (95)$$

$$v_{hd} = - \frac{\partial \phi_{hd}}{\partial y} = \sum_{i=0}^5 C_i \cdot \frac{U}{4\pi} \int_a^b \frac{-3 (x-\xi) \cdot (y-\eta) \cdot \xi^i \cdot d\xi}{r^5} \quad (96)$$

$$w_{hd} = - \frac{\partial \phi_{hd}}{\partial z} = \sum_{i=0}^5 C_i \cdot \frac{U}{4\pi} \int_a^b \frac{-3 (x-\xi) \cdot (z-\zeta) \cdot \xi^i \cdot d\xi}{r^5} \quad (97)$$

where the line doublet extends in the x-direction from a to b and is located perpendicular to the η - ξ plane.

STREAMLINE TRACING

By introducing the velocity components derived in the previous section into Equation (10) and then integrating, we can obtain the streamlines of the flow. Equation (10) can be solved numerically by Range-Kutta methods when the starting points of the streamlines are known. To obtain a desired accuracy of the streamlines, however, the Kutta-Merson method of integrating the differential equations has been chosen. This method automatically regulates the step-length used in tracing streamlines so that small step-lengths are used in regions where there are extreme changes in curvature—such as close to the bow contour, for instance—and larger step-lengths are used in regions where the changes in u , v , and w are gradual.

To determine proper starting points for the streamlines, it has been found advantageous to determine the stagnation point on the bow contour and then to trace the bow contour streamline in the center plane above and below the stagnation point. Starting points for the streamlines can afterwards be chosen on the bow contour, slightly offset from the centerplane. The forebody is obtained by choosing an appropriate number of starting points and then tracing streamlines from the bow contour rearward.

IV. DESCRIPTION OF THE COMPUTER PROGRAM

PROGRAM STRUCTURE

Figure 5 shows the program structured as overlays. The program reads input data with overlay (1,0) in core. Then overlay (2,0) is brought into core to compute the wavemaking resistance from input singularity distributions. The wavemaking resistance may be optimized to obtain the new singularity distributions under a set of design constraints. At this stage, overlay (3,0) may be brought into core to replace overlay (2,0). Streamlines corresponding to the input or optimized singularity distributions can now be traced to see whether the ship hull form they represent is practical.

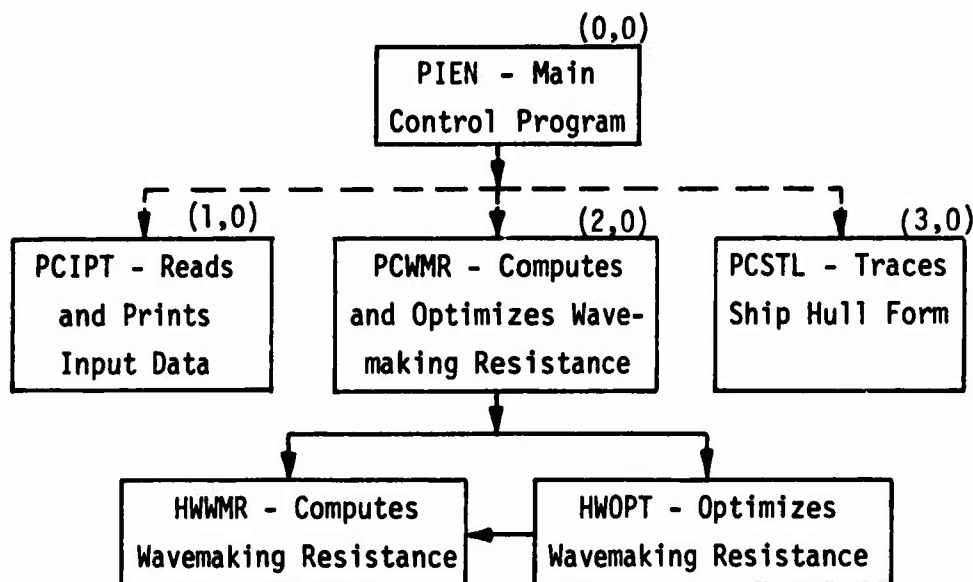
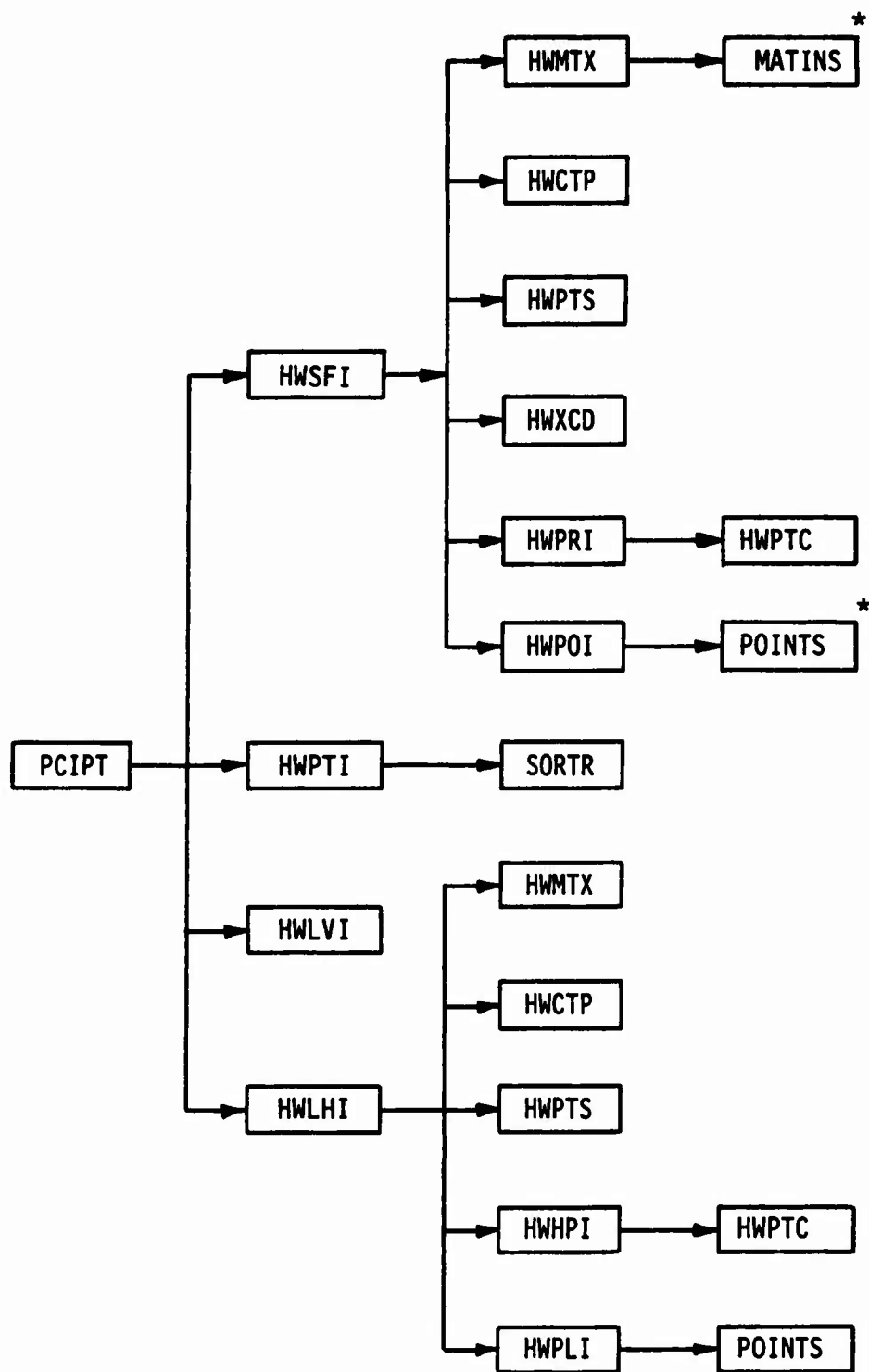


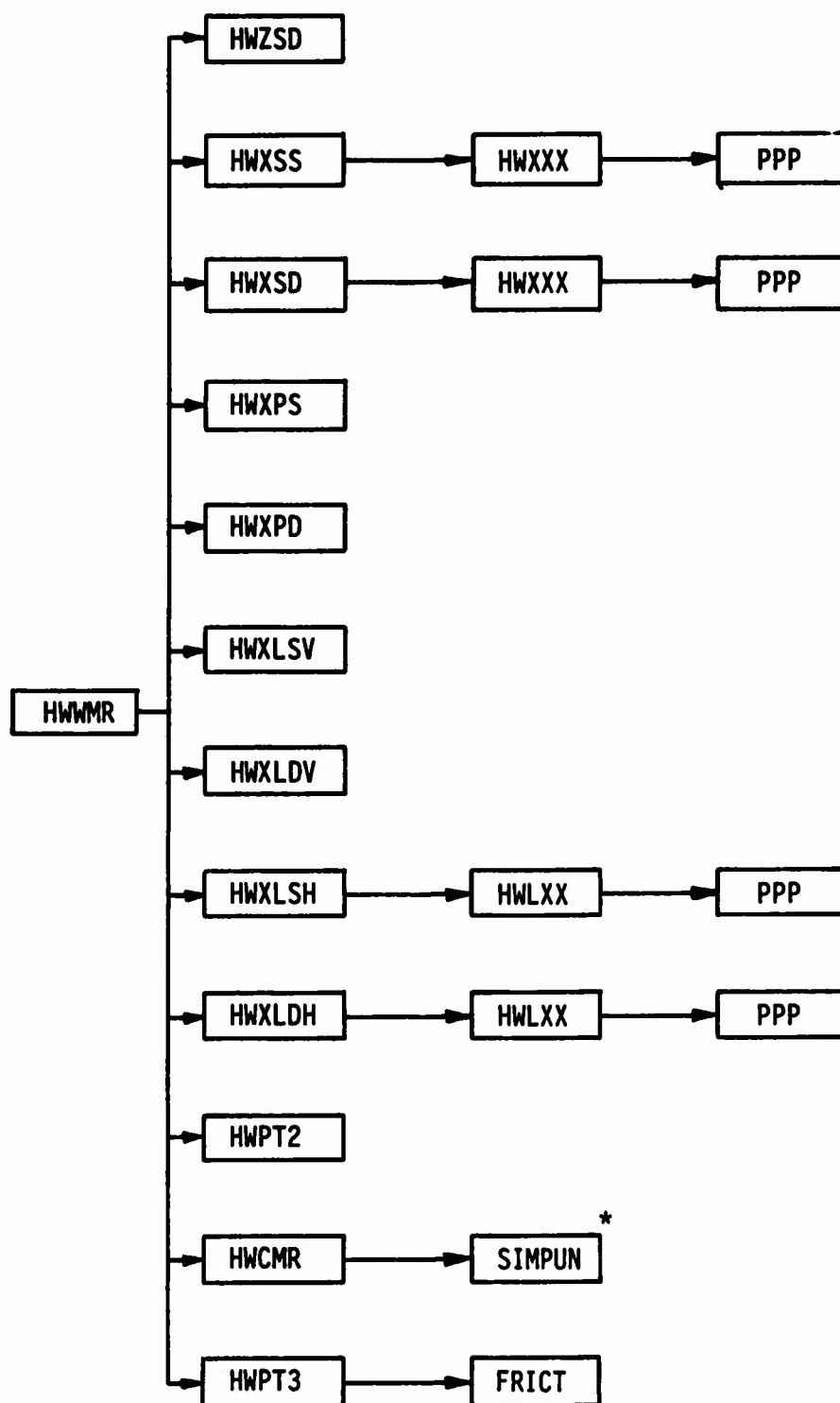
Figure 5 - Program Overlay Structure

Figures 6 through 9 which follow show the organization of programs within each overlay.



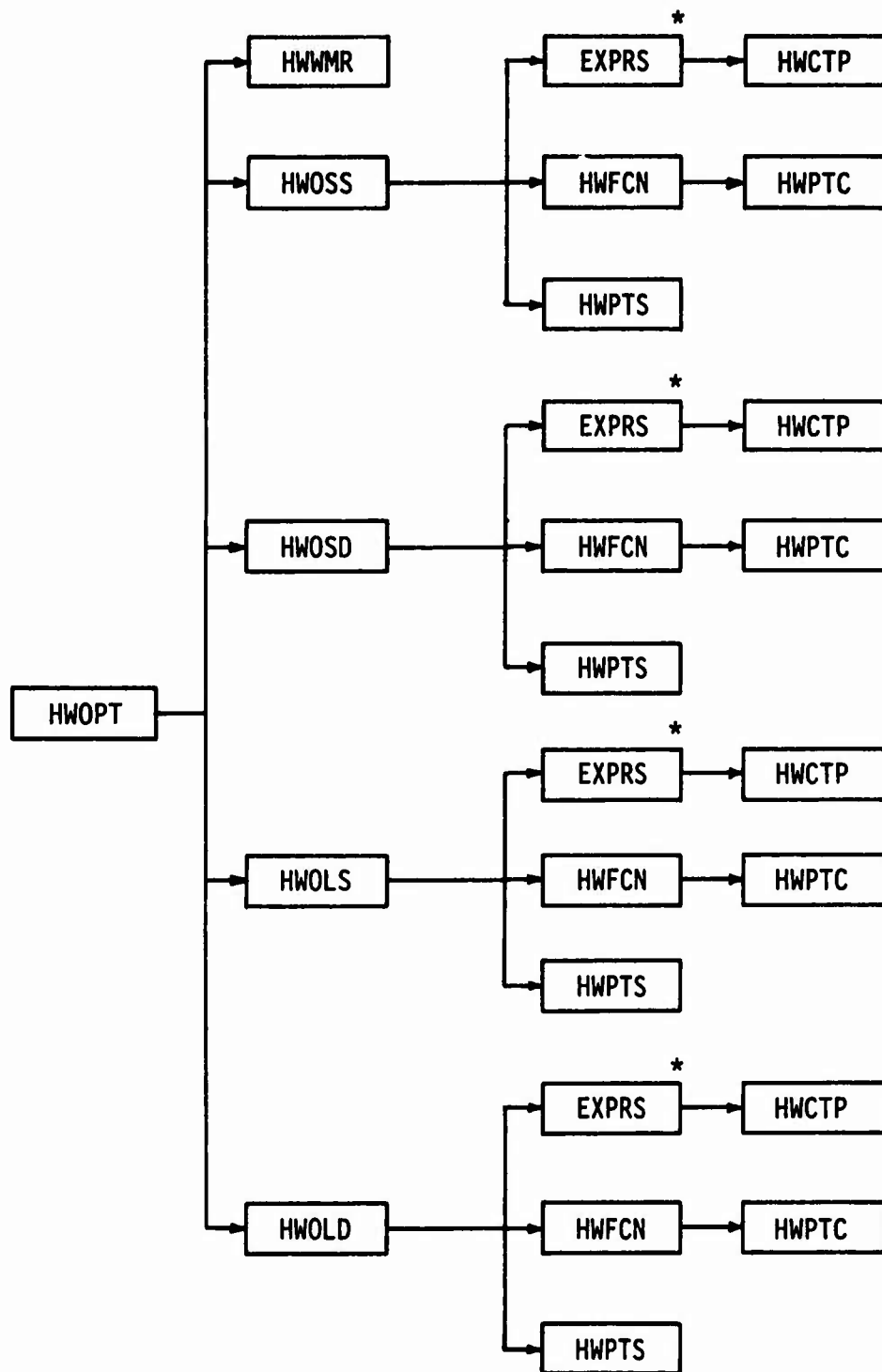
* NSRDC Library Subroutines.

Figure 6 - Block Diagram For (1,0) Overlay -
Input Data Processing



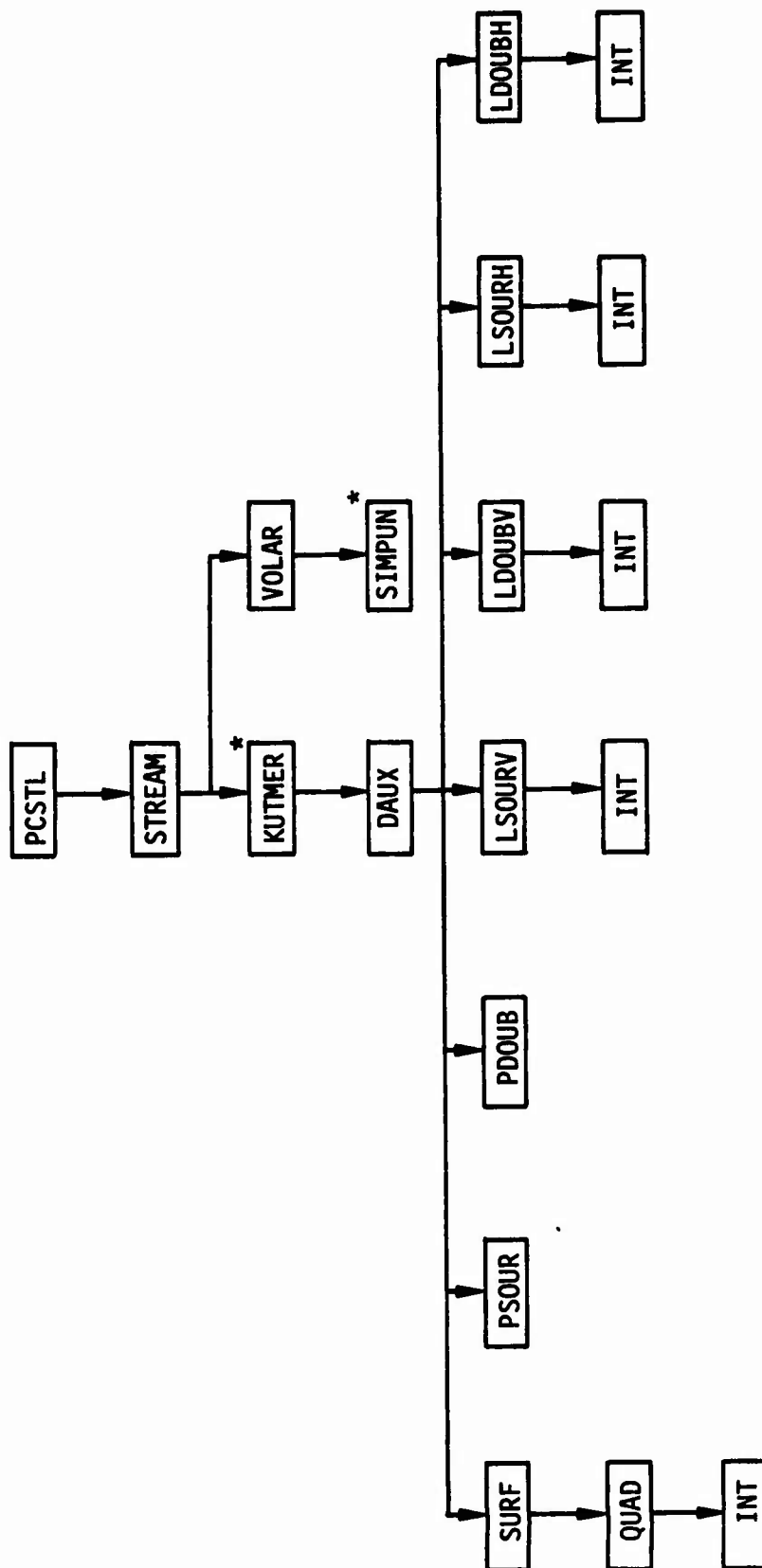
*NSRDC Library Subroutines

Figure 7 - Block Diagram for (2,0) Overlay -
Wavemaking Resistance Computation



*Subroutines described by Gray.¹¹

Figure 8 - Block Diagram for (2,0) Overlay -
Wavemaking Resistance Optimization



*NSRDC Library Subroutines.

Figure 9 - Block Diagram For (3,0) Overlay - Streamline Tracing

SUBROUTINE DESCRIPTIONS

The following pages contain detailed functional descriptions of the various subroutines of the Pien Wavemaking Resistance Computation Program. A complete alphabetical listing of the subroutines by overlay follows:

(0,0) Overlay	Page
PIEN	50

(1,0) Overlay	Page
HWCTP	51
HWHP1	52
HWLHI	53
HWLVI	54
HWMTX	55
HWPLI	56
HWPOI	57
HWPRI	58
HWPTC	59
HWPTI	60
HWPTS	61
HWSFI	62
HWXCD	63
PCIPT	64
SORTR	65

(2,0) Overlay	Page
(WRC)* FRICT	66
HWCMR	67
HWLXX	68
HWPT2	69
HWPT3	70
HWWMR	71
HWXLDH	72
HWXLDV	73
HWXLSH	74
HWXLSV	75
HWXPD	76
HWXPS	77
HWXSD	78
HWXSS	79
HWXXX	80
HWZSD	81
PCWMR	82
PPP	83
(WRO)**HWCTP	51
HWFCN	84
HWOLD	85
HWOLS	86
HWOPT	87
HWOSD	88
HWOSS	89
HWPTC	59
HWPTS	61

(3,0) Overlay	Page
DAUX	90
INT	91
LDOUBH	92
LDOUBV	93
LSOURH	94
LSOURV	95
PCSTL	96
PDOUB	97
PSOUR	98
QUAD	99
STREAM	100
SURF	101
VOLAR	102

* Wavemaking Resistance Computation

**Wavemaking Resistance Optimization

Preceding page blank

PROGRAM PIEN

Function:

This program is the main program in the (0,0) overlay.

Calling Format:

PROGRAM PIEN (OUTPUT, TAPE6=OUTPUT, INPUT, TAPE5=INPUT)

Detailed Description:

Program PIEN first initializes several arrays and then calls in the programs in the (1,0) overlay.

Subroutines Called:

PCIPT

SUBROUTINE HWCTP

Function:

This subroutine computes solutions of the six linear simultaneous equations.

Calling Format:

CALL HWCTP (L, SV, KP, D, R, PV)

Description of Parameters:

L	An indicator: = 1 The forebody = 2 The aftbody
SV(6)	Contains Matrix (23C)
KP	A printout indicator: ≠ 1 No printout = 1 Print array PV
D,R	D=a, R=b (Figure 3)
PV(6)	Contains Matrix (23a)

Detailed Description:

Subroutine HWCTP solves Equation (23). If the value in KP is 1, the program prints out the values of Matrix (23a).

Subroutines Called:

None

SUBROUTINE HWHPI

Function:

This routine reads input data in "point" form for singularity distribution of surface source-sink and doublets.

Calling Format:

CALL HWHPI (CLH, SCH, L)

Description of Parameters:

CLH(10,4) Refer to the description of CLSH or CLDH in Appendix A.

SCH(2) Scaling factors

L An indicator:
= 1 The forebody
= 2 The aftbody

Detailed Description:

Subroutine HWHPI reads in the strength of a singularity distribution in "point" form and then calls the POINTS subroutine to compute the coefficients of a 5th-degree polynomial which is an approximation based upon the "point" data.

Subroutine Called:

POINTS

SUBROUTINE HWLHI

Function:

This subroutine reads and prints the input data for horizontal source-sink and doublets.

Calling Format:

CALL HWLHI

Detailed Description:

Subroutine HWLHI reads in the integration interval for the singularity distribution, and then calls the HWMTX subroutine to compute Matrix (24) for both the fore and aftbody section. It then reads the strength of singularity distribution presented in one of three forms: as coefficients, as parameters, or as "points". If in parameter form, subroutine HWPLI is called; if in "point" form, subroutine HWHPI is called. The program writes out all of the input data read.

If $11 \leq KWR \leq 20$ or if $31 \leq KWR \leq 40$, the program prints only the input data contained in "COMMON" storage.

Subroutines Called:

HWCTP, HWMTX, HWHPI, HWPLI, HWPTS

SUBROUTINE HWLVI

Function:

This subroutine reads and prints input data for vertical line source-sinks and doublets.

Calling Format:

CALL HWLVI

Detailed Description:

Subroutine HWLVI reads in and prints out the CLSV and CLDV arrays which contain information pertaining to the vertical line source-sinks and doublets.

Subroutines Called:

None

SUBROUTINE HWMTX

Function:

Sets up six simultaneous linear equations and computes the inverse matrix for the coefficients of the equations.

Calling Format:

CALL HWMTX (L, CMS, D, R)

Description of Parameters:

L The index of the three-dimensional array CMS, ($1 \leq KL \leq 4$)
CMS(6,6,4) Refer to the description of CMH or CMS in Appendix A.
D,R D=a, R=b (See Figure 3)

Detailed Description:

HWMTX first fills the CMS array with Matrix (23b) for surface source-sink/doublet or horizontal line source-sink/doublet, then calls Subroutine MATINS to compute Matrix (24).

Subroutines Called:

MATINS

SUBROUTINE HWPLI

Function:

This subroutine reads input data in the parametric form for the horizontal source-sinks or doublets.

Calling Format:

CALL HWPLI (CLH, CMH, PV, SCH, L, K)

Description of Parameters:

CLH(10,4) Refer to description of CLSH or CLDH in Appendix A.

CMH(6,6,4) Refer to Appendix A.

PV(6,2,4) Contains Matrix (23a) for either the horizontal source-sink or the doublet.

SCH(2) Scaling factors

L An indicator:
= 1 The forebody
= 2 The aftbody

K An indicator:
= 0 Horizontal source-sink
= 2 Horizontal doublets

Detailed Description:

Subroutine HWPLI reads in six parameters of Matrix (23a) for horizontal source-sink or doublet and then calls HWPTC subroutine to convert the six parameters into coefficient form (Matrix (23c)).

Subroutine Called:

HWPTC

SUBROUTINE HWPOI

Function:

This routine reads input data in "point" form for singularity distribution of surface source-sink and doublets.

Calling Format:

CALL HWPOI (CES, SCS, L)

Description of Parameters:

CES (I,J,L) Refer to description of CESS or CESD in Appendix A.

SCS(4,2) Scaling factors

L An indicator:
 =1 The forebody
 =2 The aftbody

Detailed Description:

Subroutine HWPOI reads in the strength of a singularity distribution in "point" form and then calls the POINTS subroutine to compute the coefficients (Matrix (23c)) of a 5th-degree polynomial which is an approximation based upon the "point" data.

Subroutine Called:

POINTS

SUBROUTINE HWPRI

Function:

This subroutine reads input data in the parametric form for the surface source-sinks or doublets.

Calling Format:

CALL HWPRI (XS, CMS, CES, PV, SCS, L, K)

Description of Parameters:

XS(2,2) Refer to the description of XSS or XSD in Appendix A.

CMS(6,6,4) Refer to Appendix A.

CES(6,4,4) Refer to description of CESS or CESD in Appendix A.

PV(6,2,2) Contains Matrix (23a) for either the surface source-sink or the doublet.

SCS(4,2) Scaling factors

L An indicator:
= 1 The forebody
= 2 The aftbody

K An indicator:
= 0 Surface source-sink
= 2 Surface doublets

Detailed Description:

Subroutine HWPRI reads in six parameters of Matrix (23a) for surface source-sink or doublet and then calls HWPTC subroutine to convert the six parameters into coefficient form (Matrix (23c)).

Subroutine Called:

HWPTC

SUBROUTINE HWPTC

Function:

This subroutine converts solutions of a set of six simultaneous linear equations into coefficients.

Calling Format:

CALL HWPTC (L, PV, KP, D, R, SV, J, CMS)

Description of Parameters:

L An indicator:
 = 1 The forebody
 = 2 The aftbody

PV(6) Contains Matrix (23a)

KP A printout direction:
 ≠ 1 No printout
 = 1 Both parameters and coefficients of the six
 equations are to be printed

D,R D=a, R=b (See Figure 3).

SV(6) Contains Matrix (23c)

J Contains the value of j+1 of Equation (18)

CMS (6,6) Refer to description of CMS or CMH in Appendix A.

Detailed Description:

This subroutine solves Equation (25) using Matrices (24) and (23a). If the value in KP is 1, the program prints out the values of Matrices (23a) and (23c).

Subroutines Called:

None

SUBROUTINE HWPTI

Function:

This subroutine reads input data for point source-sink and doublet.

Calling Format:

CALL HWPTI

Detailed Description:

Subroutine HWPTI reads the scaling factors (PSL(I), I=1,5) for each group of point source-sinks or doublets, and scales each point source-sink or doublet as follows:

$$\text{PINS}(1,*) = \text{PINS}(1,*) * \text{PSL}(1) + \text{PSL}(5)$$
$$\text{PINS}(2,*) = \text{PINS}(2,*) * \text{PSL}(2)$$
$$\text{PINS}(3,*) = \text{PINS}(3,*) * \text{PSL}(3)$$
$$\text{PINS}(4,*) = \text{PINS}(4,*) * \text{PSL}(4)$$

It then calls Subroutine SORTR to sort the array PINS or PIND into descending order according to the ξ -value of each data point.

Subroutine Called:

SORTR

SUBROUTINE HWPTS

Function:

This routine interprets a 5th-degree polynomial equation.

Calling Format:

CALL HWPTS (L, SV, J, KPL)

Description of Parameters:

L	An indicator: = 1 The forebody = 2 The aftbody
SV(6)	Contains Matrix (23c)
J	Value of j+1 of Equation (18)
KPL	Not used

Detailed Description:

Subroutine HWPTS evaluates and prints out a 5th-degree polynomial (Equation (18)) for the interval $x = -1.3$ to $x = 1.3$ with increment size 0.1.

Subroutines Called:

None

SUBROUTINE HWSFI

Function:

This subroutine reads and prints the input data for surface source-sink and doublets.

Calling Format:

CALL HWSFI

Detailed Description:

Subroutine HWSFI reads in the variable defining the η -surface and the integration for the singularity distribution, and then calls the HWMTX subroutine to compute Matrix (24) for both the fore and aftbody sections. It then reads the strength of singularity distribution supplied in one of three forms: as coefficient, as parameters, or as "points". If the input data is in parameter form, the subroutine HWRPI is called; if in "point" form, the subroutine HWPOI is called. When the value in NIT is greater than one, the η -surface will be subdivided into NIT subsegments by calls to HWXCD. The program writes out all of the input data read.

If $11 \leq KWR \leq 20$ or if $31 \leq KWR \leq 40$, the program prints only the input data contained in COMMON storage.

Subroutines Called:

HWCTP, HWMTX, HWPOI, HWPRI, HWPTS, HWXCD

SUBROUTINE HWXCD

Function:

This subroutine approximates an n -surface by using a number of straight line segments.

Calling Format:

CALL HWXCD (\downarrow X1, \downarrow X2, \downarrow K1, \downarrow K2, \downarrow XD, \downarrow L)

Description of Parameters:

X1,X2	The beginning and the end of a straight line segment
K1	The number of the straight line segments ($1 \leq K1 \leq 4$)
K2	An indicator: = 1 Surface source-sink = 2 Surface doublet
XD	Distance between X1 and X2 ($X2 - X1$)
L	An indicator: = 1 The forebody = 2 The aftbody

Detailed Description:

Subroutine HWXCD computes A_1 and A_2 of Equation (13) and stores the results into the AAA and BBB arrays respectively. For description of arrays AAA and BBB, refer to Appendix A.

Subroutines Called:

None

SUBROUTINE PCIPT

Function:

This subroutine, the main controlling routine in the (1,0) overlay, acts as the executive program for input-data processing.

Calling Format:

CALL AETSKC(5HPCIPT)

Detailed Description:

Subroutine PCIPT reads in the printout titles, the ten calculation flags, the Froude numbers, and other variables. Depending upon the calculation-flag values, it may then call upon other subroutines to read input data for a surface source-doublet, a point source-doublet, a vertical-line source-doublet, or a horizontal-line source-doublet. It will then transfer control to PCWMR in the (2,0) overlay or to PCSTL in the (3,0) overlay, depending upon the value of the input parameter KWR.

Subroutines Called:

HWSFI, HWPTI, HWLVI, HWLHI, PCWMR, PCSTL

SUBROUTINE SORTR

Function:

This subroutine sorts an array into descending order.

Calling Format:

CALL SORTR(KP,PIN,NP)

Description of Parameters:

KP(100) The array PIN in its original order.
PIN(4,100) Refer to the description of PINS of PIND in Appendix A.
NP Refer to description of NPS of NPD in Appendix A.

Detailed Description:

Subroutine SORTR arranges the contents of the PIN array in a descending order according to the first element PIN(1,*) of the array.

Subroutines Called:

None

FUNCTION FRICT

Function:

This function computes the coefficient of frictional resistance.

Calling Format:

FRICT (VS, SL, IFT)

Description of Parameters:

VS	Ship speed
SL	Ship length
IFT	Indicator:
	=1 ATTC formula used
	=2 ITTC formula used

Detailed Description:

Function FRICT computes the coefficient of frictional resistance by using the formulas in Section 3, Chapter VII of Comstock.⁷

Subroutine called:

None

SUBROUTINE HWCMR

Function:

This subroutine computes the coefficient of wavemaking resistance.

Calling Format:

CALL HWCMR

Detailed Description:

Subroutine HWCMR first sums up the various wave amplitude functions. After squaring A_c (Equation (56)) and A_s (Equation (57)), it calls the function SIMPUN for the integration of the sum of these squares to obtain the coefficient of wavemaking resistance as shown in Equation (55).

Subroutine Called:

SIMPUN

SUBROUTINE HWLXX

Function:

This routine computes the integration term on the right side of Equations (51) and (52) or (53) and (54).

Calling Format:

CALL HWLXX (XS, XE, IND, L)

Description of Parameters:

XS,XE	Starting and ending point of the integration interval in the ξ -direction
IND	An indicator: = 1 Surface source-sink = 2 Surface doublet
L	An indicator: = 1 The forebody = 2 The aftbody

Subroutine Called:

PPP

SUBROUTINE HWPT2

Function:

This subroutine prints amplitude functions of the cosine and sine wave.

Calling Format:

CALL HWPT2 (KFW)

Description of Parameters:

KFW Index to the number of different wave amplitudes to be printed.

Detailed Description:

HWPT2 first prints values at different degrees of the cosine wave amplitude functions of surface source-sink (Eq.(37)), surface doublet (Eq. (39)), point source-sink (Eq. (43)), point doublet (Eq. (45)), vertical line source-sink (Eq. (47)), vertical line doublet (Eq. (49)), horizontal line source-sink (Eq. (51)) and horizontal line doublet (Eq. (53)) and then prints values at different degrees of the sine wave amplitude functions of surface source-sink (Eq. (38)), surface doublet (Eq. (41)), point source-sink (Eq. (44)), point doublet (Eq. (46)), vertical line source-sink (Eq. (48)), vertical line doublet (Eq. (50)), horizontal line source-sink (Eq. (52)) and horizontal line doublet (Eq. (54)).

Subroutine Called:

None

SUBROUTINE HWPT3

Function:

This routine prints the speed-length ratio, coefficients of frictional and wavemaking resistance, and horsepower at different ship speed.

Calling Format:

CALL HWPT3

Detailed Description:

Subroutine HWPT3 first reads from input the length of ship, wetted surface of the ship, and other information. It then enters into a DO loop. In the DO loop, HWPT3 prints the Froude number, speed-length ratio, coefficients of frictional and wavemaking resistance, and horsepower at different ship speeds.

Subroutine Called:

FRICT

SUBROUTINE HWMR

Function:

This subroutine is the main execution program for the wavemaking resistance computation.

Calling Format:

CALL HWMR

Detailed Descriptions:

Subroutine HWMR contains two main iterative loops. The outer loop is for the computation of the wavemaking resistance at specific Froude numbers beginning with FDS and ending with FDE with the increment FDI. The inner loop is for the computation of the amplitude function of the waves at the directional angles between 0 and 85 degrees; the cosine and sine components of the wave amplitude functions are then computed by the successively called subroutines HWXSS, HWXSD, HWXPS, HWXPD, HWXLSV, HWXLDV, HWXLSH, and HWXLDH. These wave amplitudes are stored in the WAMP array. The last row of the 7X7 triangular matrix TSC, which corresponds to the Matrices of Equations (63) and (65), is also filled here for the optimization of wavemaking resistance. When the inner-loop computation is complete, the wavemaking resistance (Equation (55)) is computed by a call to HWCMR. The computations are saved in the CRW array.

Before the program returns, the wavemaking resistance and wave amplitude are printed out.

Subroutines Called:

HWXSS, HWXSD, HWXPS, HWXPD, HWLSV, HWLDV, HWLSH, HWLDH, HWCMR, HWPT2, HWPT3, HWZSD

SUBROUTINE HWXLDH

Function:

This routine computes the cosine and sine components of wave amplitudes generated by the horizontal line doublet.

Calling Format:

CALL HWXLDH

Detailed Description:

This routine computes Equations (53) and (54) and stores the computed wave amplitudes in the WAMP array. The first six rows of the TSC array for the optimization of wavemaking resistance are also filled if the value in KLP is 1.

Subroutines Called:

HWLXX

SUBROUTINE HWXLDV

Function:

This routine computes the cosine and sine components of wave amplitude generated by the vertical line doublet.

Calling Format:

CALL HWXLDV

Detailed Description:

Subroutine HWXLDV computes Equations (49) and (50) and stores the computed wave amplitudes into the WAMP array.

Subroutines Called:

None

SUBROUTINE HWXLSH

Function:

This routine computes the cosine and sine components of wave amplitudes generated by the horizontal line source-sink.

Calling Format:

CALL HWXLSH

Detailed Description:

Subroutine HWXLSH computes Equations (51) and (52) and stores the computed wave amplitudes in the WAMP array. The first six rows of the TSC array for the optimization of wavemaking resistance are also filled if the value in KLP is 1.

Subroutines Called:

HWLXX

SUBROUTINE HWXLSV

Function:

This routine computes the cosine and sine components of wave amplitudes generated by the vertical line source-sink.

Calling Format:

CALL HWXLSV

Detailed Description:

This routine computes Equations (47) and (48) and stores the computed wave amplitudes into the WAMP array.

Subroutines Called:

None

SUBROUTINE HWXPD

Function:

This routine computes the cosine and sine components of wave amplitudes generated by point doublets.

Calling Format:

CALL HWXPD

Detailed Description:

Subroutine HWXPD evaluates Equations (45) and (46) for every point doublet and stores the computed wave amplitude into the WAMP array.

Subroutine Called:

None

SUBROUTINE HWXPS

Function:

This routine computes the cosine and sine components of wave amplitudes generated by point source-sinks.

Calling Format:

CALL HWXPS

Detailed Descriptions:

Subroutine HWXPS evaluates Equations (43) and (44) for every point source-sink and stores the computed wave amplitudes into the WAMP array.

Subroutines Called:

None

SUBROUTINE HWXSD

Function:

This routine computes the cosine and sine components of wave amplitudes generated by the surface doublet..

Calling Format:

CALL HWXSD

Detailed Description:

Subroutine HWXSD computes Equations (39) and (41) for both fore and aft sections and stores the computed wave amplitudes in the WAMP array. The first six rows of the TSC array for the optimization of wavemaking resistance are also filled if the value in KLP is 1.

Subroutine Called:

HWXXX

SUBROUTINE HWXSS

Function:

This subroutine computes the cosine and sine components of the wave amplitudes generated by the surface source-sink.

Calling Format:

CALL HWXSS

Detailed Description:

Subroutine HWXSS computes Equations (37) and (38) for each n -surface segment and stores the wave amplitudes computed in the WAMP array. The first six rows of the TSC array for the optimization of wavemaking resistance are filled if the value in KLP is 1.

Subroutine Called:

HWXXX

SUBROUTINE HWXXX

Function:

This routine computes Equations (35) and (36) or (40) and (42) for one η -surface segment.

Calling Format:

CALL HWXXX (\downarrow XS, \downarrow XE, \downarrow K, \downarrow IND, \downarrow L)

Description of Parameters:

XS,XE	The starting and ending points for integration interval in the ξ -direction
K	The number of η -surface subsegments
IND	An indicator: = 1 Surface source-sink = 2 Surface doublet
L	An indicator: = 1 The forebody = 2 The aftbody

Detailed Description:

Subroutine HWXXX first fills the arrays TXP, R and S. It then enters into a loop to compute Equations (35) and (36) or (40) and (42), depending on the value of IND.

Subroutine Called:

PPP

SUBROUTINE HWZSD

Function:

This routine computes Equation (30).

Calling Format:

CALL HWZSD

Detailed Description:

Subroutine HWZSD computes Equation (30) for both fore and aft sections and stores the results in the ZSD array.

Subroutines Called:

None

PROGRAM PCWMR

Function:

This program is the main program in the (2,0) overlay.

Calling Format:

CALL AETSKC(5LPCWMR)

Detailed Description:

Program PCWMR calls in either HWWMR or HWOPT depending upon the value of KWR. It then calls in the (1,0) overlay to process other input data.

Subroutines Called:

HWOPT, HWWMR, PCIPT

FUNCTION PPP

Function:

This routine computes Equations (35), (36), (40) and (42) for one i value of one n -surface subsegment.

Calling Format:

PPP (CSG, SNG, HAP, HAN, R1, R2, R3, R4, S1, S2, S3, S4, TXP1, TXP2, TXP3,
TXP4, A, B, DCX, DCT, IND)

Description of Parameters:

See the program listing of HWXXX

Detailed Description:

Function PPP has two entry points, PPP and QQQ; the former for the computation of cosine components, Equations (35) and (36), and the latter for the computation of the sine components, Equations (40) and (42). Upon entry, the value of IND is checked: If IND = 1, the equation for the surface source-sink is computed; if IND = 2, the equation for the surface doublet is computed.

Subroutines Called:

None

SUBROUTINE HWFCN

Function:

This subroutine computes a coefficient of the wavemaking resistance.

Calling Format:

CALL HWFCN (PAR, PART, N2RET, PD, PR, CM, CEF, CR)

Description of Parameters:

PAR(6) Six parameters for modifying the singularity distribution

PART(6) Six parameters for modifying the singularity distribution of the last trial

N2RET Indicator of search status:
= 1 First
= 2 Subsequent trial
= 3 End of search (last trial)

PD,PR PD=a, PR=b (See Figure 3)

CM(6,6) Refer to description of CMS or CMH in Appendix A

CEF(6) Six coefficients corresponding to the six parameters of PAR

CR Contains a value computed by Eq. (55)

Detailed Description:

Subroutine HWFCN first converts the six parameters, PAR(6), to six coefficients CEF(6) (Equation (25)) and then computes the coefficient (CR) of wavemaking resistance.

Subroutine Called:

HWPTC

SUBROUTINE HWOLD

Function:

This routine determines the six parameters for the horizontal line doublet of either forebody or aftbody that produce the lowest wavemaking resistance.

Calling Format:

CALL HWOLD

Detailed Description:

Subroutine HWOLD makes successive calls to Subroutine EXPRS to randomly determine a set of six parameters corresponding to the horizontal line doublet (Equation (58)). In each successive call, Subroutine HWFCN computes the wavemaking resistance using the six parameters generated. Subroutine EXPRS then compares the wavemaking resistance value just computed with the lowest value obtained thus far. If the newly computed value is lower, the six parameters used to produce this lower value will replace the six parameters previously saved. At the end of the search, the six parameters saved (those parameters which produced the lowest wavemaking resistance value) will be converted into their coefficient values and these values will be added to the values of the original horizontal line doublet.

Subroutines called:

EXPRS, HWCTP, HWFCN, HWPTS

SUBROUTINE HWOLS

Function:

This routine determines the six parameters for the horizontal line source-sink of either forebody or aftbody that produce the lowest wavemaking resistance.

Calling Format:

CALL HWOLS

Detailed Description:

Subroutine HWOLS makes successive calls to Subroutine EXPRS to randomly determine a set of six parameters corresponding to the horizontal line source-sink (Equation (58)). In each successive call, Subroutine HWFCN computes the wavemaking resistance using the six parameters generated. Subroutine EXPRS then compares the wavemaking resistance value just computed with the lowest value obtained thus far. If the newly computed value is lower, the six parameters used to produce this lower value will replace the six parameters previously saved. At the end of the search, the six parameters saved (those parameters which produced the lowest wavemaking resistance value) will be converted into their coefficient values and these values will be added to the values of the original horizontal line source-sink.

Subroutines called:

EXPRS, HWCTP, HWFCN, HWPTS

SUBROUTINE HWOPT

Function:

This subroutine is the executive program for the minimization of wavemaking resistance.

Calling Format:

CALL HWOPT

Detailed Description:

Subroutine HWOPT reads in the data for the optimization process. Using the data provided, the program optimizes one singularity distribution for either the forbody or the aftbody using a single J value. It then calls HWWMR to store data into the array TSC, after which it calls one of the following subroutines to evaluate the six coefficients of Equation (58): HWOSS (for surface source-sink), HWOSD (for surface doublet), HWOLS (for horizontal line source-sink), or HWOLD (for horizontal line doublet). For detailed description, refer to Figure 4.

Subroutine called:

HWOLS, HWOLD, HWOSS, HWOSD, HWWMR

SUBROUTINE HWOSD

Function:

This routine determines the six parameters for the surface doublet of either forebody or aftbody that produce the lowest wavemaking resistance.

Calling Format:

CALL HWOSD

Detailed Description:

Subroutine HWOSD makes successive calls to Subroutine EXPRS to randomly determine a set of six parameters corresponding to the surface doublet (Equation (58)). In each successive call, Subroutine HWFCN computes the wavemaking resistance using the six parameters generated. Subroutine EXPRS then compares the wavemaking resistance value just computed with the lowest value obtained thus far. If the newly computed value is lower, the six parameters used to produce this lower value will replace the six parameters previously saved. At the end of the search, the six parameters saved (those parameters which produced the lowest wavemaking resistance value) will be converted into their coefficient values and these values will be added to the values of the original surface doublet.

Subroutines called:

EXPRS, HWCTP, HWFCN, HWPTS

SUBROUTINE HWOSS

Function:

This routine determines the six parameters for the surface source-sink of either forebody or aftbody that produce the lowest wavemaking resistance.

Calling Format:

CALL HWOSS

Detailed Description:

Subroutine HWOSS makes successive calls to Subroutine EXPRS to randomly determine a set of six parameters corresponding to the surface source-sink (Equation (58)). In each successive call, Subroutine HWFCN computes the wavemaking resistance using the six parameters generated. Subroutine EXPRS then compares the wavemaking resistance value just computed with the lowest value obtained thus far. If the newly computed value is lower, the six parameters used to produce this lower value will replace the six parameters previously saved. At the end of the search, the six parameters saved (those parameters which produced the lowest wavemaking resistance value) will be converted into their coefficient values and these values will be added to the values of the original surface source-sink.

Subroutines called:

EXPRS, HWCTP, HWFCN, HWPTS

SUBROUTINE DAUX

Function:

This routine directs the calling of other routines to calculate the u, v, w contributions from the various singularity distributions.

Calling Format:

CALL DAUX (A, B, F)

Description of Parameters:

A Contains the x-value of a streamline point being evaluated
B(2) Contains the y- and z-values of a streamline point being evaluated
F(2) Contains slopes of the streamline points being evaluated

Detailed Description:

Subroutine DAUX checks on each singularity distribution calculation flag periodically to determine if the contribution from that particular type of distribution is to be calculated. If it is, a call is made to the appropriate routine. When the calculation is completed, 4π is added to the U component (that is, the normalized steady flow $V = 4\pi$) and the slopes of the streamlines are calculated from the streamline formula, Equation (10).

Subroutines Called:

SURF, PSOUR, PDOUB, LSOURV, LDOUBV, LSOURH, LDOUBH

SUBROUTINE INT

Function:

This routine performs an integration of one variable of a specific family of functions over some definite limits.

Calling Format:

CALL INT (XXI, YET, Z, F, G, S, D)

Description of Parameters:

$$S(I) = \int_G^F \frac{x^{I-1} dx}{(x^2 - 2 \cdot Z \cdot x + XXI^2 + YET^2 + Z^2)^{3/2}} \quad I = 1, 2, \dots, 7$$

$$D(I) = \int_G^F \frac{x^{I-1} dx}{(x^2 - 2 \cdot Z \cdot x + XXI^2 + YET^2 + Z^2)^{5/2}} \quad I = 1, 2, \dots, 8$$

Detailed Description:

In order to save multiplications and other arithmetic operations later, subroutine INT begins by calculating several frequently used intermediate quantities. Then, by checking the various distribution calculation flags, those values (and only those values) of S and D needed by the calling routine are determined by using the limits in the analytical solutions of the above integrals.

Subroutines Called:

None

SUBROUTINE LDOUBH

Function:

This routine calculates the u, v, w contribution from all horizontal line doublets.

Calling Format:

CALL LDOUBH ([↑]ULDH, [↑]VLDH, [↑]WLDH)

Description of Parameters:

ULDH	}	u, v, w components, respectively, of the streamline velocity
VLDH		
WLDH		

Detailed Description:

Subroutine LDOUBH performs the same operations on horizontal-line doublets that LSOURH performs on horizontal-line source-sinks (See Equations (95) through (97).)

Subroutines Called:

INT

SUBROUTINE LDOUBV

Function:

This routine calculates the u, v, w contributions from all vertical-line doublets.

Calling Format:

CALL LDOUBV (ULDV, VLDV, WLDV)

Description of Parameters:

ULDV	}	u, v, w components, respectively, of the streamline velocity
VLDV		
WLDV		

Detailed Description:

Subroutine LDOUBV performs the same operations on vertical-line doublets that LSOURV performs on vertical-line source-sinks (See Equations (87) through (89).)

SUBROUTINE LSOURH

Function:

This routine calculates the u, v, w contributions from all horizontal line source-sinks.

Calling Format:

CALL LSOURH (ULSH, VLSH, WLSH)

Description of Parameters:

ULSH	}	u, v, w components, respectively, of the streamline velocity
VLSH		
WLSH		

Detailed Description:

After setting the distribution calculation flag to active (i.e., making KLSH <0), subroutine LSOURH calculates YY and ZZ. The integration over the line source-sink is performed and the results used to calculate the contributions. Each line is also checked to see if it is off the centerline and/or below the water plane. If it is, the corresponding appropriate image line source-sinks are deactivated by being made positive again. (See Equations (91) through (93).)

Subroutines Called:

INT

SUBROUTINE LSOURV

Function:

This routine calculates the u, v, w contributions from all vertical line source-sinks.

Calling Format:

CALL LSOURV (ULSV, VLSV, WLSV)

Description of Parameters:

ULSV	}	u, v, w components, respectively, of the streamline velocity.
VLSV		
WLSV		

Detailed Description:

After setting the distribution calculation flag to active (by making KLSV<0), subroutine LSOURV calculates XX, YY and ZZ. The integrations over the line source-sink and its image are performed and the results used to calculate the contributions. When the line is not on the centerline, an image source-sink distribution is created on the other side and the contribution from that image and its image above the waterplane is calculated. KLSV is then deactivated by being made positive again. (See Equations (83) through (85).)

Subroutines Called:

INT

SUBROUTINE PCSTL

Function:

This routine is the main program in the (3,0) overlay.

Calling Format:

CALL AETSKC (5LPCSTL)

Detailed Description:

After Subroutine PCSTL initializes several variables, it calls STREAM to trace the streamlines and then calls in the (1,0) overlay to process other input data.

Subroutines Called:

STREAM, PCIPT

SUBROUTINE PDOUB

Function:

This routine calculates the u, v, w contribution from all point doublets.

Calling Format:

CALL PDOUB (UPDD, VPDD, WPDD)

Description of Parameters:

UPDD	}	u, v, w components, respectively, of the streamline velocity.
VPDD		
WPDD		

Detailed Description:

Subroutine PDOUB performs the same operations on point doublets that PSOUR performs on point source-sinks. (See Equations (79) through (81).)

Subroutines Called:

None

SUBROUTINE PSOUR

Function:

This routine calculates the u, v, w contributions from all point source-sinks.

Calling Format:

CALL PSOUR (UPSD, VPSD, WPSD)

Description of Parameters:

UPSD	}	u, v, w components, respectively, of the streamline velocity
VPSD		
WPSD		

Detailed Description:

Each point source-sink is examined to see if it is off the centerline and/or below the waterplane. If it is, appropriate image source-sinks are created. The contributions from the source-sink and any images are then calculated. (See Equations (75) through (77).)

Subroutines Called:

None

SUBROUTINE QUAD

Function:

Using a 10-point Gaussian quadrature method, this routine numerically evaluates the double integrals used in calculating the u, v, w contributions from the surface distributions.

Calling Format:

CALL QUAD (XL, XU, S, IFL)

Description of Parameters:

XL, XU Limits of Gaussian interval being evaluated over
S(3) Array containing the u, v, w contributions
IFL Flag indicating which side of η -surface is being evaluated.
IFL>0, $\eta > 0$; IFL<0, $\eta < 0$.

Detailed Description:

This routine evaluates the six double integrals in Equations (67), (68), (69), (71), (72) and (73).

The entire integration is performed so as to avoid any unnecessary duplication of arithmetic computation and thus to save time. The actual calculation of the functions and the summing of the results for these ten points is performed separately for the source and doublet cases, with the results being stored in the array D. D(1) contains the u component of the velocity, D(2) the v, and D(3) the w. These results are then multiplied by the appropriate distribution coefficient and summed into the TT array. Finally, a last postmultiplication is performed on TT corresponding to the multiplication by b-a in the quadrature formula. The final results are summed into S for return to SURF.

Subroutines Called:

INT

SUBROUTINE STREAM

Function:

This routine acts as the executive for the actual streamline calculations.

Calling Format:

CALL STREAM

Detailed Description:

Subroutine STREAM first reads in the number of stations, the number of streamlines, the station-number option, the offset scaling factor, and other variables. It then reads the x-value of streamline stations and the initial y and z offsets for each streamline. The Kutta-Merson routine KUTMER is then called, a loop being provided each time with the x, y, z coordinates of the present streamline point and the Δx to the next station. The routine KUTHER returns the x, y, z coordinates of the next point. These points are saved and then printed out when the last station is reached or when KUTMER fails to meet the error criteria specified in EPS and A.

Subroutines Called:

KUTMER

SUBROUTINE SURF

Function:

This routine calculates the u, v, w contribution from the surface source-sink and doublet distributions.

Calling Format:

CALL SURF (A, B, C)

Description of Parameters:

A }
B } u, v, w components, respectively, of the streamline velocity.
C }

Detailed Description:

Subroutine SURF initializes IFL and then calculates the value of ET. Y is checked to see if it has penetrated the η -surface, in which case a message is printed out. XINT is then calculated and preparations are made to begin the integration on the +y side of the η -surface in the +x direction. XL and XU are calculated, with XL being the last value of XX and XU being $XX + XINT * J^2$. Starting at 1, J increases by 1 for each interval. When $J > 5$, the remaining portion of the η -surface integration in that direction is computed in one final step. The values of XL and XU are checked to see that they (1) stay within the η -surface limits, (2) lie outside of the parallel body lengths, and (3) both lie on the same fore and aft section. Changes are made to XL, XU and/or XX where appropriate to meet the above conditions. Then if $XL \geq XU$, a call is made to the Gaussian quadrature routine QUAD which will calculate the actual contribution over the interval XL→XU. This process is repeated until the integration interval reaches the forward end of the η -surface, $x = 1.0$. The whole procedure is then repeated to perform the integration from X in the -x direction and then again to do the integration in both directions on the - η side of the η -surface.

Subroutines Called:

QUAD

SUBROUTINE VOLAR

Function:

This routine computes the value and wetted surface for the strut or lower hull for SWATH ship.

Calling Format:

CALL VOLAR (OFF, ZS, KPT, YM, ZZZ, KXS, KXE)

Description of Parameters:

OFF	Offset scaling
ZS	Depth of the strut or lower hull
KPT	Station number options: =1 Traces streamline at every station =2 Traces streamline at every other station
YM	Beam of the strut or the lower hull
ZZZ	Draft of the strut
KXS	Station number that marks the fore point of the bow at the waterline
KXE	Station number that marks the aft point of the stern at the waterline

Detailed Description:

Subroutine VOLAR calls subroutine SIMPUN to compute the volume and wetted surface for the strut or lower hull of the SWATH ship.

Subroutine called:

SIMPUN

ACKNOWLEDGMENT

The author is grateful for the opportunity to work with Dr. P. C. Pien and for his continuing guidance and help with the development of the computer program.

APPENDIX A

VARIABLES IN COMMON

The variable names used in COMMON throughout the program are described in the pages that follow. The User's Manual contains detailed descriptions of the input data variables. If the input data variables are also included in COMMON, only the names of the input data variables and the corresponding numbers of the cards containing their descriptions are indicated.

- AAA(N,L,K) The value of A_1 used in Equation (13) to approximate the η -surface
- N The number of straight-line segments ($N \leq 4$) defining the η -surface
- L The portion of the ship under consideration:
 =1 Forebody
 =2 Aftbody
- K The singularity distribution to be calculated:
 =1 Surface source-sink
 =2 Surface doublet
 =3 Reserved for interactive graphics use
 =4 Reserved for interactive graphics use
- AKZ A constant defined as $\frac{K_0}{\cos \theta}$ where $K_0 = g/v^2$
- BBB(N,L,K) The value of A_2 used in Equation (13) to approximate the η -surface. The values for N,L, and K are the same as those for AAA(N,L,K) above
- BEM [Defined on input data card C8]
- BEXT(N) Values of exponents for exponential random search, where $N=3$
- BKZ A constant defined as $K_0 \tan \theta \sec \theta$, where $K_0 = g/v^2$

Preceding page blank

CESD(I,J,L) Coefficients of Equation (16) for the surface doublet,
where $1 \leq I \leq 6$ and $1 \leq J \leq 4$

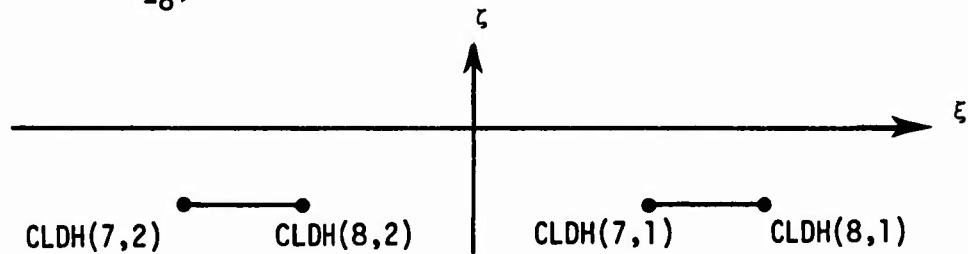
- L** Hull portion to be considered:
- =1 Forebody
 - =2 Aftbody
 - =3 Reserved for interactive graphics use
 - =4 Reserved for interactive graphics use

CESS(I,J,L) Coefficients of Equation (16) for the surface source-sink,
where $1 \leq I \leq 6$ and $1 \leq J \leq 4$

- L** Hull portion to be considered:
- =1 Forebody
 - =2 Aftbody
 - =3 Reserved for interactive graphics use
 - =4 Reserved for interactive graphics use

CLDH(I,L) Information defining horizontal-line doublet

- I** Indicator:
- =1 }
 . } Coefficients of Equation (20)
 . }
 6 }
 - =7 }
 =8 } Integration interval in the ξ -direction



- =9 The distance from the centerline of the line doublet to the ζ - ξ plane
- =10 The distance from the center of the line doublet to the ξ - η plane

L Hull portion to be considered:

=1 Forebody

=2 Aftbody

=3 Reserved for interactive graphics use

=4 Reserved for interactive graphics use

CLDV(J,L)

Information defining vertical line doublet

J

Indicator:

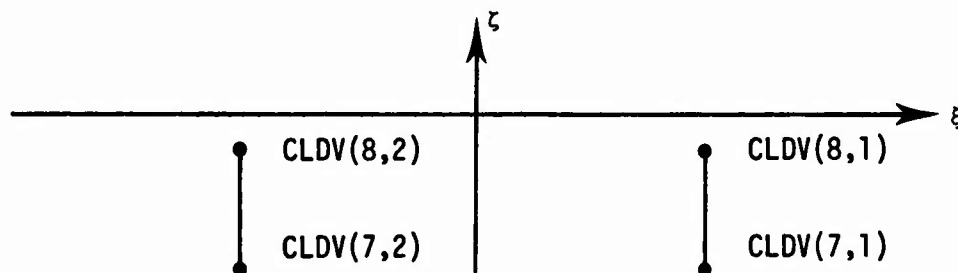
=1
.
.
.
4

} Coefficients of Equation (19)

=5 Contains distance from the centerline of the
line-doublet to the η - ζ plane

=6 Contains distance from the centerline of the
line-doublet to the ζ - ξ plane

=7
=8 } Contains integration interval in the ζ -direction



L Hull portion to be considered:

=1 Forebody

=2 Aftbody

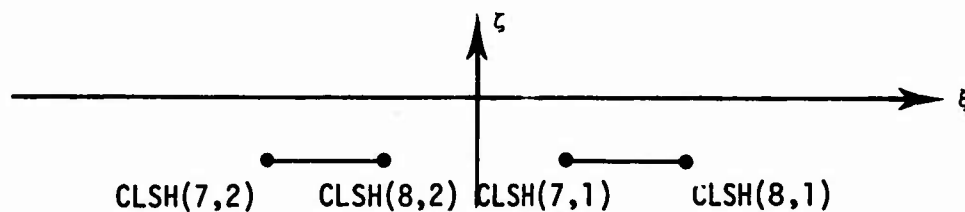
=3 Reserved for interactive graphics use

=4 Reserved for interactive graphics use

CLSH(I,L) Information defining horizontal line source-sink

I Indicator:

=1)
 : } Coefficients of Equation (20)
 :
 6)
 =7)
 =8) Integration interval in the ξ -direction



=9 Distance from centerline of the line source-sink to the ζ - ξ plane

=10 Distance from center of the line source-sink to the ξ - η plane

L Hull portion to be considered:

=1 Forebody
 =2 Aftbody
 =3 Reserved for interactive graphics use
 =4 Reserved for interactive graphics use

CLSV(J,L) Information defining the vertical line source-sink

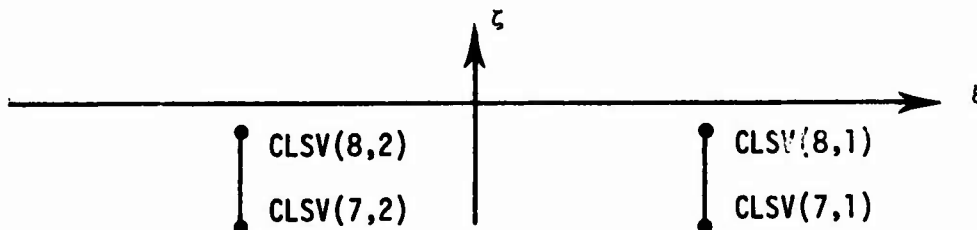
J Indicator:

=1)
 : } Contains coefficients for Equation (19)
 :
 4)

=5 Distance from the centerline of the line source-sink to the η - ζ plane

=6 Distance from the centerline of line source-sink to the ζ - ξ plane

=7)
 =8) Integration interval in the ζ -direction



- L Hull portion to be considered:
 =1 Forebody
 =2 Aftbody
 =3 Reserved for interactive graphics use
 =4 Reserved for interactive graphics use
- CMH(M,N,L) Coefficients of the Matrix (24) for horizontal-line source-sink and doublet, where M=7 and N=7
- L Hull portion to be considered:
 =1 Forebody, horizontal line source-sink
 =2 Aftbody, horizontal line source-sink
 =3 Forebody, horizontal line doublet
 =4 Aftbody, horizontal line doublet
- CMS(M,N,L) Coefficients of the Matrix (24) for surface source-sink and doublet, where M=7 and N=7
- L Hull portion to be considered:
 =1 Forebody, surface source-sink
 =2 Aftbody, surface source-sink
 =3 Forebody, surface doublet
 =4 Aftbody, surface doublet
- CN3(N) Constants defined as $\text{Cos}^3 \theta$ where $1 \leq N \leq \text{NDG}$
- CRW(N) Wavemaking resistance Equation (55) at different Froude numbers, where $1 \leq N \leq \text{NDG}$
- CSN A constant defined as $\text{Cos} \theta$
- DDR [Defined on input data card C24]
- DEG(N) The values in degree of direction angle where $1 \leq N \leq \text{NDG}$ and $0 \leq \text{DEG}(N) \leq 85^\circ$

DGR(N) Information for numerical integration of Equation (55)

N Indicator:

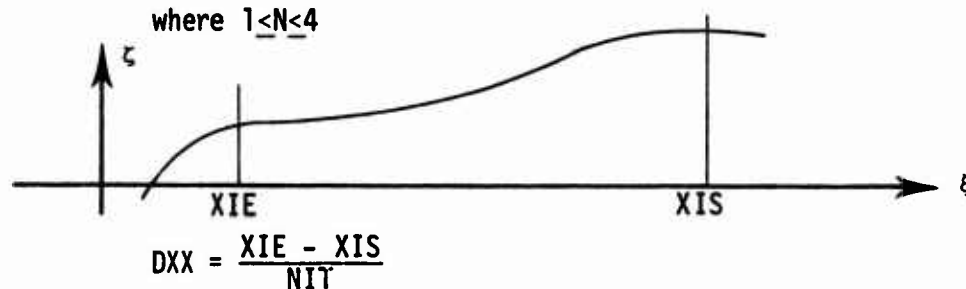
=1 Initial increment size, in degrees

=2 Upper limit of the integration where $0 \leq DGR(2) \leq 85^\circ$

=3 } Those points (degrees) at which the increment size
 . } is to be reduced by half
 . }
 10 }

DIN The increment size of θ for current use in the numerical integration of Equation (55)

DXX(L,N) Integration subinterval for surface source-sink doublet where $1 \leq N \leq 4$



FDE [Defined on input data card C3]

FDI [Defined on input data card C3]

FDP(N) [Defined on input data card C76]

FDS [Defined on input data card C3]

FDW(N) [Defined on input data card C4]

FND Variable NDY in floating-point format

FRD(N) Froude numbers at which wavemaking resistance will be evaluated, $1 \leq N \leq MFD$

KAYT(N) [Defined on input data card C72]

KBD [Defined on input data card C5]

KBS [Defined on input data card C5]

KED(J,L) Indicators for the calculation of coefficients of the surface doublet

J An indicator:
 =0 CESD(I,J,L) = 0, I= 1,...6
 =1 CESD(I,J,L) \neq 0, I=1,...6

L Hull portion to be considered:
 =1 Forebody
 =2 Aftbody

KES(J,L) Indicators for the calculation of coefficients of the
 surface source-sink:

J An indicator:
 =0 CESS(I,J,L) = 0, I = 1,...6
 =1 CESS(I,J,L) \neq 0, I = 1,...6

L Hull portion to be considered:
 =1 Forebody
 =2 Aftbody

KLDH [Defined on input data card C5]

KLDV [Defined on input data card C5]

KLP An indicator used in the optimization process:
 =1 Forebody
 =2 Aftbody

KLSH [Defined on input data card C5]

KLSV [Defined on input data card C5]

KOP(K) [Defined on input data card C73]

KPD [Defined on input data card C5]

KPI(K) [Defined on input data card C7]

KPR(K) [Defined on input data card C6]

KPS [Defined on input data card C5]

KSD [Defined on input data card C5]

KSS [Defined on input data card C5]

KWP	An indicator used in the optimization process: =0 No optimization =1 Optimization for the forebody =-1 Optimization for the aftbody
KWR	[Defined on input data card C2]
KWZ	The current KZP value
KZP(N)	[Defined on input data card C74]
LING	An indicator: =0 Standard option in which the first random number chosen is compared to .5 to determine the search region for each trial =1 The random number is compared with a variable instead of with a constant of .5
MDG	A constant which is the maximum dimension for the arrays DEG and THE, where MDG = 100
MEND	The number of stations in the streamline tracing
MFD	A constant which is the maximum number of Froude numbers allowed, where MFD = 30
NDG	The index to the arrays DEG and THE; $1 \leq NDG \leq MDG$
NDY	[Defined on input data card C8]
NFD	The index to the array FRD. $1 \leq NFD \leq MFD$
NFP	[Defined on input data card C75]
NFW	The index to the array FDW. $1 \leq NFW \leq MFW$
NGR	A constant which is the number of times the variable DIN will be divided by 2
NIT	[Defined on input data card C8]
NPD	The total number of point-doublets read from the input file

NPS The total number of point-source-sinks read from the input file

NTI A constant which is the i value in the Equation (15), where NTI=6

NTJ A constant which is the j value in the Equation (15), where NTJ=4

NTS A constant, where NTS=8

NZP [Defined on input data card C74]

N2EXP Number of exponents, where N2EXP=3

N2PAR Number of search parameters, where N2PAR=6

PALS(I,N,L) Parameters of the singularity distribution of the horizontal line source-sink and doublet

I Indicator:

=1
 .
 .
 .
 .
 6 } The six parameters

N An indicator:

=1 Used in the interactive graphics

=2 Currently used

L Hull portion to be considered:

=1 Forebody, horizontal line source-sink

=2 Aftbody, horizontal line source-sink

=3 Forebody, horizontal line doublet

=4 Aftbody, horizontal line doublet

PARD(I,N,L) Parameters of the singularity distribution of the surface doublet

I Indicator:

=1
 :
 :
 :
 6 } The six parameters

N Indicator:
 =1 Reserved for interactive graphics
 =2 Currently used

L Hull portions to be considered:
 =1 Forebody
 =2 Aftbody

PARH(6) [Defined on input data card C79]

PARL(6) [Defined on input data card C78]

PARS(I,N,L) Parameters for the singularity distribution of the surface source-sink

I Indicator:
 =1
 .
 .
 .
 6 } The six parameters

N Indicator:
 =1 Reserved for interactive graphics
 =2 Currently used

L Hull portion to be considered:
 =1 Forebody
 =2 Aftbody

PCY [Defined on input data card C2]

PIE A constant which is equal to π

PIND(K,N) [Defined on input data card C42]

PINS(N,N) [Defined on input data card C40]

PMD(L) The lengths of the parallel mid-body for surface doublet computation

L Hull portion to be considered:
 =1 Forebody
 =2 Aftbody

PMS(L) The lengths of the parallel midbody for surface source-sink computation

 L Hull portion to be considered
 =1 Forebody
 =2 Aftbody

PS(L) The lengths of the parallel midbody of either surface source-sink or doublet

 L Hull portion to be considered:
 =1 Forebody
 =1 Aftbody

RAD The constant 57.2958

RKZ The variable which is defined k_0 where $k_0 = g/v^2$

RLM The variable $K_0 \cdot \text{SEC}^2 \theta$

SNE The variable $\text{Sin} \theta$

T Same as for ZRH

TEF(I,J) A temporary array used to store coefficients of singularity distributions in the optimization of wavemaking resistance

THE(N) Direction angles in radius, where $1 \leq N \leq 100$

TSC(M,N,K) Coefficients of Matrices (63) and (65)

 K Indicator:
 =1 Matrix (63)
 =2 Matrix (65)

WAMP(N,L,K) The wave amplitudes at different direction angles, where $1 \leq N \leq \text{NDG}$

 L Hull portion to be considered:
 =1 Forebody
 =2 Aftbody

K Indicator:
 =1 Surface source-sink
 =2 Surface doublet
 =3 Point source-sink
 =4 Point doublet
 =5 Vertical line source-sink
 =6 Vertical line doublet
 =7 Horizontal line source-sink
 =8 Horizontal line doublet

WTP(N) [Defined on input data card C77]

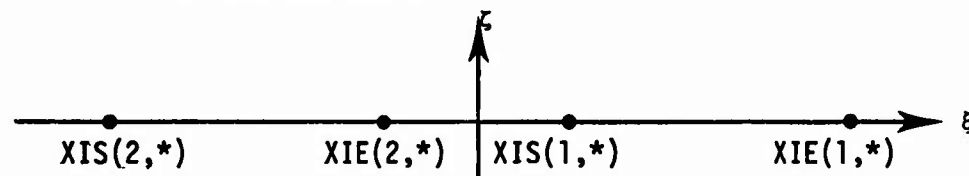
X X-values of a streamline point at which evaluation of u, v, w is being made

XIE(L,K) Integration intervals for surface source-sink and doublet

L Hull portion to be considered:

 =1 Forebody
 =2 Aftbody

K Indicator:
 =1 Surface source-sink
 =2 Surface doublet



XIS(L,K) The integration intervals for surface source-sink and doublet (see preceding figures)

L Hull portion to be considered:

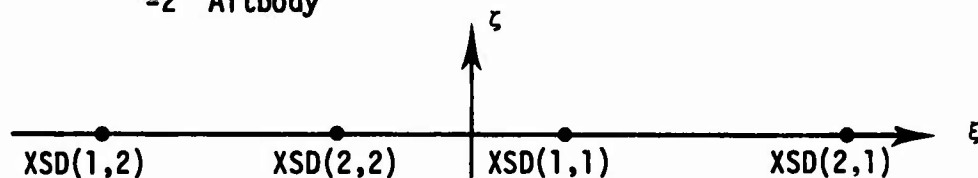
 =1 Forebody
 =2 Aftbody

K Indicator:
 =1 Surface source-sink
 =2 Surface doublet

XSD(K,L) Integration intervals for the surface doublet

K Indicator:
 =1 Starting point
 =2 Ending point

L Hull portion to be considered:
 =1 Forebody
 =2 Aftbody



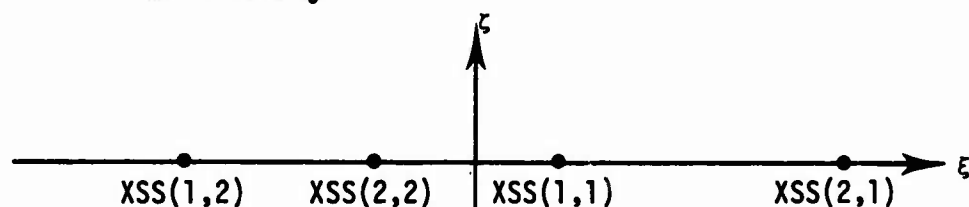
XSDC(I) Equation (35), where $I=1,2,\dots,6$

XSDS(I) Equation (36), where $I=1,2,\dots,6$

XSS(K,L) Integration intervals for the surface source-sink

K Indicator:
 =1 Start point
 =2 End point

L Hull portion to be considered:
 =1 Forebody
 =2 Aftbody



XX(M,N) X-values of streamlines

M Number of streamline stations where $1 \leq M \leq 61$

N Number of streamlines where $1 \leq N \leq 6$

Y Y-values of a streamline point at which evaluation of U, V, W is being made

YY(M,N)	Y-values of streamlines
M	Number of streamline stations $1 \leq M \leq 61$
N	Number of streamlines, $1 \leq N \leq 6$
Z	Z-values of a streamline point at which evaluation of U,V,W is being made
ZER	A constant set to 0.0000001
ZLS	Result of Equation (30), for horizontal line source-sink or doublet
ZRH	[Derived on input data card C8]
ZSD(J)	Result of Equation (30), for surface source-sink or doublet
ZZ(M,N)	Z-values of streamlines
N	Number of streamline stations, $1 \leq M \leq 61$
N	Number of station-lines, $1 \leq N \leq 6$

APPENDIX B

COMPARISONS OF COEFFICIENTS OF THEORETICAL WAVEMAKING RESISTANCE AND RESIDUAL RESISTANCE OF SWATH'S III, IV, V, AND RC-2

In this appendix, resistances derived from experimental tests of certain SWATH models are compared with wavemaking resistances predicated for the SWATH designs by the Pien program. Four recently developed SWATH models are used in the comparison: SWATH's III, IV, and V, developed at the Naval Ship Research and Development Center, and SWATH RC-2, developed at the Naval Undersea Center. The SWATH-model experimental tests were informally documented within the Center conducting the experiment.

The coefficient of the wavemaking resistance C_W is defined as

$$R_W / (1/2) \rho \cdot S \cdot V$$

where R_W is the wavemaking resistance in pounds
 ρ is the mass density
 S is the wetted surface for both strut and lower hull
 V is the ship speed in feet per second

Since L_e was selected as the effective ship length for the experimental tests,* L_e was used in the Pien program also for the computation of the speed-length ratio $V/\sqrt{L_e}$ where V is the ship speed in knots. The limitations of wavemaking resistance theory are well known; hence several

$$* L_e = \frac{S_s \cdot L_s + S_h \cdot L_h}{(S_s + S_h)}$$

where L_s is the length of the strut
 L_h is the length of the lower hull
 S_s is the wetted surface of the strut
 S_h is the wetted surface of the lower hull

simplifications were considered desirable in computing the hull geometry from a singularity distribution as discussed in Pien's paper on "Motion and Resistance of a Low-Waterplane-Area Catamaran."⁸ Nevertheless, as the Figures 10 to 37 which compare the C_r (residual resistance coefficient) and the C_w (wavemaking resistance coefficient) show, the Pien program is more than adequate for estimating the resistance for a proposed SWATH design. This program is also a useful tool for making systematic parametric studies of SWATH ships.

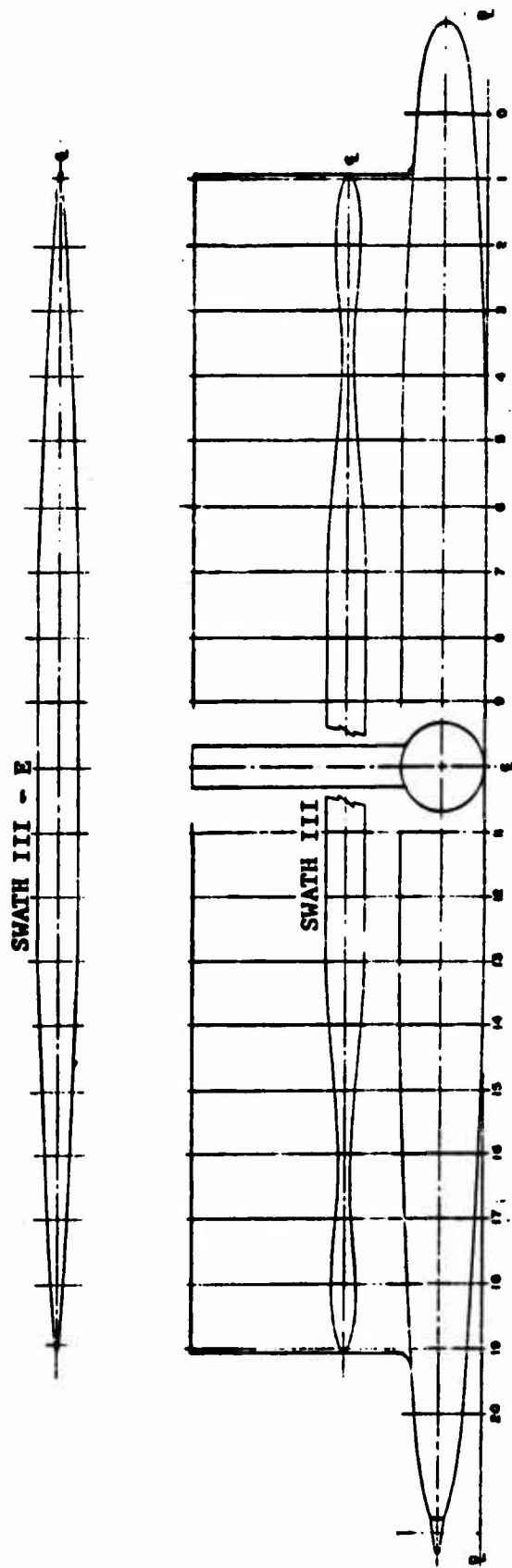


Figure 10 - Abbreviated Lines and Profile for SWATH III Represented by Models 5276 and 5276E

ITEMS	SHIP		MODEL	
	HULL	STRUT	HULL	STRUT
LENGTH IN FT.	287.00	226.50	14.07	11.10
BEAM IN FT.	17.30	8.00	0.85	0.39
DESIGN SPEED IN KNOTS	32.00		7.08	
C _p	0.758		0.758	
C _v		0.72		0.72
C _x	0.785	0.982	0.785	0.982
EFFECTIVE LENGTH IN FT.	265.80			

FIGURE NO.	TEST NO.	DRAFT(FT)	HULL SPACING*	DISPL. (TON)	WET SURF. (FT ²)	TEST CONDITIONS
3	27	32.00	75.00	4,050.00	38,390.00	Free to trim and heave
4	2	28.00	75.00	3,756.00	34,708.00	Free to trim and heave
5	4	25.00	75.00	3,537.00	31,980.00	Free to trim and heave

* From center to center at midship.

Figure 11 - Ship and Experimental Model Test Data for SWATH III (Model 5276)

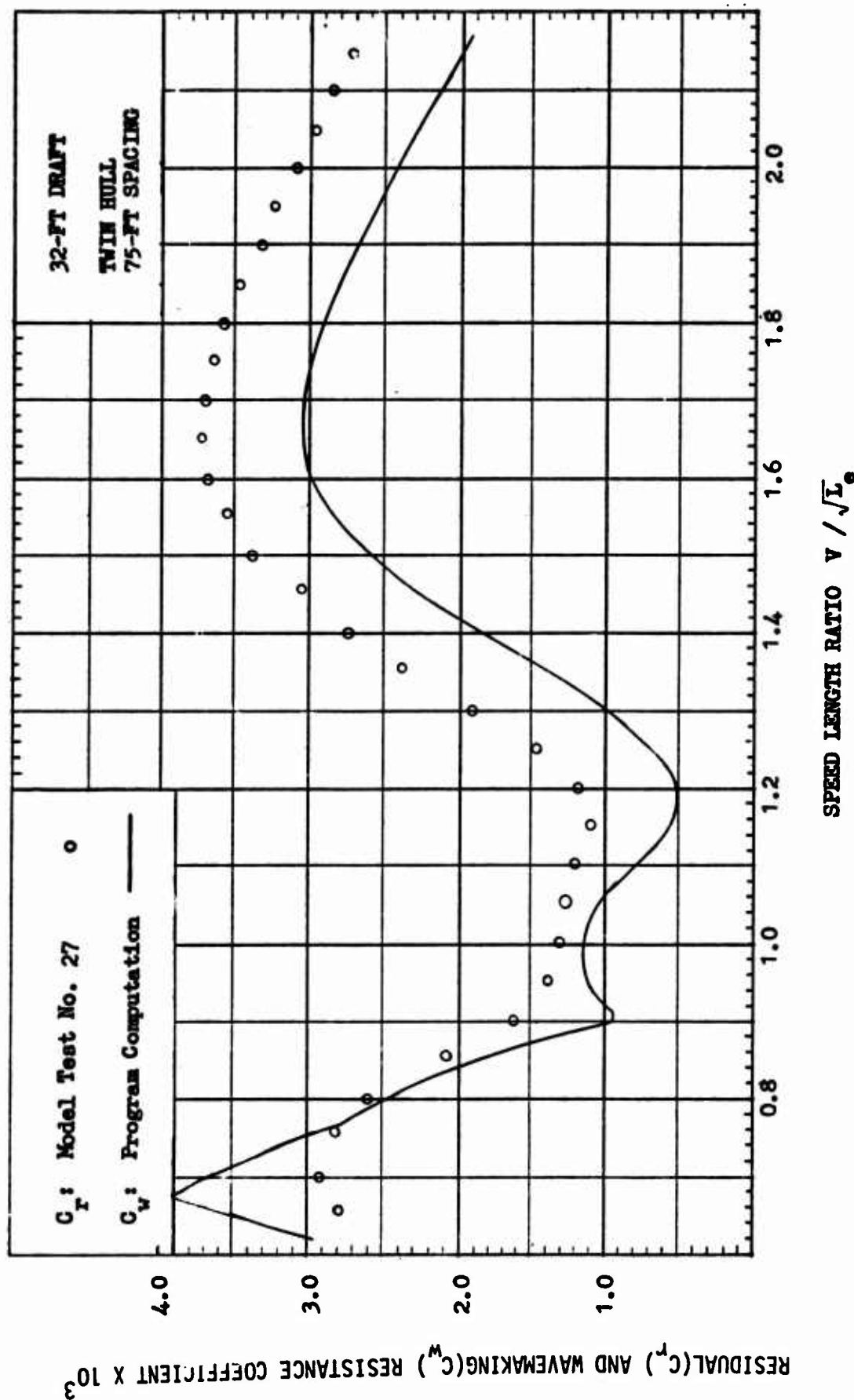


Figure 12 - Residual and Wavemaking Resistance Coefficients versus Speed-Length Ratio for SWATH III (Model 5276) at a 32-Foot Draft

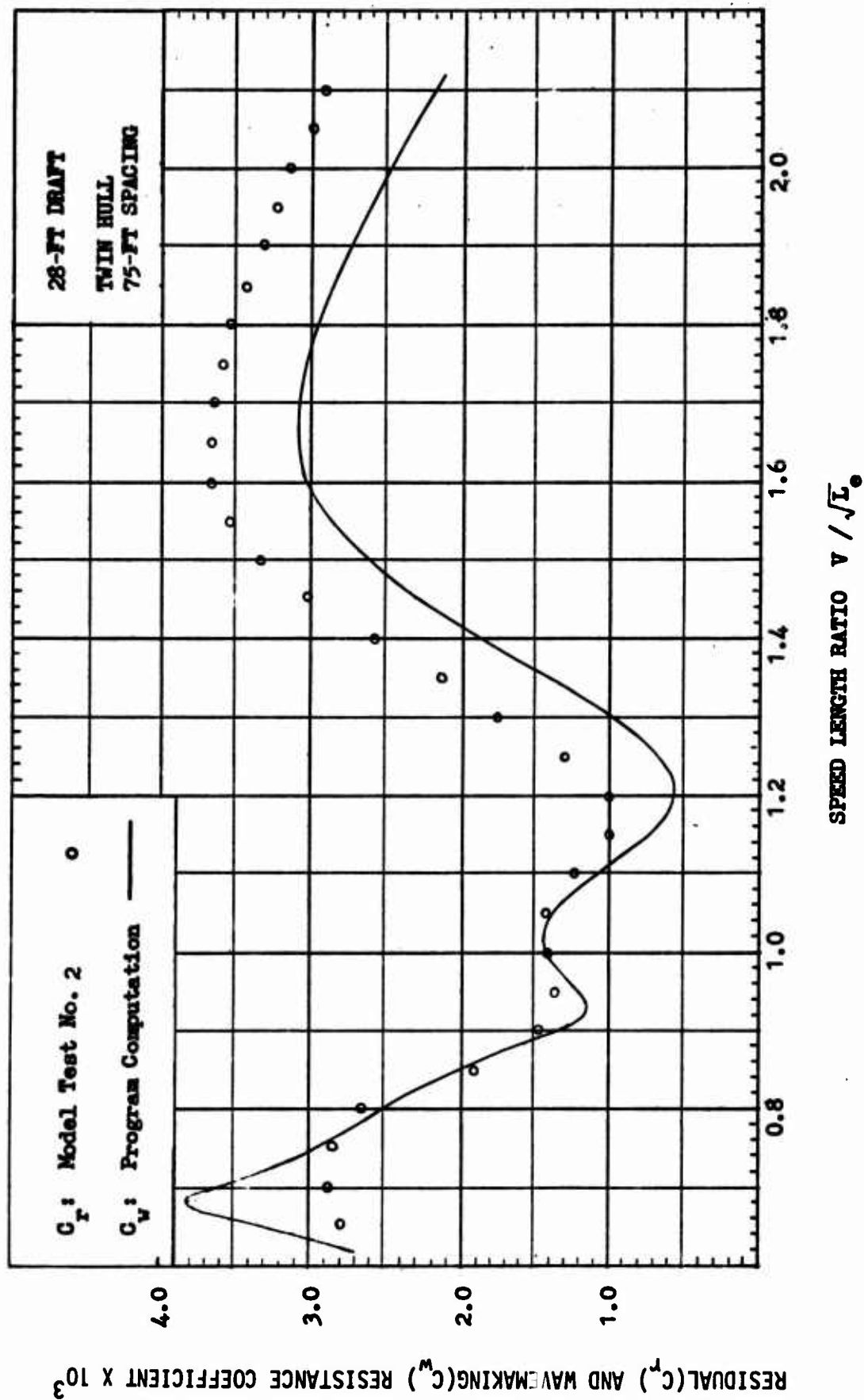


Figure 13 - Residual and Wavemaking Resistance Coefficients versus Speed-Length Ratio for SWATH III (Model 5276) at a 28-Foot Draft

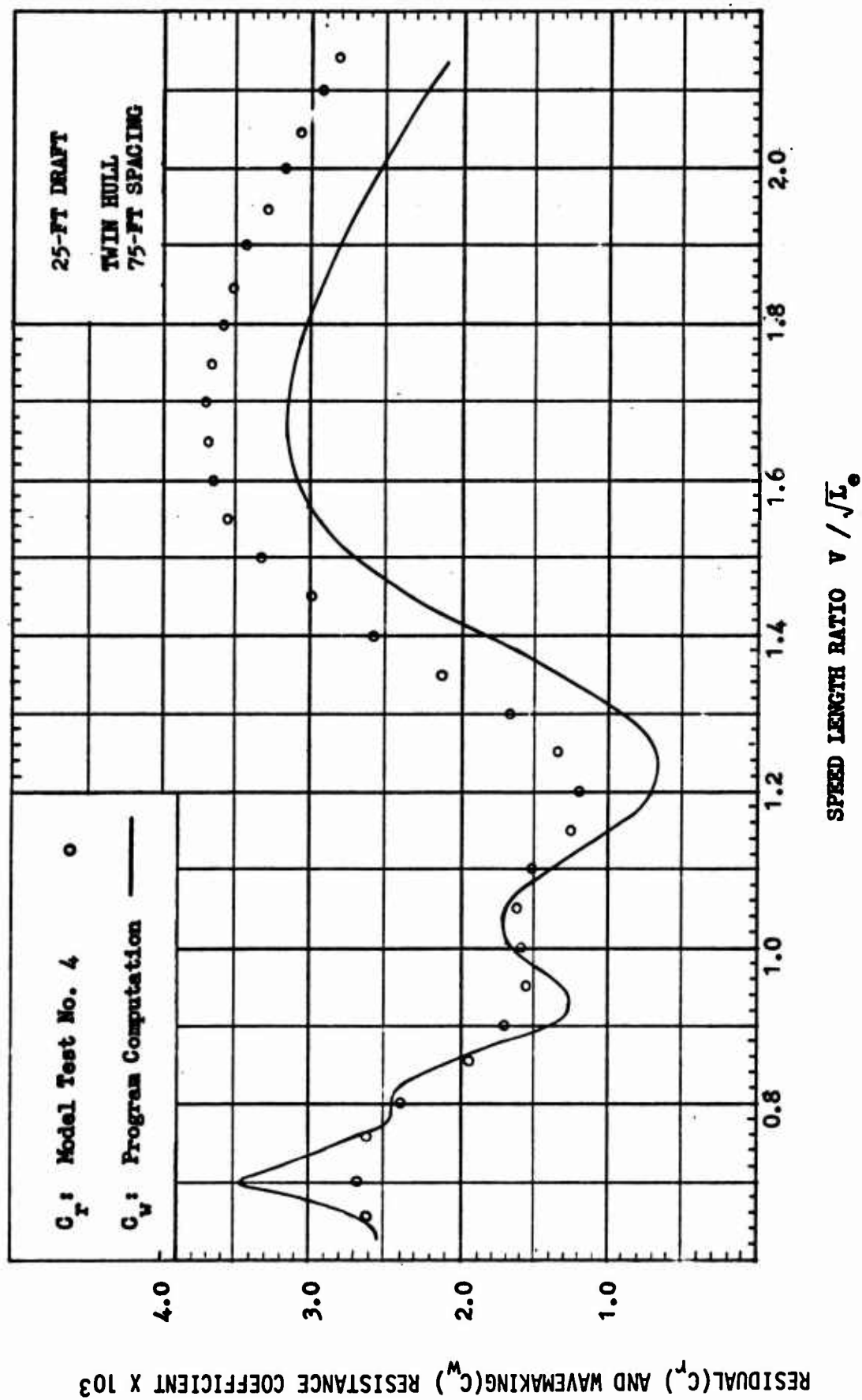


Figure 14 - Residual and Wavemaking Resistance Coefficients versus Speed-Length Ratio for SWATH III (Model 5276) at a 25-Foot Draft

ITEMS	SHIP		MODEL	
	HULL	STRUT	HULL	STRUT
LENGTH IN FT.	287.00	226.50	14.07	11.10
BEAM IN FT.	17.30	8.00	0.85	0.39
DESIGN SPEED IN KNOTS	32.00		7.08	
C _p	0.758		0.758	
C _v		0.74		0.74
C _x	0.795	0.982	0.795	0.982
EFFECTIVE LENGTH IN FT.	265.80			

FIGURE NO.	TEST NO.	DRAFT (FT)	HULL SPACING*	DISPL. (TON)	WET SURF. (FT ²)	TEST CONDITIONS
7	501	32.00	.00	2,045.00	18,663.00	Captive
8	502	28.00	.00	1,887.00	16,826.00	Captive
9	503	25.00	.00	1,772.00	15,449.00	Captive

* From center to center at midship.

Figure 15 - Ship and Experimental Model Test Data for SWATH III (Model 5276E)

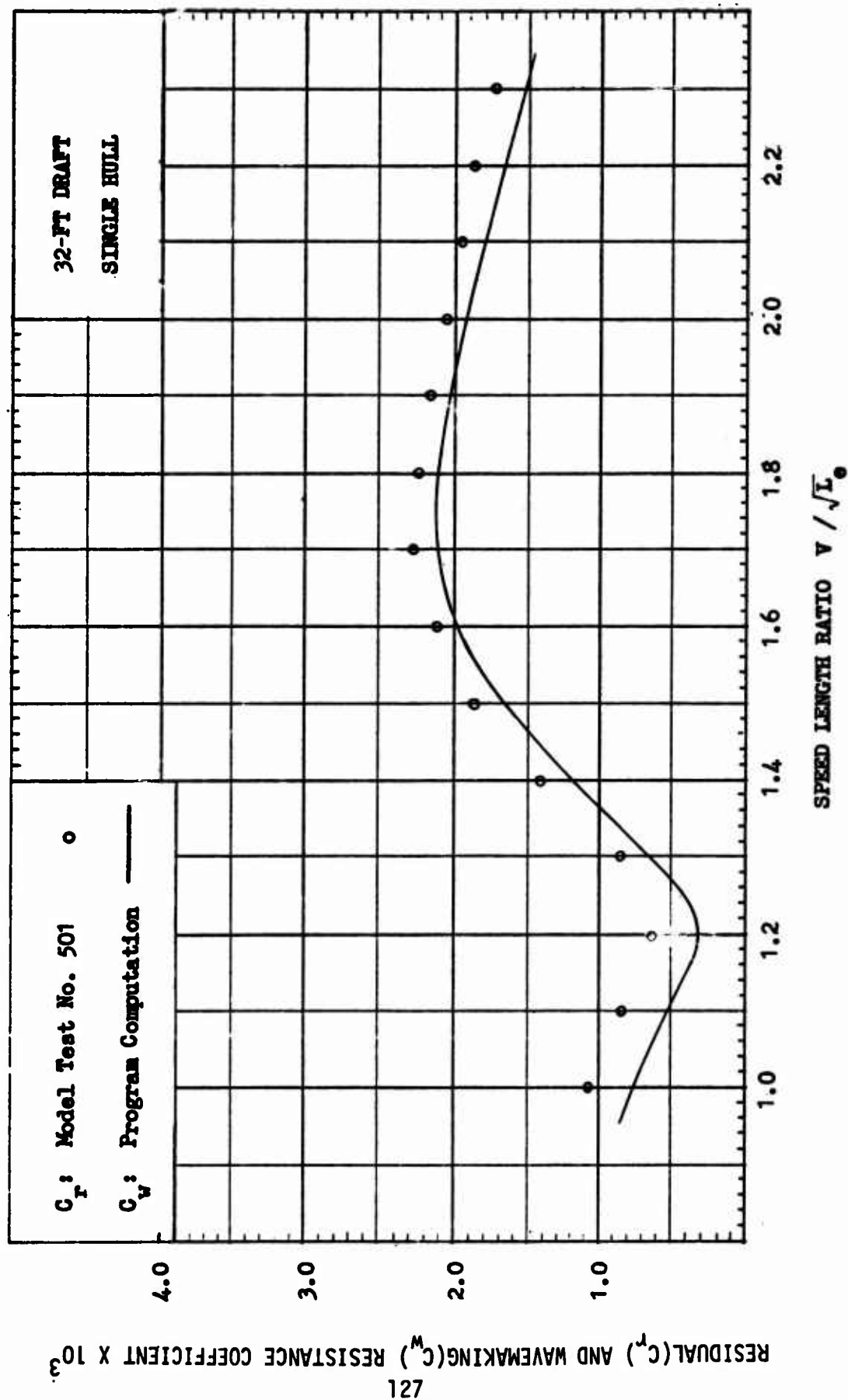


Figure 16 - Residual and Wavemaking Resistance Coefficients versus Speed-Length Ratio for SWATH III (Model 5276E) at a 32-Foot Draft

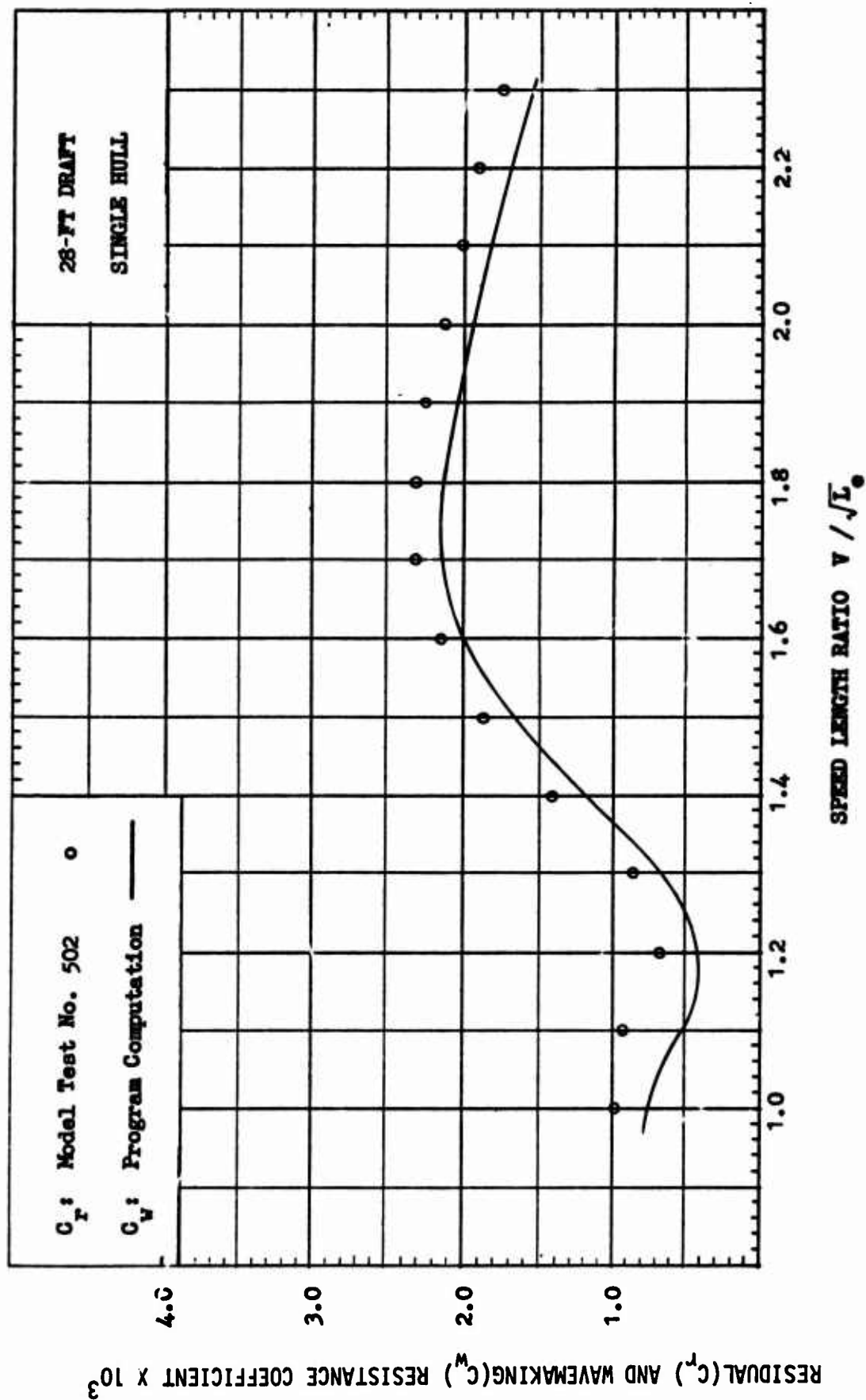


Figure 17 - Residual and Wavemaking Resistance Coefficients versus Speed-Length Ratio for SWATH III (Model 5276E) at a 28-Foot Draft

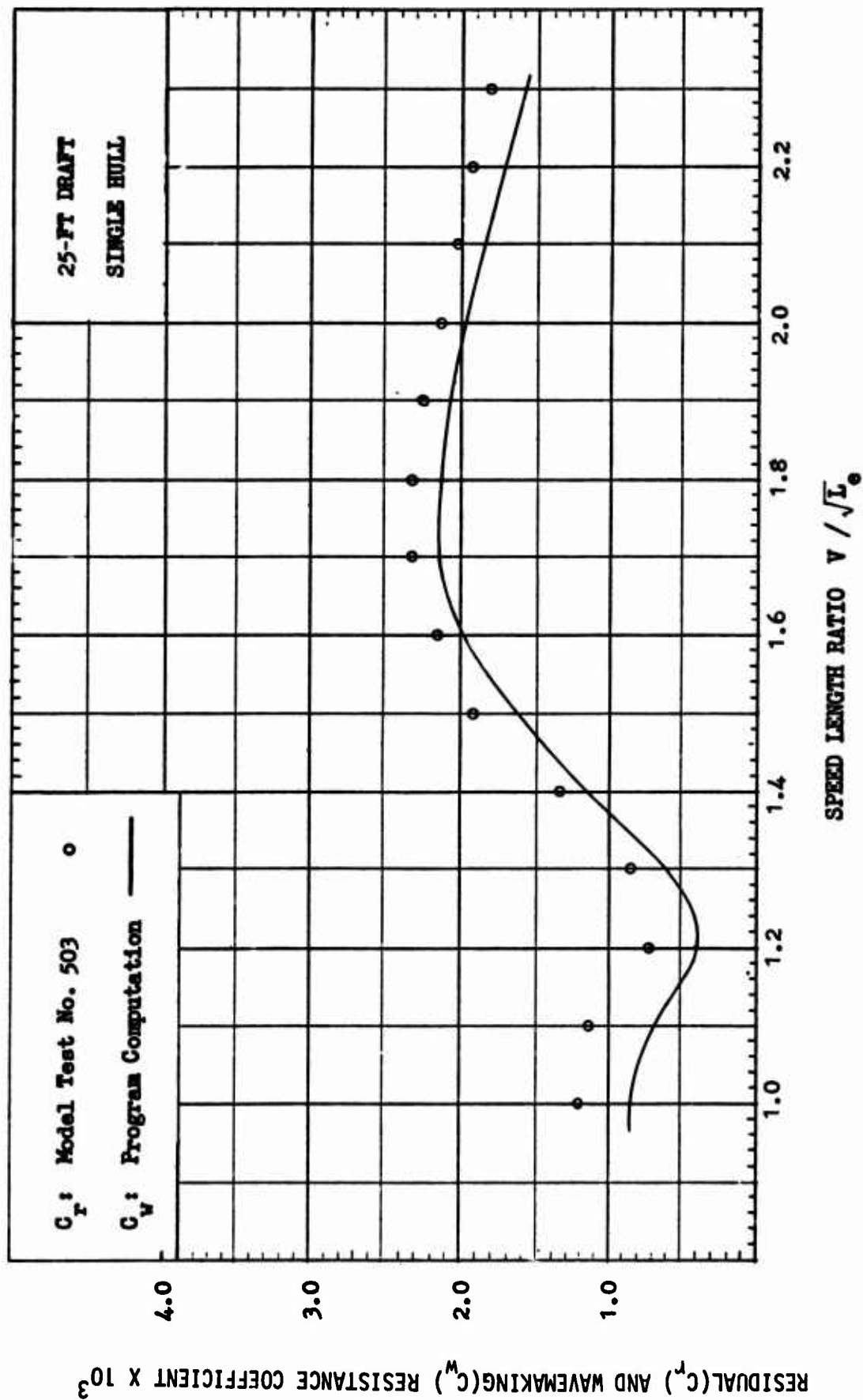


Figure 18 - Residual and Wavemaking Resistance Coefficients versus Speed-Length Ratio for SWATH III (Model 5276E) at a 25-Foot Draft

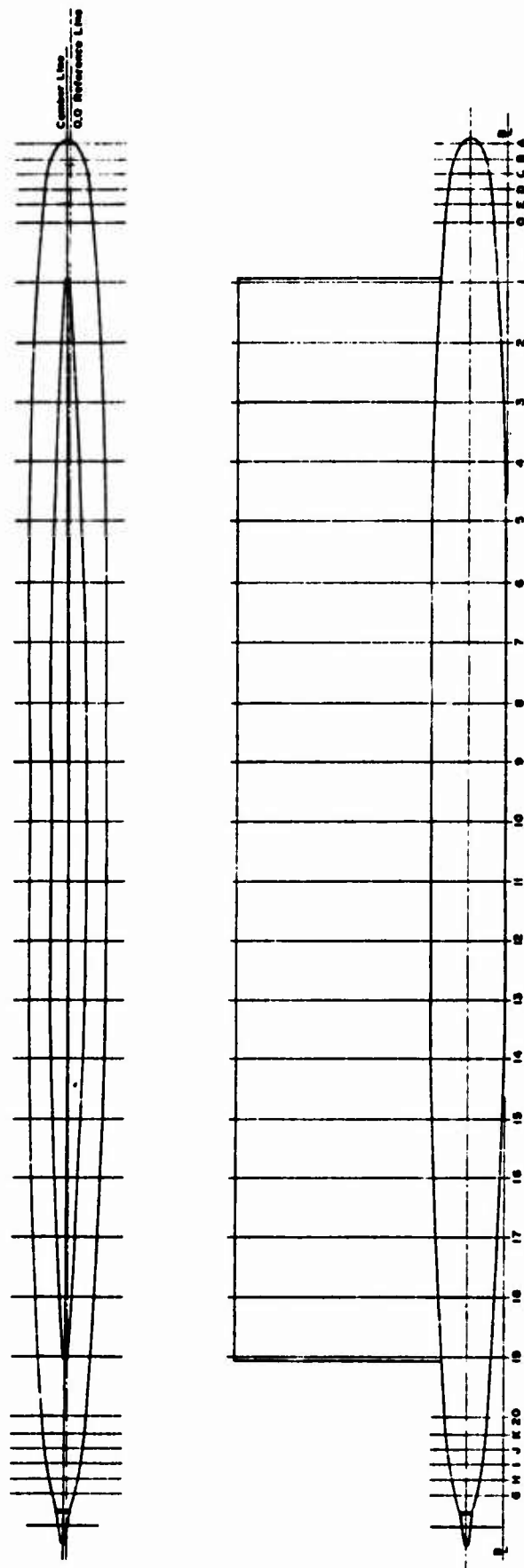


Figure 19 - Abbreviated Lines and Profile for SWATH IV Represented by Model 5287

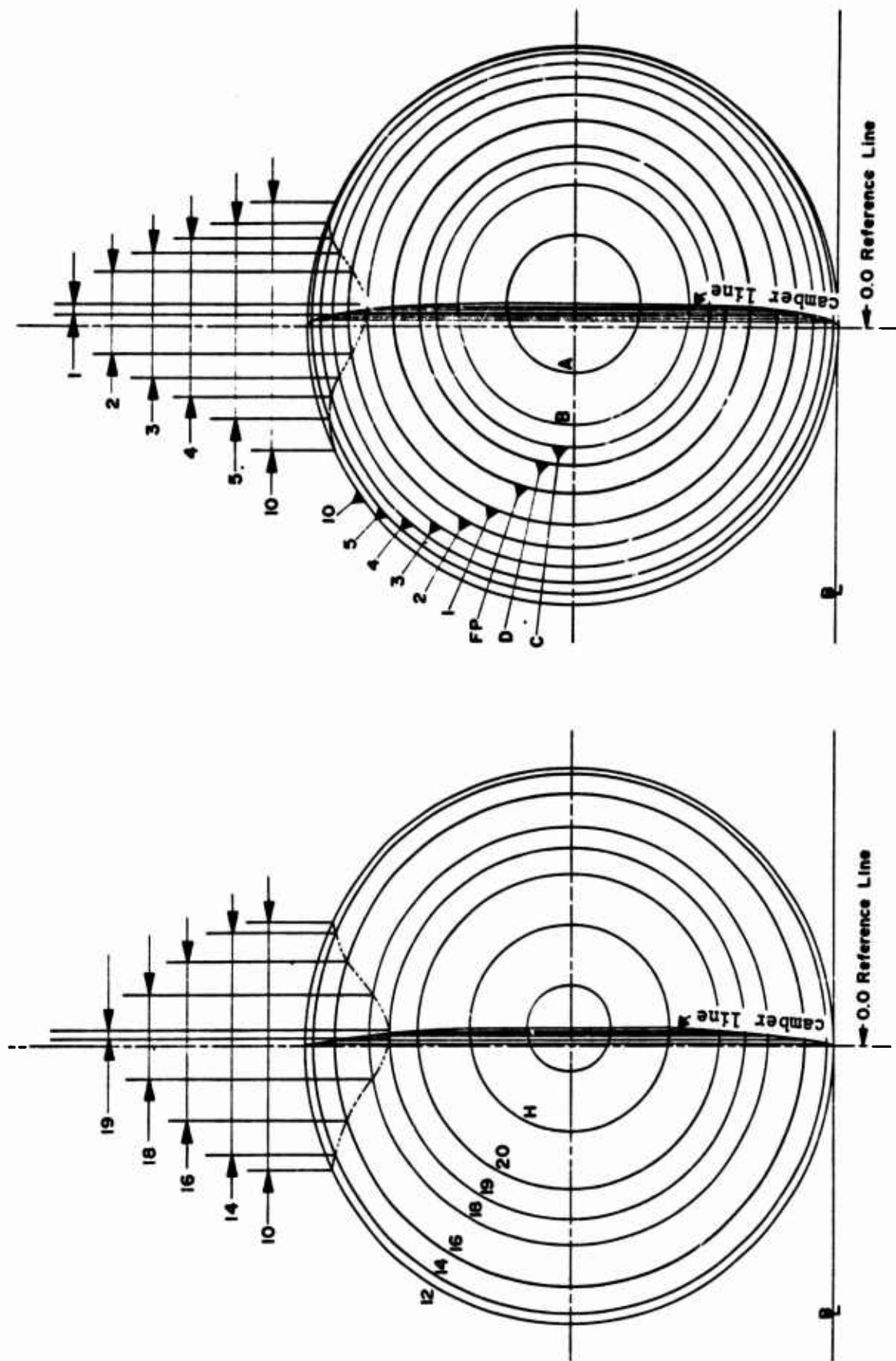


Figure 20 - Abbreviated Body Plan for SWATH IV (Model 5287)

ITEMS	SHIP		MODEL	
	HULL	STRUT	HULL	STRUT
LENGTH IN FT.	287.58	226.70	14.10	11.12
BEAM IN FT.	18.00	8.00	0.88	0.39
DESIGN SPEED IN KNOTS	32.00		7.08	
C _p	0.758		0.758	
C _w		0.74		0.74
C _x	0.785	0.987	0.785	0.987
EFFECTIVE LENGTH IN FT.	268.20			

FIGURE NO.	TEST NO.	DRAFT(FT)	HULL SPACING	DISPL. (TON)	WET SURF. (FT ²)	TEST CONDITIONS
13	1	32.00	75.00	4,270.00	38,710.00	Free to heave and trim
14	3	28.00	75.00	3,930.00	35,080.00	Free to heave and trim
15	9	25.00	75.00	3,730.00	32,360.00	Free to heave

* From center to center at midship.

Figure 21 - Ship and Experimental Model Test Data for SWATH IV (Model 5287)

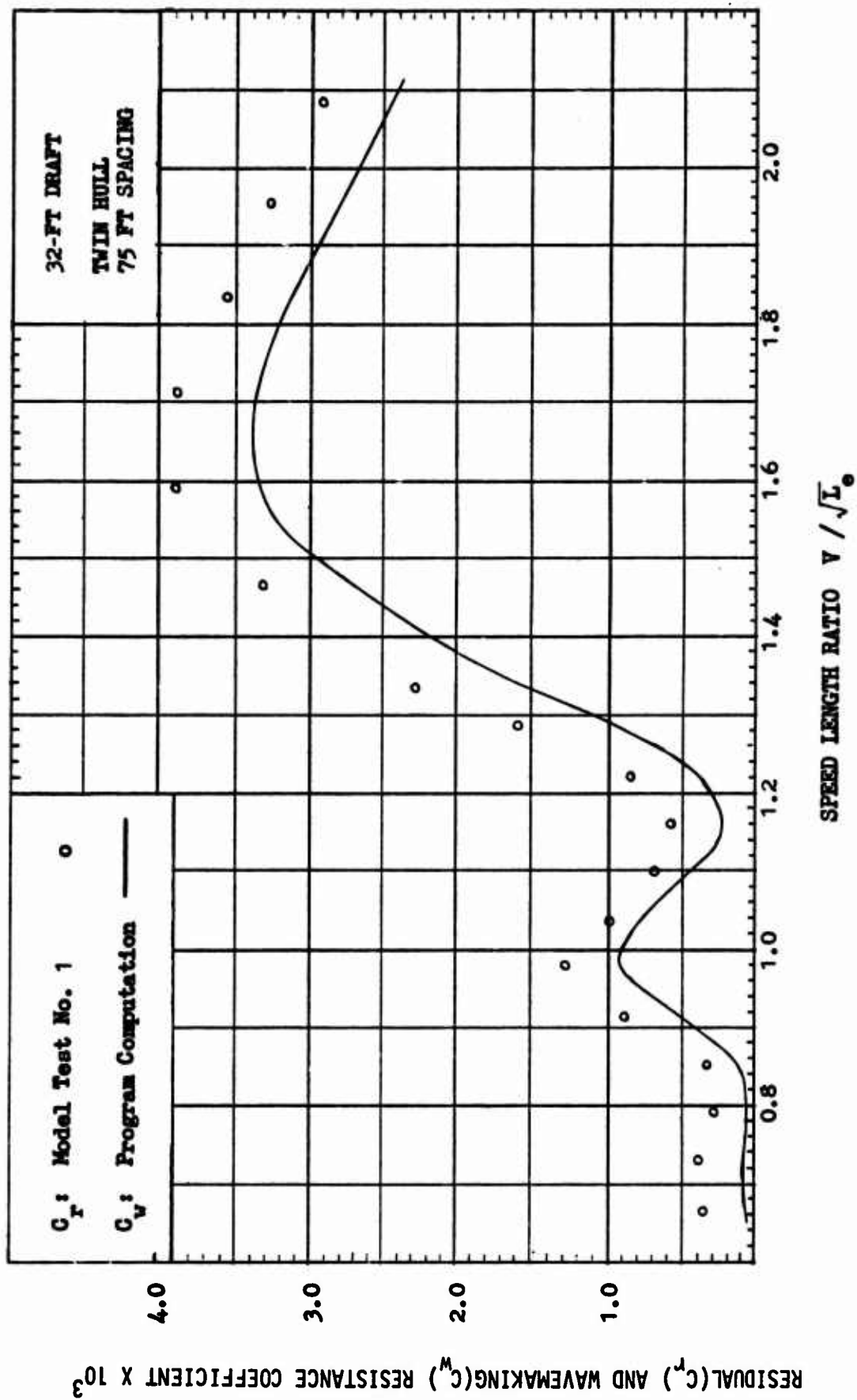


Figure 22 - Residual and Wavemaking Resistance Coefficients versus Speed-Length Ratio for SWATH IV (Model 5287) at a 32-Foot Draft

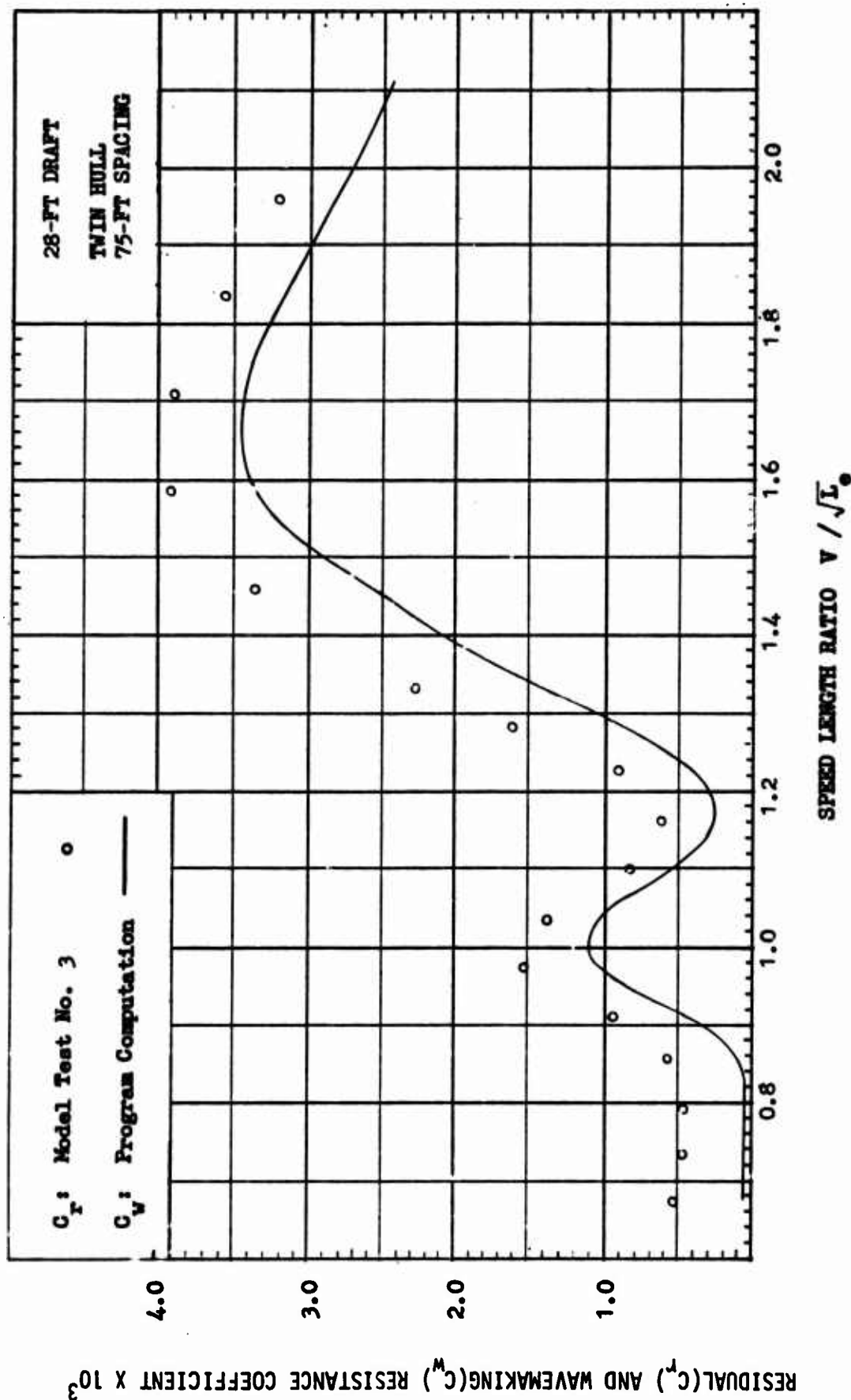


Figure 23 - Residual and Wavemaking Resistance Coefficients versus Speed-Length Ratio for SWATH IV (Model 5287) at a 28-Foot Draft

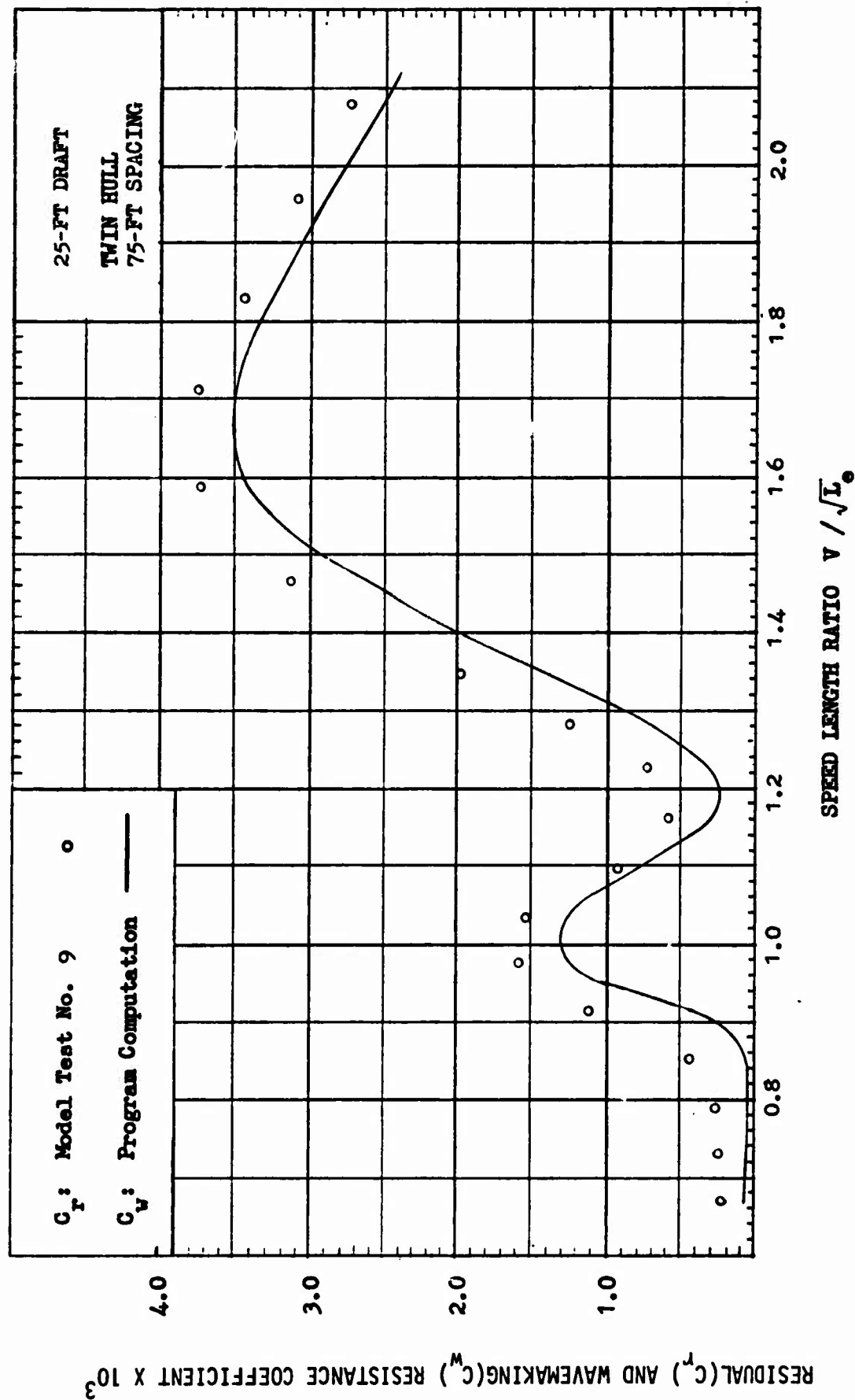


Figure 24 - Residual and Wavemaking Resistance Coefficients versus Speed-Length Ratio for SWATH IV (Model 5287) at a 25-Foot Draft

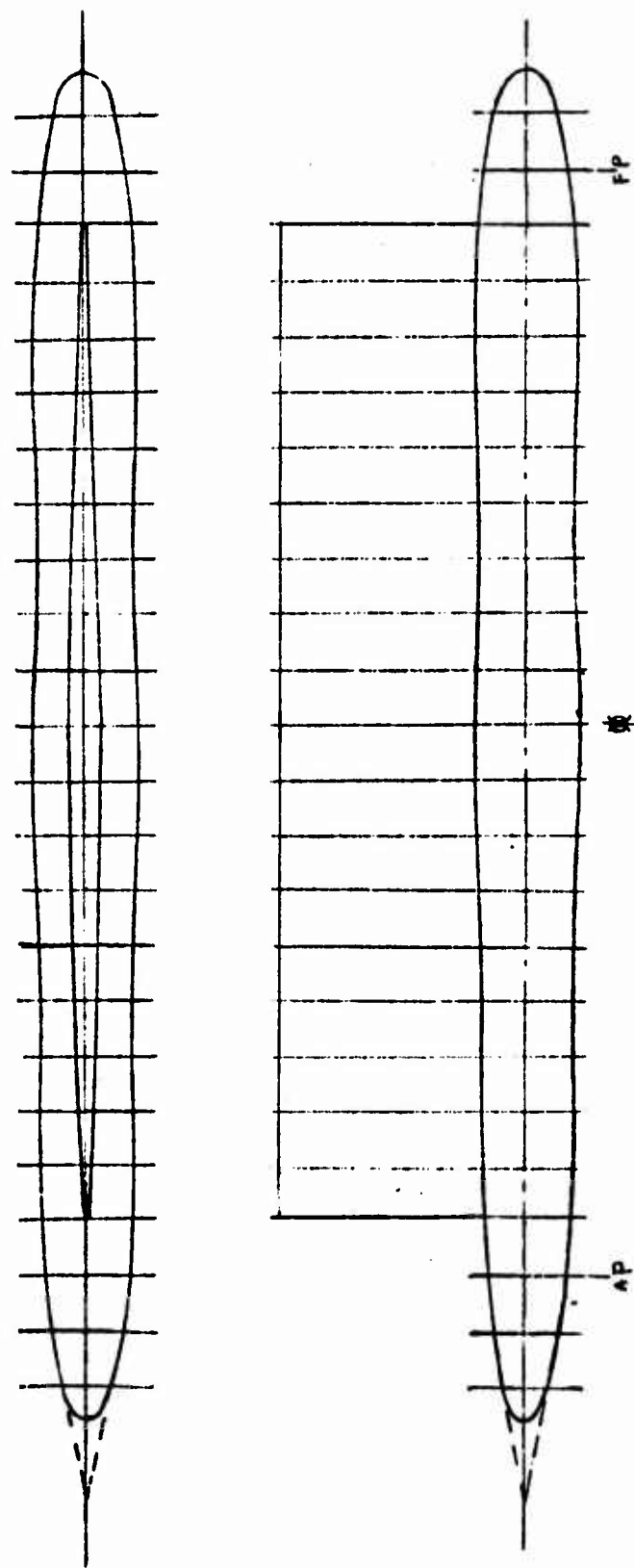


Figure 25 - Abbreviated Lines and Profile for SWATH V Represented by Model 5301

ITEMS	SHIP		MODEL	
	HULL	STRUT	HULL	STRUT
LENGTH IN FT.	259.72	191.05	15.012	11.043
BEAM IN FT.	20.622	6.833	1.192	0.395
DESIGN SPEED IN KNOTS				
C_p	0.777		0.777	
C_v		0.518		0.518
C_x	0.785	0.99	0.785	0.99
EFFECTIVE LENGTH IN FT.	242.80			

FIGURE NO.	TEST NO.	DRAFT(FT)	HULL SPACING	DISPL. (TON)	WET SURF. (FT ²)	TEST CONDITIONS
18	5	36.27	.00	2,244.00	20,298.00	Captive
19	12	32.00	.00	2,161.00	18,657.00	Captive
20	1	26.27	.00	2,051.00	16,474.00	Captive

* From center to center at midship.

Figure 26 - Ship and Experimental Model Test Data for SWATH V (Model 5301)

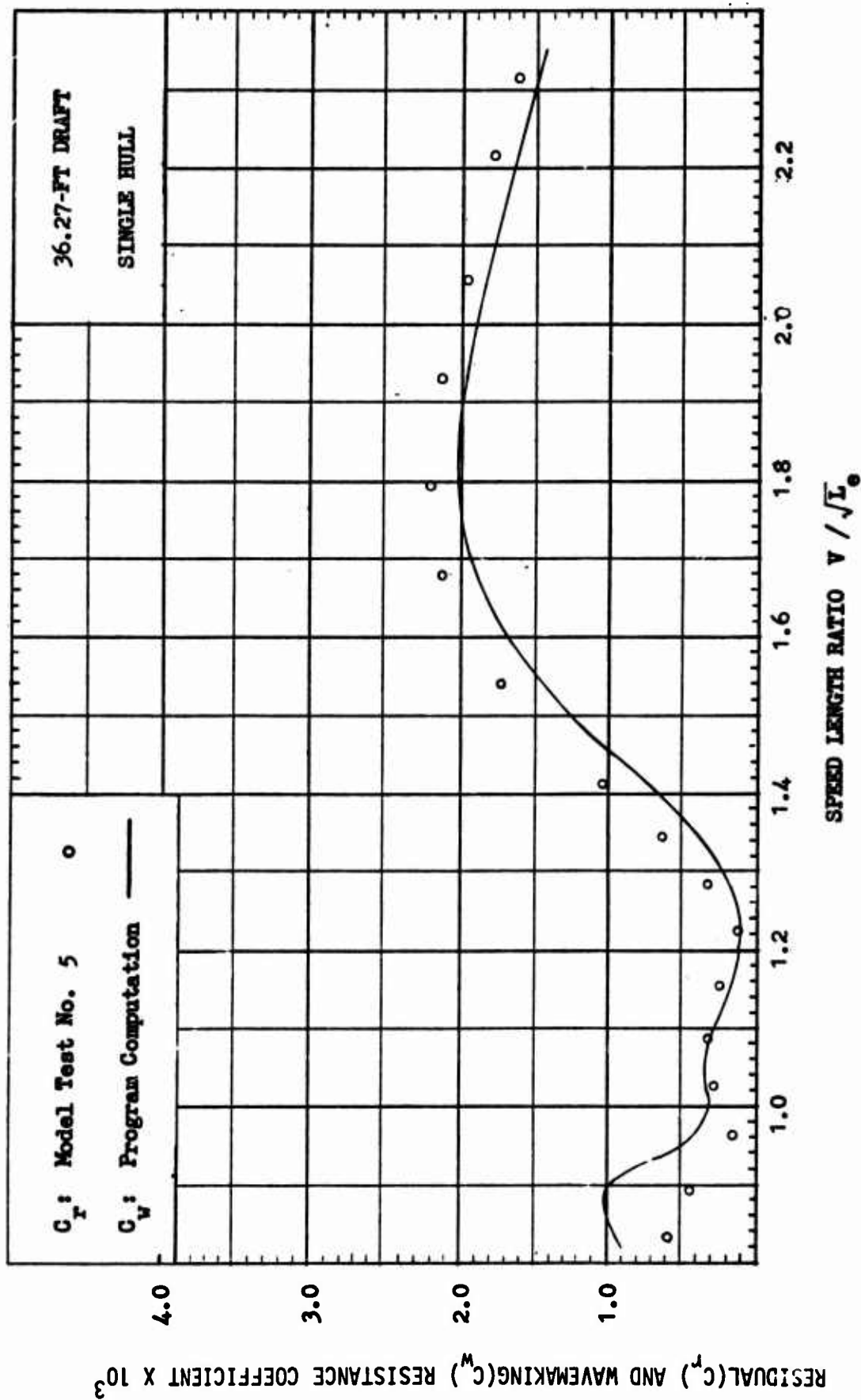


Figure 27 - Residual and Wavemaking Resistance Coefficients versus Speed-Length Ratio for SWATH V (Model 5301) at a 36.27-Foot Draft

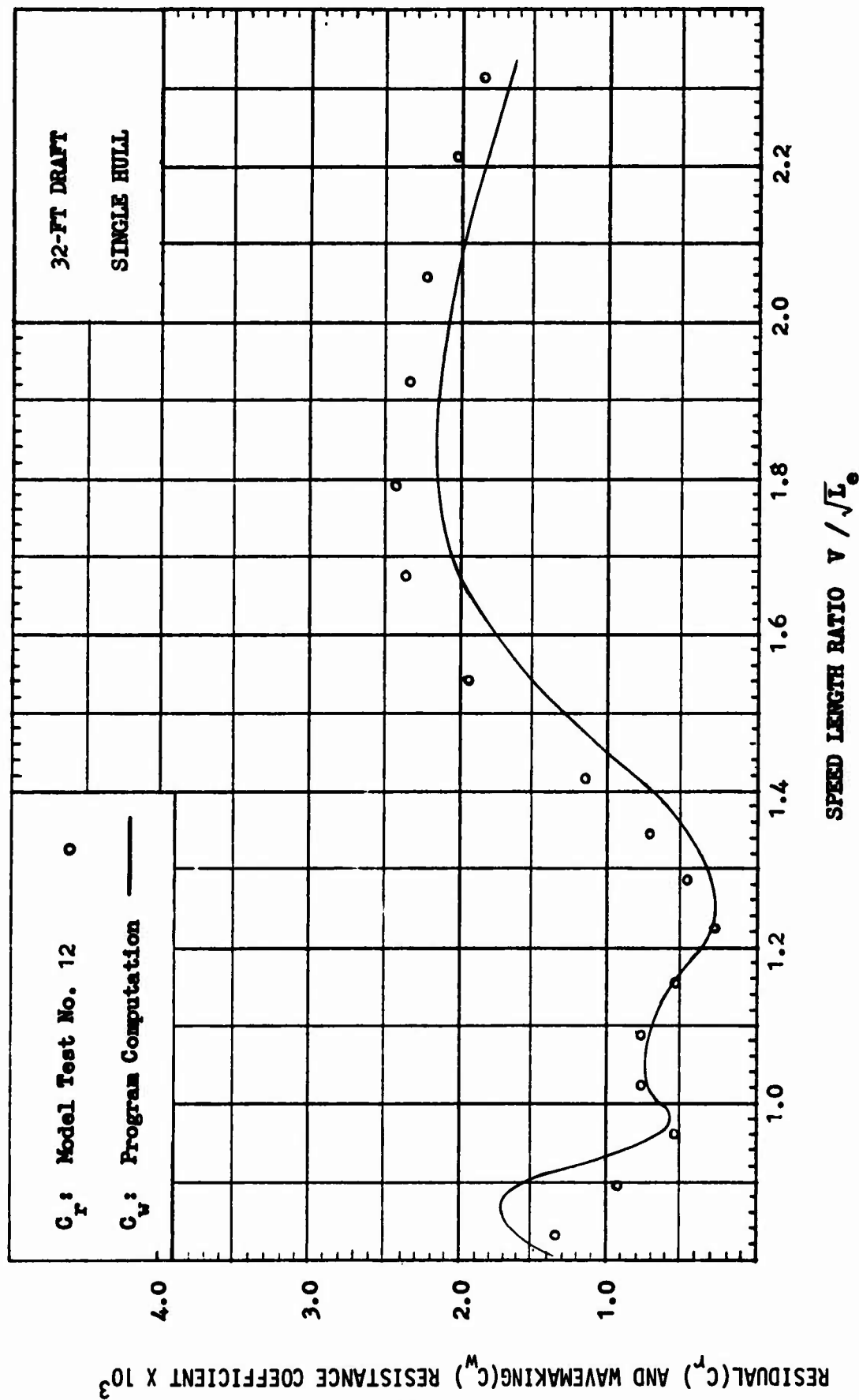


Figure 28 - Residual and Wavemaking Resistance Coefficients versus Speed-Length Ratio for SWATH V (Model 5301) at a 32-Foot Draft

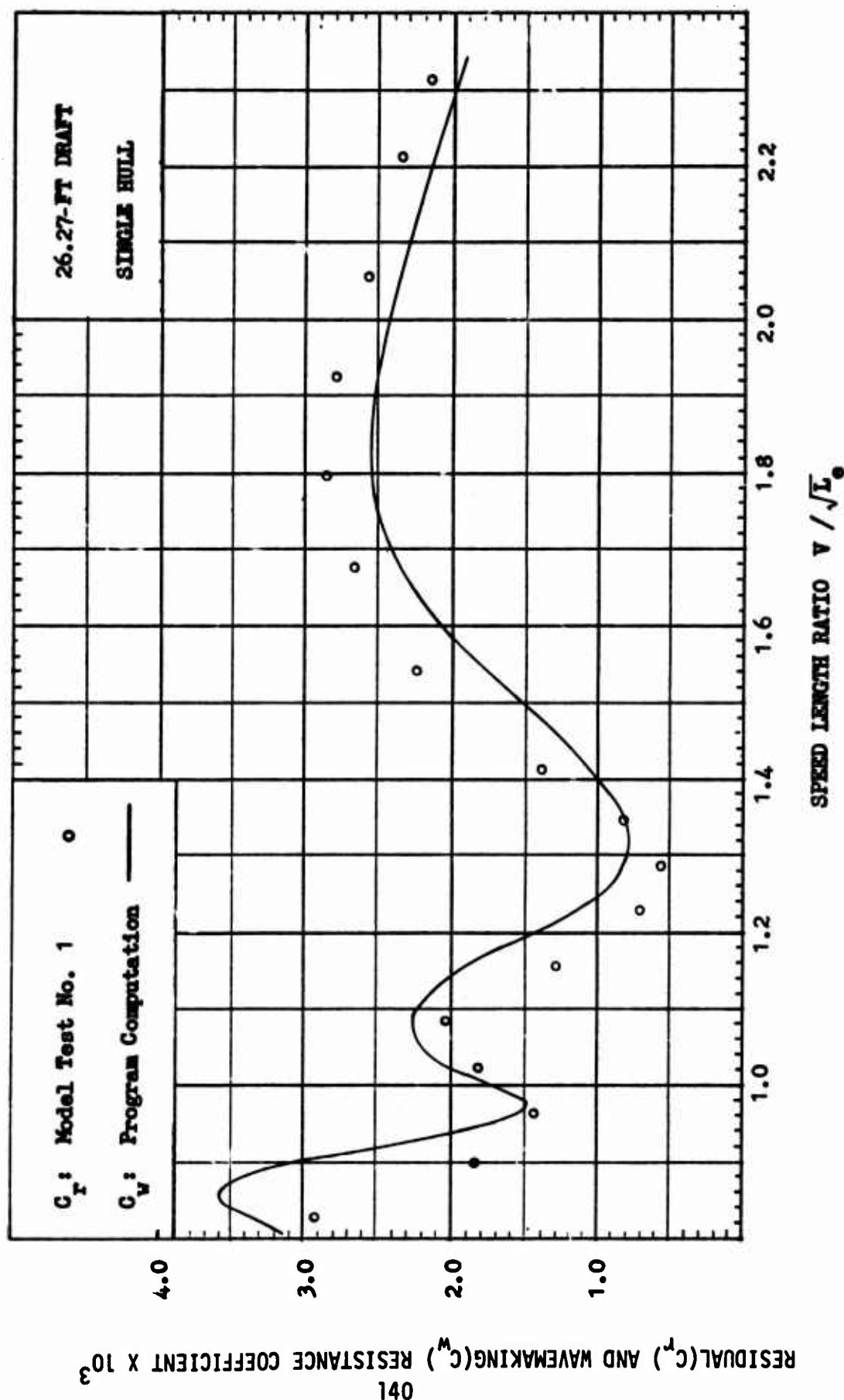


Figure 29 - Residual and Wavemaking Resistance Coefficients versus Speed-Length Ratio for SWATH V (Model 5301) at a 26.27-Foot Draft

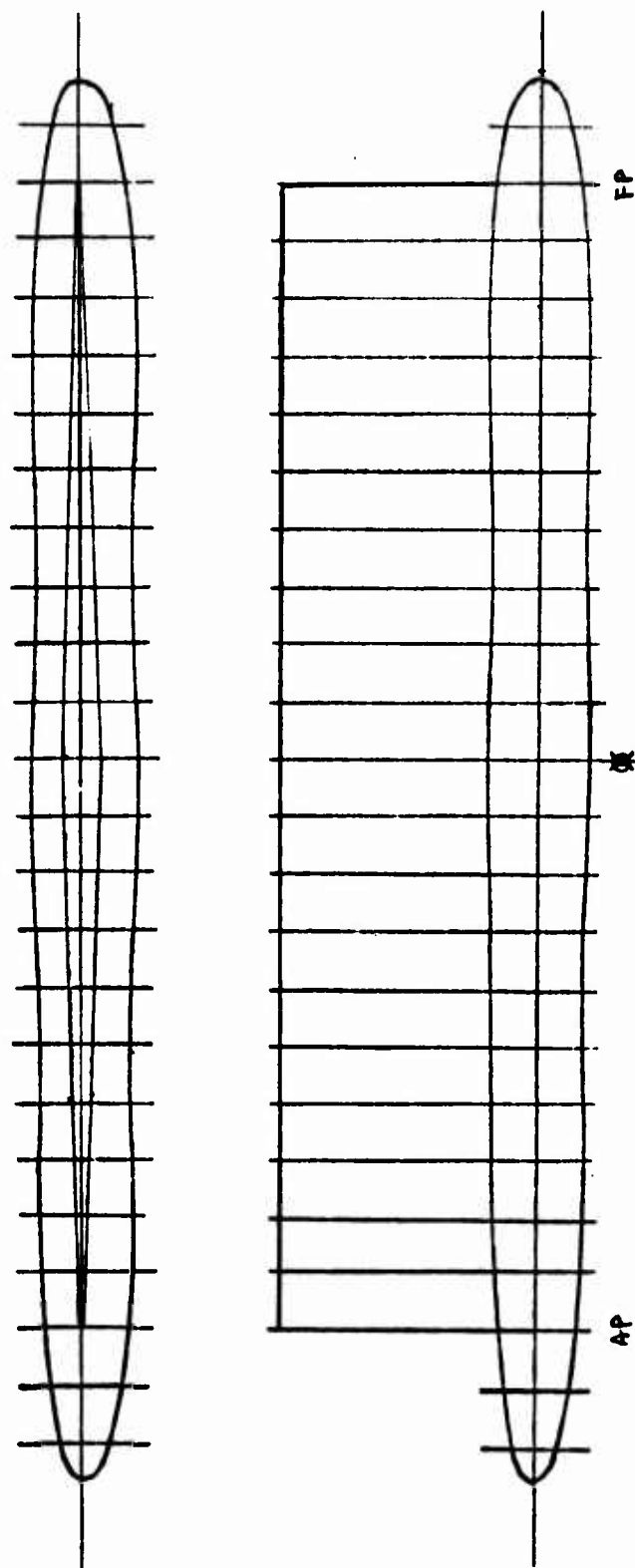


Figure 30 - Abbreviated Lines and Profile for SWATH V Represented by Model 5301-1

ITEMS	SHIP		MODEL	
	HULL	STRUT	HULL	STRUT
LENGTH IN FT.	259.72	212.285	15.012	12.27
BEAM IN FT.	20.622	6.833	1.192	0.395
DESIGN SPEED IN KNOTS				
C_p	0.777		0.777	
C_v		0.706		0.706
C_x	0.785	0.981	0.785	0.981
EFFECTIVE LENGTH IN FT.	246.50			

FIGURE NO.	TEST NO.	DRAFT(FT)	HULL SPACING*	DISPL.(TON)	WET SURF.(FT ²)	TEST CONDITIONS
23	7	38.00	0.00	2,460.0	21,467.00	Captive
24	8	32.00	0.00	2,284.00	18,924.00	Captive

* From center to center at midship.

Figure 31 - Ship and Experimental Model Test Data for SWATH V (Model 5301-1)

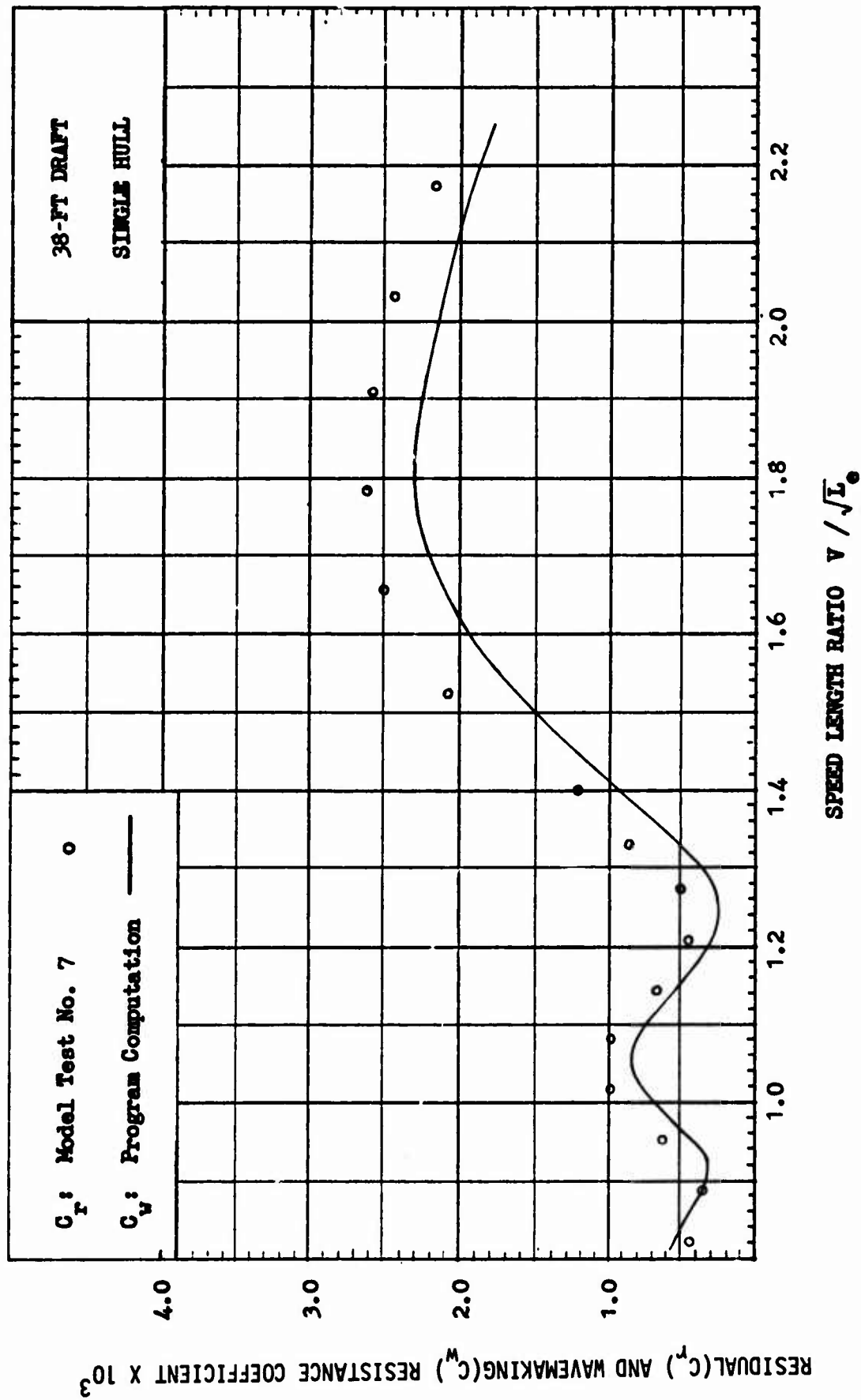


Figure 32 - Residual and Wavemaking Resistance Coefficients versus Speed-Length Ratio for SWATH V (Model 5301-1) at a 38-Foot Draft

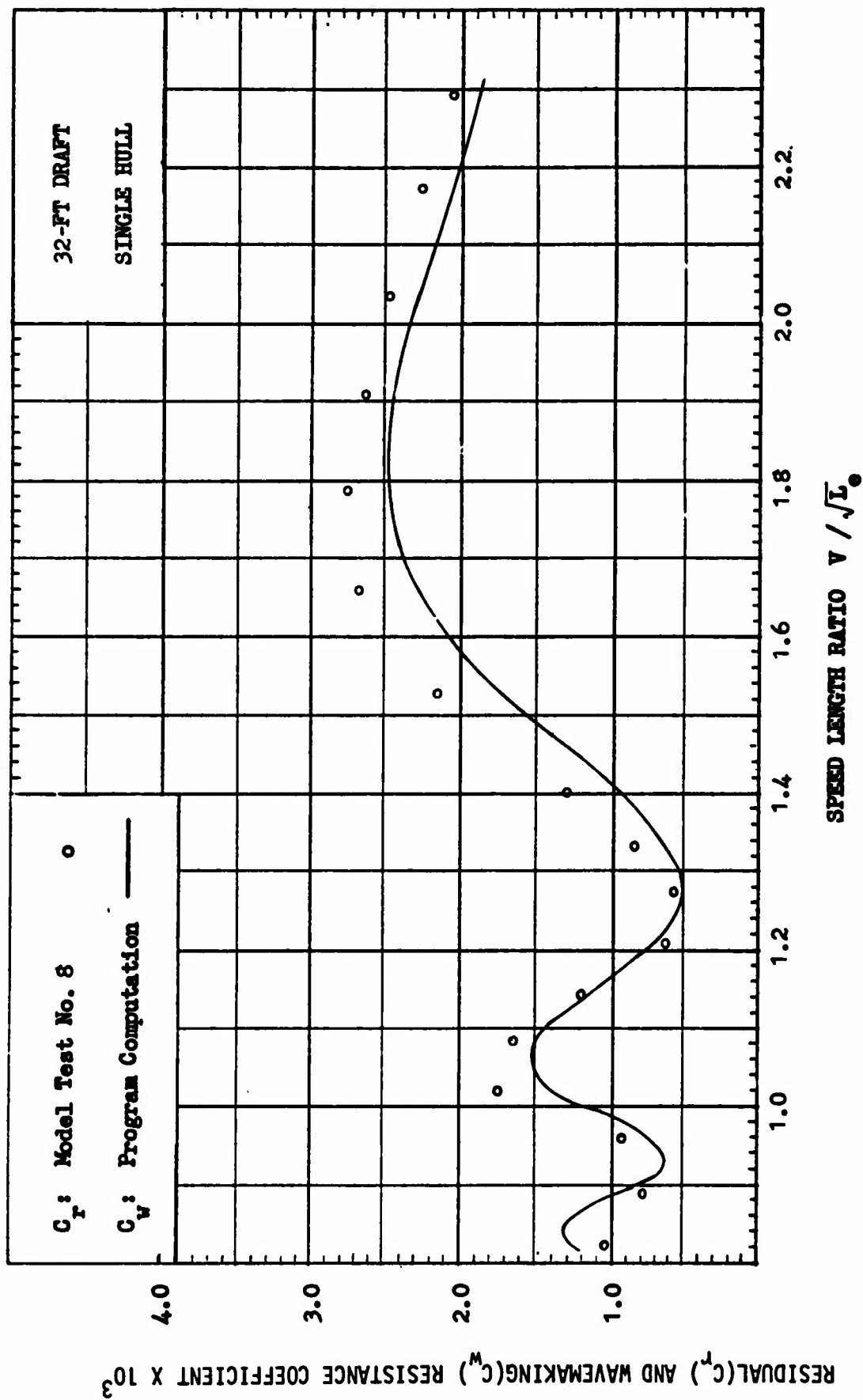


Figure 33 - Residual and Wavemaking Resistance Coefficients versus Speed-Length Ratio for SWATH V (Model 5301-1) at a 32-Foot Draft

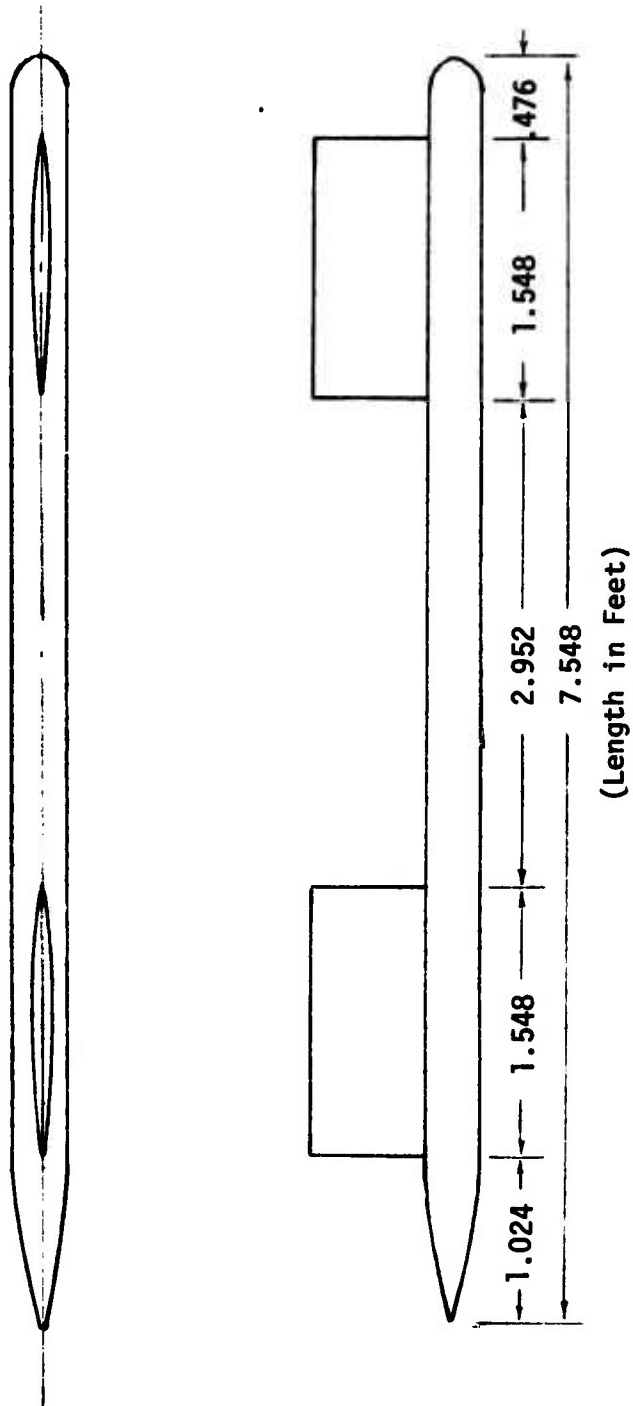


Figure 34 - Abbreviated Lines and Profile for SWATH RC-2

ITEMS	SHIP		MODEL	
	HULL	STRUT	HULL	STRUT
LENGTH IN FT.	317.00	65.00	7.548	1.548
BEAM IN FT.	14.00	5.00	.333	.119
DESIGN SPEED IN KNOTS				
C _p	0.946			
C _v		0.72		
C _x				
EFFECTIVE LENGTH IN FT.	307.6			

FIGURE NO.	TEST NO.	DRAFT(FT)	HULL SPACING*	DISPL.(TON)	WET SURF.(FT ²)	TEST CONDITIONS
27		28.00	123.00	2,995.00	29,493.00	
28		21.00	123.00	2,811.00	27,673.00	

* From center to center at midship.

Figure 35 - Ship and Experimental Model Test Data for SWATH RC-2

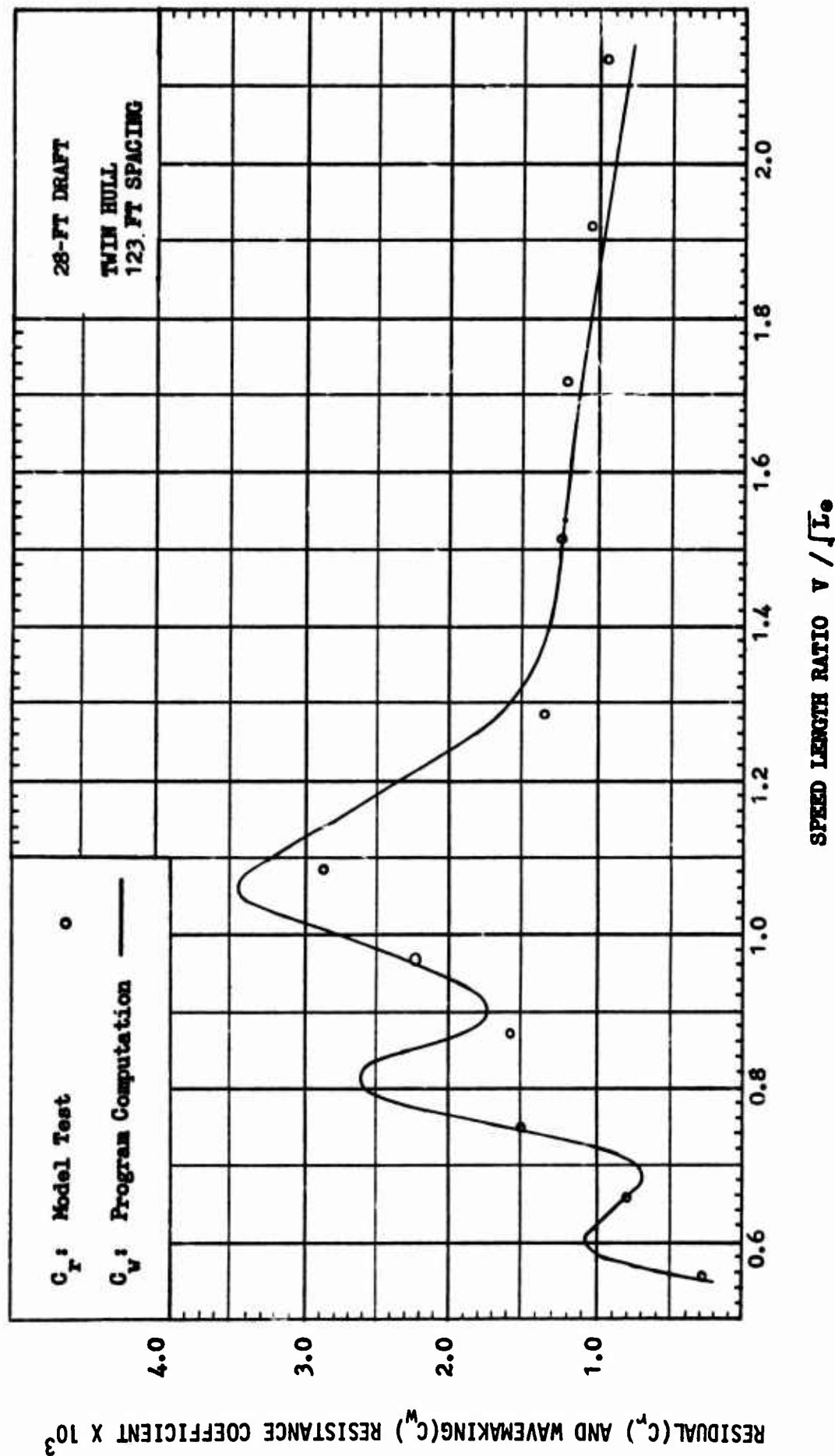


Figure 36 - Residual and Wavemaking Resistance Coefficients versus Speed-Length Ratio for SWATH KC-2 at a 28-Foot Draft

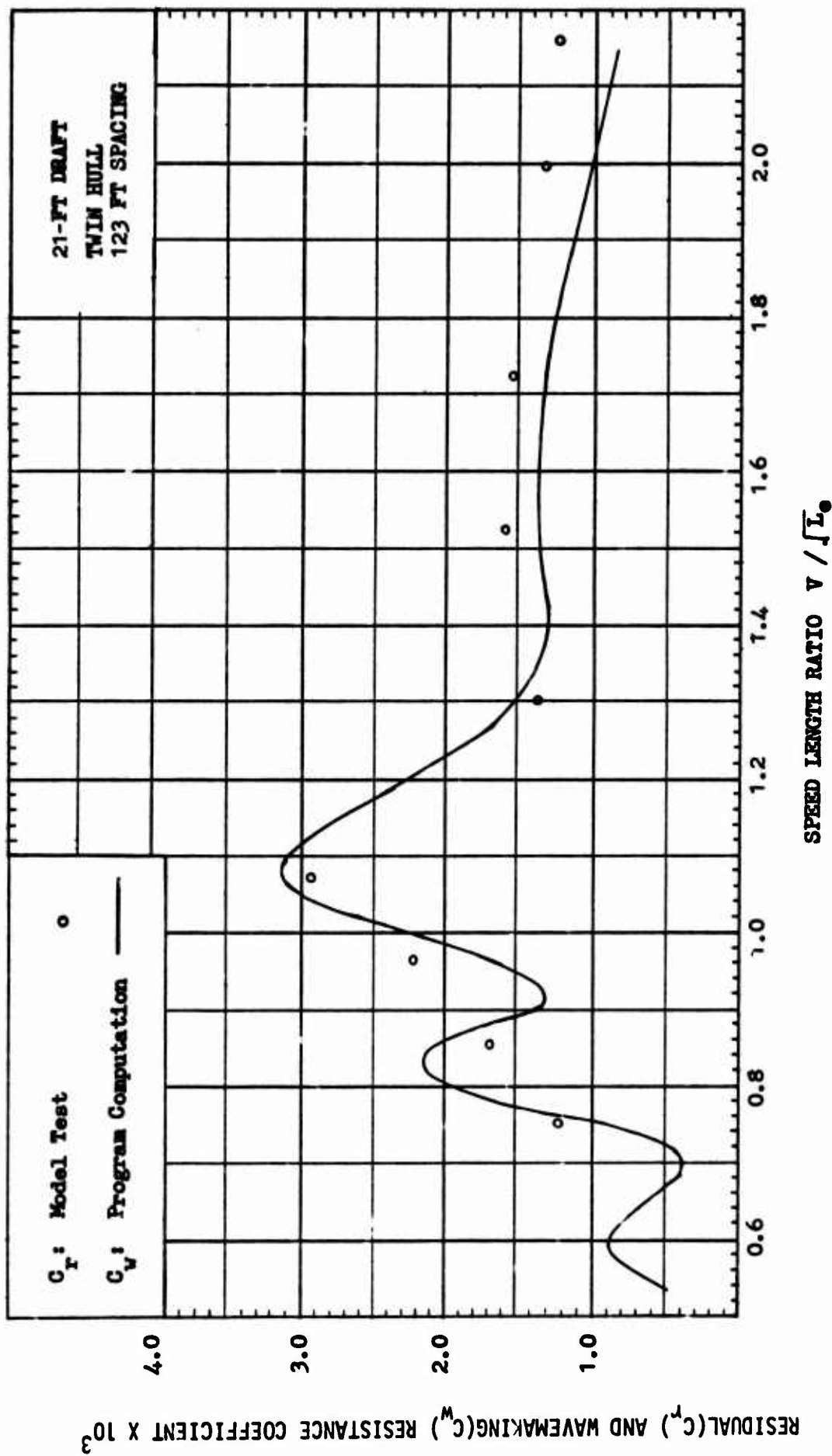


Figure 37 - Residual and Wavemaking Resistance Coefficients versus Speed-Length Ratio for SWATH RC-2 at a 21-Foot Draft

REFERENCES

1. Michell, J. H., "The Wave-Resistance of a Ship," *Philosophical Magazine*, Vol. 45 (1898).
2. Havelock, T. H., "Wave Patterns and Wave Resistance," *Transaction INA*, Vol. 74 (1934).
3. Havelock, T. H., "Calculation of Wave Resistance," *Proceedings of the Royal Society, London, England, Series A*, Vol. 144 (1934).
4. Pien, P. C., and W. I. Moore, "Theoretical and Experimental Study of Wavemaking Resistance of Ships," *International Seminar on Theoretical Wave Resistance*, University of Michigan, Ann Arbor, Michigan (Aug 1963).
5. Pien, P. C., "The Application of Wave-Making Resistance Theory to the Design of Ship Hulls with Low Resistance," *Fifth Symposium on Naval Hydrodynamics*, Bergen, Norway (Sept 1964).
6. Pien, P. C. and J. Strom-Tejsen, "A Hull Design Procedure for High Speed Displacement Ships," *Proceedings of 1963 Diamond Jubilee International Meeting*, SNAME (1968).
7. Comstock, J., "Principles of Naval Architecture," *The Society of Naval Architects and Marine Engineers* (1967).
8. Pien, P. C. and C. M. Lee, "Motion and Resistance of a Low-Water-plane-Area Catamaran," *Ninth Symposium on Naval Hydrodynamics*, Paris, France (Aug 1972).
9. Chen, R., "The Pien Wavemaking Resistance Computation Program - Part 2 User's Manual," *Naval Ship Research and Development Center Report 4371* (Apr 1975).
10. Inui, T., "Wave-Making Resistance of Ships," *Transaction of SNAME* (1962).
11. Gray, M., "A Survey of Current Optimization Methods," *Naval Ship Research and Development Center Report 3605* (Jan 1971).